

AD-A159 535

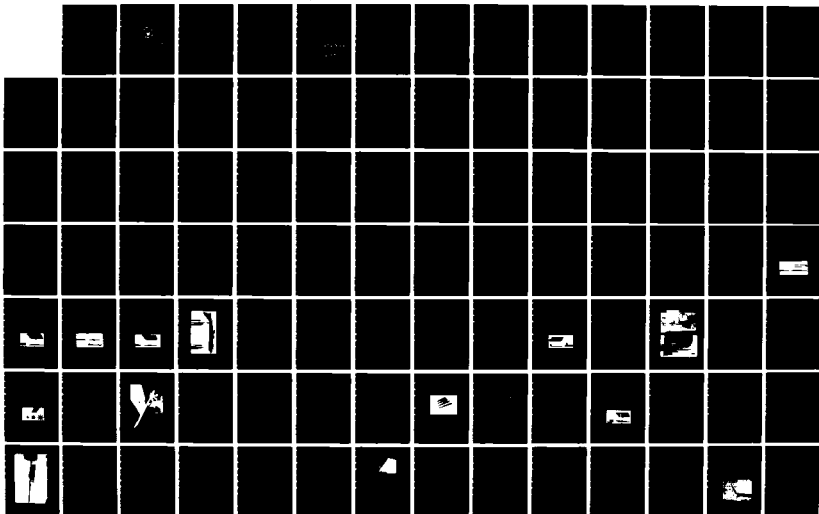
TRAILING VORTEX ATTENUATION DEVICES(U) NAVAL
POSTGRADUATE SCHOOL MONTEREY CA K G HEFFERNAN JUN 85

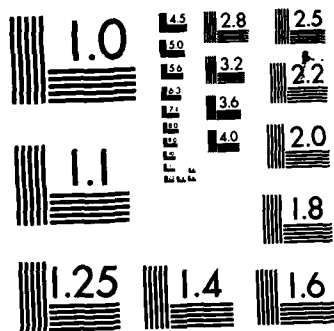
1/2

UNCLASSIFIED

F/G 28/4

NL





MICROCOPY RESOLUTION TEST CHART
NATIONAL BUREAU OF STANDARDS-1963-A

9

AD-A159 535

NAVAL POSTGRADUATE SCHOOL

Monterey, California



DTIC
ELECTE
SEP 25 1985
S 96 A D

THESIS

TRAILING VORTEX ATTENUATION DEVICES

by

Kenneth G. Heffernan

June 1985

Thesis Advisor:

T. Sarpkaya

Approved for public release; distribution is unlimited.

DTIC FILE COPY

85 9 21 000

Unclassified

SECURITY CLASSIFICATION OF THIS PAGE (When Data Entered)

REPORT DOCUMENTATION PAGE		READ INSTRUCTIONS BEFORE COMPLETING FORM
1. REPORT NUMBER	2. GOVT ACCESSION NO. AD A159535	3. RECIPIENT'S CATALOG NUMBER
4. TITLE (and Subtitle) Trailing Vortex Attenuation Devices		5. TYPE OF REPORT & PERIOD COVERED Dual Master's Thesis; June 1985
7. AUTHOR(s) Kenneth G. Heffernan		6. PERFORMING ORG. REPORT NUMBER
9. PERFORMING ORGANIZATION NAME AND ADDRESS Naval Postgraduate School Monterey, California 93943		8. CONTRACT OR GRANT NUMBER(s)
11. CONTROLLING OFFICE NAME AND ADDRESS Naval Postgraduate School Monterey, California 93943		10. PROGRAM ELEMENT, PROJECT, TASK AREA & WORK UNIT NUMBERS
14. MONITORING AGENCY NAME & ADDRESS (if different from Controlling Office)		12. REPORT DATE June 1985
		13. NUMBER OF PAGES 109
		15. SECURITY CLASS. (of this report) Unclassified
		15a. DECLASSIFICATION/DOWNGRADING SCHEDULE
16. DISTRIBUTION STATEMENT (of this Report) Approved for public release; distribution is unlimited.		
17. DISTRIBUTION STATEMENT (of the abstract entered in Block 20, if different from Report)		
18. SUPPLEMENTARY NOTES		
19. KEY WORDS (Continue on reverse side if necessary and identify by block number) Trailing Vortices		
20. ABSTRACT (Continue on reverse side if necessary and identify by block number) Trailing vortices generated by large aircraft pose a serious hazard to other planes. Numerous studies have been carried out to destroy them either before and/or after their formation. The present investigation is a survey and critical assessment of all the known active/passive devices and wingtip modifications proposed to achieve vortex attenuation. It is concluded that some devices, such as the wing tip sails, have promise in affecting the vortex roll-up in the vicinity of the aircraft. However		

DD FORM 1473
1 JAN 73

EDITION OF 1 NOV 65 IS OBSOLETE
S N 0102-LF-014-6601

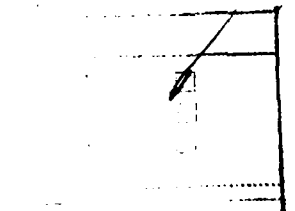
Unclassified

SECURITY CLASSIFICATION OF THIS PAGE (When Data Entered)

Unclassified

SECURITY CLASSIFICATION OF THIS PAGE (When Data Entered)

more data and analysis on this and other devices are needed before they can be incorporated into existing aircraft or future designs.

		
EY		
Dist		
Assessment of		
Dist		
AI	Assessment of	Special



S/N 0102- LF-014-6601

Unclassified

SECURITY CLASSIFICATION OF THIS PAGE(When Data Entered)

Approved for public release; distribution is unlimited.

Trailing Vortex Attenuation Devices

by

Kenneth G. Heffernan
Lieutenant, United States Navy
B.S., United States Naval Academy, 1978

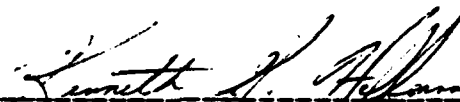
Submitted in partial fulfillment of the
requirements for the degree of

MASTER OF SCIENCE IN MECHANICAL ENGINEERING
and the degree of
MASTER OF SCIENCE IN AERONAUTICAL ENGINEERING

FROM THE

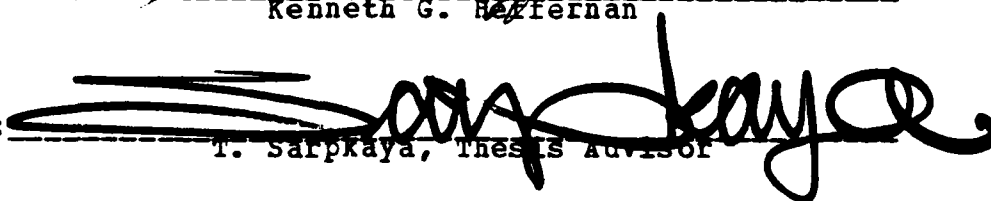
NAVAL POSTGRADUATE SCHOOL
June 1985

Author:



Kenneth G. Heffernan

Approved by:



T. Sarpkaya, Thesis Advisor



M. F. Platzler, Chairman,
Department of Aeronautics



P. J. Marto, Chairman,
Department of Mechanical Engineering



John M. Dyer,
Dean of Science and Engineering

ABSTRACT

Trailing vortices generated by large aircraft pose a serious hazard to other planes. Numerous studies have been carried out to destroy them either before and/or after their formation. The present investigation is a survey and critical assessment of all the known active/passive devices and wingtip modifications proposed to achieve vortex attenuation. It is concluded that some devices, such as the wing tip sails, have promise in affecting the vortex roll-up in the vicinity of the aircraft. However, more data and analysis on this and other devices are needed before they can be incorporated into existing aircraft or future designs.

TABLE OF CONTENTS

I.	INTRODUCTION	12
II.	BRIEF REVIEW OF THE FUNDAMENTAL ASPECTS OF WINGTIP VORTICES	13
III.	EXPERIMENTAL EVALUATION OF THE VORTEX MINIMIZATION DEVICES	22
	A. INTRODUCTION	22
	B. ACTIVE DEVICES	24
	C. PASSIVE DEVICES	29
IV.	SUMMARY	39
V.	CONCLUSIONS	46
	APPENDIX A: FIGURES	47
	LIST OF REFERENCES	104
	INITIAL DISTRIBUTION LIST	109

LIST OF TABLES

I	Horizontal Separation Requirements	22
II	Categorical Listing of Vortex Attenuating Devices	24
III	Induced Rolling Moment Coefficients for Various Devices	28
IV	Biplane Winglet Addition Efficiency Factors . . .	37
V	Recapitulation of the Advantages and Disadvantages of Active Devices	40
VI	Recapitulation of the Advantages and Disadvantages of Passive Devices	41

LIST OF FIGURES

1	Formation of Wake Vortex Showing Induced Velocities	47
2	Sketch of Trailing Vortex System	47
3	Trailing Vortex Hazard Potentials	48
4	Sketch of the Induced Flow	48
5	Test Arrangement in NASA Facilities	49
6	Arrangement of the Langley Vortex Research Facility	50
7	Effects of Central Jet on the Measured Tangential and Axial Mean Velocity Profiles	51
8	Effects of Central Jet on the Rolling Moment Coefficient	52
9	Sketch and Close-Up Views of a Forward Blowing Jet	53
10	Sketch and Close-Up Views of a Rearward Blowing Jet	54
11	Sketch and Close-Up Views of a Downward Blowing Jet	55
12	Sketch and Close-Up Views of a Deflected Jet	56
13	Basic Model of a Boeing 747 Aircraft	57
14	Effect of Engine Reverse Thrust on the Vortex Induced Rolling Moment Coefficient on a Learjet Probe Model	58
15	Sketch of a Spanwise Extended Blowing Tube	59
16	Effect on Lift-to-Drag Ratio from Spanwise Extended Tube Blowing	59
17	Effect on Lift-to-Drag Ratio from Spanwise Extended Tube Blowing at Transport Model Wingtip	60

18	Rolling Moments Measured by a Small-Wing Model at 7.5 Spans Downstream a Transport Model with a Blowing Tube	60
19	Sketch of Individually Controlled Discrete Wingtip Jets	61
20	Two Typical Wingtip Jet Configurations	62
21	Sketch and Close-Up Views of a Blown Flap	63
22	Effect of a Blown Flap on the Vortex Velocity Distribution	64
23	Wingtip-Mounted Engines on a Transport Model: Front and Side Views	65
24	B-747 Wake Vortex Disturbance on a T-37B Probe Aircraft--Oscillating Ailerons and Spoilers	66
25	Sketch of Fixed Crossed Blades (Four Inch)	67
25a	Sketch of Fixed Crossed Blades (Eight Inch)	67
26	Sketch and Close-Up Views of Wingtip Mounted Splines	68
27	Sketch of Spline Assembly at Wingtip	69
28	Photograph of the Spline Assembly on the Wingtip	70
29	Sketch of Cabled Drogue Cone and Cabled Chute	71
30	Sketch and Close-Up Views of a Vortex Generator	72
31	Sketch of Wingfins on a Transport Aircraft Model	73
32	Summary of Reductions in Rolling Moment Coefficient for Various Wingfin Configurations (7.8 Spans Downstream)	74
33	Parabolic Wingfins	75
34	Vortex Strength Term vs. Fin Angle of Attack	76
35	Maximum Vortex Strength Term vs. Fin Aspect Ratio	77
36	Wingtip Mounted Spoiler	78
37	Variation of Rolling Moment Coefficient with Distance behind a Basic Model: No Device, Spoiler, Spline	79

38	Variation of Rolling Moment Coefficient with Distance behind a Flapped Model: No Device, Spoiler, Spline	80
39	Sketch of Flight Spoilers on a B-747 Aircraft Model	81
40	Photograph of Flight Spoilers on a B-747 Aircraft Model: Segments 1 and 2 Deflected 45 Degrees	82
41	Variation of Rolling Moment Coefficient with Distance behind the B-747 Aircraft Model (Spoiler Deflection)	83
42	Three View Sketch of DC-10 Model with Flaps Retracted	84
43	Sketch of Flight Spoilers on a DC-10 Model	85
44	Variation of Rolling Moment Coefficient with Distance behind the DC-10 Aircraft Model (Spoiler Deflection)	86
45	Three View Sketch of B-747 Model with Flaps Retracted	87
46	Photograph of Porous Wingtip	88
47	Nondimensional Maximum Tangential Velocity vs. Lift Coefficient	88
48	Maximum Tangential Velocity vs. Downstream Distance	89
49	Lift Distribution on O-1A Wing with and without Porous Tip	89
50	Wingtip Edge Shape Configurations	90
51	Changeover Position from Axial Velocity Excess to Axial Velocity Deficit behind NACA 6412 Wing Section	91
52	Comparison of Axial Velocity Profile for Various Wingtip Edge Shapes (20 Chordlengths Downstream)	92

53	Comparison of Tangential Velocity Profile for Various Wingtip Edge Shapes (20 Chordlengths Downstream)	93
54	Sketch of End Plate and Wingtip Extension	94
55	Photograph of Whitcomb Winglet	94
56	Geometric Drawing of the Whitcomb Winglet	95
57	Incremental Lift Coefficient Variation for Constant Drag Cefficient ($M=0.78$)	96
58	Tangential Velocity Profile Downstream Whitcomb Winglet (5 Chordlengths)	97
58a	Tangential Velocity Profile Downstream Whitcomb Winglet (20 Chordlengths)	97
59	Axial Velocity Profile Downstream Whitcomb Winglet (5 Chordlengths)	98
59a	Axial Velocity Profile Downstream Whitcomb Winglet (20 Chordlengths)	98
60	Spanwise Pressure Distribution for Various Wingtip Edge Shapes and Whitcomb Winglet	99
61	Spanwise Load Distribution of Whitcomb Winglet ($M=0.78$)	100
62	Forces on an Auxiliary Surface Mounted on the Tip of a Wing	101
63	View of Paris Aircraft Fitted with Wingtip Sails	101
64	Wingtip Sail Geometry	102
65	Effect of Wingtip Sails on Lift-Induced Drag	103
66	Sketch of Biplane Winglet	103

ACKNOWLEDGEMENTS

The author wishes to express his sincere appreciation to Distinguished Professor T. Sarpkaya for his invaluable guidance, advice and encouragement during this research. His wealth of knowledge and dedication to the advancement of science are truly inspirational.

Blowing jets have been the subject of exhaustive studies. Snedeker [Ref. 25] and Poppleton [Ref. 26] introduced axial flow directly into the vortex core and found that the tangential velocities were greatly reduced while the core radius increased (see Figure 7). However, as shown in Figure 8, the rolling moment created on an airfoil (25 chordlengths downstream) was relatively unaffected by the jet momentum. This is a point which will continuously become evident throughout this review. Reduction of tangential velocities within the vortex cannot be directly correlated with reduced rolling moments. These results were limited to very short downstream distances, indicating that the effects of axial blowing jets are not immediately manifested in vortex breakdown. Kirkman, et al. [Ref. 27 : pp. 8-13], using the Hydronautics ship model basin, tested four variations of the blowing jet: forward, rearward, downward and deflected (Figures 9-12). The investigation conducted on a 3/100 scale model of the B-747 transport aircraft (see Figure 13) emphasized far-field effects (up to 8 km full-scale) including velocity distributions and induced rolling moments on following aircraft. The model ran at Reynolds numbers of 7.5×10^5 and 9.3×10^5 in a cruise (the lift coefficient $C_L = 0.4$) and 30 degrees flapped ($C_L = 1.2$) conditions with jet momentum coefficients between 4.6×10^{-4} to 8.3×10^{-4} . With these low jet momentum coefficients, only the deflected jet produced any appreciable change in the tangential velocity distribution in comparison to the unmodified aircraft. The slight decrease, at a full-scale distance of 4.42 km downstream, may have been more a function of the protruding nozzle face, creating added turbulence, rather than that of the mass injection. At the same downstream distance, the rolling moments experienced by the following Learjet model exceeded the full aileron deflection capabilities to maintain level flight.

Active devices dynamically interact with the vortex system. These devices attempt to alter the vortex by (a) emitting a jet or sheet of air at various stations along the span, or (b) oscillating the control surfaces which vary the spanwise loading with time. Passive devices involve static interaction with the vortices. Thus, they change the characteristics of the vortex by altering or controlling the flow over the wing. Both categories involve concepts of turbulence introduction, instability initiation and counter-sign circulation. Table II is a listing of devices by category.

TABLE II
Categorical Listing of Vortex Attenuating Devices

ACTIVE	PASSIVE
Blowing Jet Blown Flap Wingtip-Mounted Jet Wingtip Propeller Spoiler & Aileron Oscillation	Spline Cabled Drogue Cone or Chute Vortex Generator Spoiler Trailing-Edge Flap Porous Wingtip Wingtip Shaping Wingtip Extension

B. ACTIVE DEVICES

Apparently, the first proposal for vortex modification by mass injection was presented by Rinehart, et al. [Ref. 24]. The mass injection principle is intended to introduce turbulence into the flow field, accelerating the destruction of the vortex. Blowing jets, blown flaps and wingtip mounted jet engines exploit this idea.

A critique of the various methods investigated to attain these goals is difficult. Much of the experimental work has been done in wind tunnels and tow tanks or by actual flight evaluation. The Reynolds numbers, aircraft configuration (cruise, approach, landing, etc.) and airfoil data (shape, aspect ratio, camber, angle of attack, etc.) differ widely between various studies. The data presented in various reports are not in a form conducive to comparison. Additionally, the characteristics of the ambient turbulence are often unreported, making the duplication of the results at other facilities rather dubious.

Most of the research that will be referenced here has been sponsored by the National Aeronautics and Space Administration (NASA). NASA uses four different facilities: The 40x80 ft. wind tunnel at NASA Ames Research Center, the Langley Vortex Research Facility (a towing basin using air as the test medium), the Vertical/Short Takeoff and Landing (V/STOL) wind tunnel at Langley Research Center and the Hydronautics Ship Model Basin in Laurel, Md. (see Figures 5, 6). An effort has been made in their investigations to alleviate some of the problems cited above. Common models, standard measurement techniques, and consistent Reynolds numbers were used in these facilities. [Ref. 23]

There is no unique way to classify all the devices that have been tested. Though several logical means of classification do come to mind: (1) The nature of the device concerned with the overall effect on the aircraft or vortices (i.e., active or passive devices); (2) Model vs. prototype; (3) Subsonic vs. supersonic; (4) Civilian vs. military; and (5) Phase of flight or configuration (i.e. landing, cruise). Partly for reasons which will become clear later, it was decided to discuss these devices in two broad categories: Active devices and Passive devices.

III. EXPERIMENTAL EVALUATION OF THE VORTEX MINIMIZATION DEVICES

A. INTRODUCTION

In the United States, the primary impetus in the advancement of vortex alleviation methods has been the drive to reduce the separation distances between aircraft. This is of particular interest in terminal areas around busy airports, where these distances restrict their potential utilization due to delays in takeoff and landing. With this vortex hazard in mind, the Federal Aviation Administration (FAA) has set the following separation requirements.

TABLE I
Horizontal Separation Requirements

Generating Aircraft Following Aircraft	Heavy	Large	Small
Heavy	4 nm	3 nm	3 nm
Large	5 nm	3 nm	3 nm
Small	6 nm	4 nm	3 nm

nm - nautical mile

300,000 lbs.	}	Heavy	}	300,000 lbs.
12,500 lbs.	}	Large	}	12,500 lbs.
	}	Small	}	

The goal of continuing research is to reduce these separation distances without sacrificing safety. In conjunction, additional research has been targeted directly at improving the cruise capabilities of the aircraft.

motion of vortices and the importance that the various parameters play in establishing and dictating the flow field. If the vortex can be accurately modeled, then the possibility exists that the vortex may be controlled or annihilated. This may be accomplished through the use of instabilities introduced into the flow or features added to the wing tips which control the size, velocities and the motion of the vortex. The ultimate goal is to modify the vortex in a manner which will improve the characteristics of the body that generates them and also to dissipate or to minimize the destructive effects of the vortices as quickly as possible following their formation.

A new vortex model has recently been introduced by Staufenbiel [Ref. 22]. It is a modified form of the Lamb model where a reduced circulation $q \Gamma_\infty$ ($q < 1$), is assigned to the core region, and the remainder, i.e., $(1-q) \Gamma_\infty$, to the outer region. This model attempts to achieve better correlation with experimental data by mathematical means and seeks to conserve both the second moment of vorticity (vortical dispersion) and the rotational energy. This leads to much smaller core radii and to increased values of the maximum tangential velocity. Even though the resulting velocity profile contains an inflection point (leading to instabilities), Staufenbiel's model has clear advantages over those proposed previously. A comparison of the models cited reveals:

- a) Betz model: Does not conserve kinetic energy and exhibits no viscous core region (solid body rotation) where the velocity goes to zero at the center;
- b) Spreiter and Sacks model: Vortical dispersion is not satisfied by the Rankine vortex alone;
- c) Lamb model: It is for a laminar vortex. Furthermore, it does not satisfy vortical dispersion. Though it may be modified to include turbulence effects by changing the kinematic viscosity to an eddy viscosity, there is no real measure of turbulence within the vortex and the choice of v_T is somewhat arbitrary.

Progress in accurately modeling the structure of a turbulent vortex has been slow in developing, and is certainly attributable to the extreme complexity of the problem. Efforts continue in seeking improvements of older models through the use of additional conservation laws and better computational techniques in order to simulate the characteristics of real vortices. Hopefully, the modeling of the vortex structure can improve the understanding of the

during the latter stages of vortex growth and has been investigated by Batchelor [Ref. 16] assuming small axial velocity as compared with the free stream velocity. As for the viscous airfoil drag terms, Brown [Ref. 17] has made a theoretical study which indicates that in the rolled up region before the vortex has spread and been dissipated by turbulent diffusion, the combination of induced and profile drag can either create an axial velocity excess or defect dependent on their magnitudes. Experimental tests [Ref. 18,19] have exhibited both velocity excess and deficit yet no method has been devised which can accurately predict what profile exists.

The axial as well as the tangential velocity distributions at any section behind the wing shows a varied dependence on certain critical parameters of wing section, wingtip shape, Reynolds number, angle of attack (AOA) and the distance of the station downstream from the wing [Ref. 20 : p. 911]. With this number of parameters, the difficulty in coming up with a single model which can accurately describe the motion of the vortex is understandable. Moreover, the experimental results which are used to compare the theoretical models are obtained mostly by intrusive means, (Hot wire anemometer, vorticity meter, bubbles, etc.) possibly disturbing the flow. Clearly the laser velocimeter, with the added high-speed spatial scanning feature, may offer a solution to this problem [Ref. 21]. It can minimize the effects of "vortex meandering" which would normally result in inaccurate velocity distributions due to spatial movement of the vortex filament. Additionally, relating wind tunnel/tow tank data to full-scale aircraft is difficult due to differences in Reynolds number (based on wing chord) which may differ by one to two orders of magnitude. Furthermore, the scale and intensity of the free-stream turbulence is easily measured/controlled in the wind tunnel but not in actual flight tests.

term be replaced by an eddy viscosity ν_T , which is a function of the vortex Reynolds number Γ_∞/ν . As with the Lamb vortex, the circulation in the core region, where the tangential velocity reaches a maximum, should be 71.6% of the overall circulation, however experimental results indicate that only 37-60% actually exists in the core [Ref. 14].

Hoffmann and Joubert [Ref. 15] have approached the analysis of the turbulent trailing vortex in yet another manner. Their analysis is along lines similar to Prandtl's law of the wall used with turbulent boundary layers, and has modeled the circulation outside the core region and a small boundary layer buffer region by the logarithmic profile;

$$\Gamma/\Gamma_1 = 1/H \ln(r/r_1) + 1 \quad (\text{eqn 2.6})$$

where Γ_1 and r_1 are the core circulation and core radius and H is a constant. This also assumes that the flow in the core region is independent of the flow outside and is of a universal form where Γ/Γ_1 is a unique function of r_1 . These last two models for turbulent vortices still fail to accurately quantify the circulation and velocity profiles and require correlation with experimental results to obtain the necessary terms, such as the eddy viscosity ν_T and the universal constant H .

There also exists an axial velocity component associated with trailing vortex flow. This axial flow is associated with the rotational motion of the vortex itself and the profile/induced drag of the wing. A low pressure region is formed in the core by the centrifugal acceleration of the fluid, and as the vortex decays downstream, the tangential velocities decrease and the core pressure increases giving a positive axial pressure gradient. This, of course, occurs

Another method which has been used to model the tangential velocity profile of laminar line vortices has been the model of Lamb [Ref. 11]. His similarity solution has assumed a constant axial velocity, which is not truly the case, and has been applied to laminar trailing vortices by replacing the time variable with z/U_0 , where z is the axial distance and U_0 is the free stream velocity. This solution is written as

$$\eta = r / (\Gamma_\infty z / U_0)^{1/2} \quad (\text{eqn 2.4})$$

$$\Gamma / \Gamma_\infty = 1 - \exp(-\eta^2 / 4\nu / \Gamma_\infty) \quad (\text{eqn 2.5})$$

where the circulation Γ is a function of the similarity variable η and Γ_∞ is the total circulation of the vortex. The Γ_∞ term presents a problem when comparing results of different origins. Some authors have taken Γ_∞ to be the wing root circulation while experimental evidence presented by Dosanjh, et al. [Ref. 12] has shown that the circulation in each of the trailing vortices is only about 60% of that at the wing root. This is due to the interaction between vortices shed off the wing-fuselage interface. On actual models these vortices are generated opposite to the trailing vortex and act to decrease the circulation.

The Lamb model has recently been preferred to others because it exhibits rigid body rotation for small radii with tangential velocity increasing linearly with radius, peaking and then decaying exponentially to zero. It has been extended to turbulent trailing vortices based on work by Squire [Ref. 13] who suggested that the kinematic viscosity

A principal model that was used when the study of aircraft trailing vortices first came to the forefront was that of Spreiter and Sacks [Ref. 5]. The roll-up wake consists of two counter rotating Rankine vortices, with the circulation concentrated in the vortex core and distributed uniformly throughout. With the circulation Γ_0 and \bar{y} set by the equations (2.1) and (2.2) above, the additional unknown of the vortex core radius was determined by requiring the conservation of kinetic energy to account for induced drag. While their assumption seemed natural, experimental data indicated that this model was not sufficient, for it overestimated the core size and underestimated the maximum tangential velocity.

Then, in 1971, the model of Betz (1932) [Ref. 6] was resurrected by Donaldson [Ref. 7] showing greater agreement with flight test data. Betz proposed that in addition to those quantities in equations (2.1) and (2.2) the second moment of vorticity, shed by each wing semi-span, should be conserved, taking the form

$$I = -\int_0^{b/2} (y-\bar{y})^2 d\Gamma(y)/dy dy = \int_0^R r^2 d\Gamma(r)/dr dr \quad (\text{eqn 2.3})$$

Donaldson et al. [Ref. 8] and Rossow [Ref. 9] have offered modifications to the original form of the Betz model which will handle spanwise loading which differ significantly from the elliptical loading. These models fail on two counts. The tangential velocity at the center of the vortex core does not go through zero, thus not truly modeling the vortex core, but allowing the tangential velocity to decay slowly from the center. Also, as pointed out by Moore and Saffman [Ref. 10], the rolled up vortex does not conserve kinetic energy.

The first method attempts to take the steady roll-up of the three dimensional vortex sheet and break it down into a two dimensional sheet which is stepped through the roll-up process at small time increments. Westwater [Ref. 3] represented the vortex sheet by a finite number of vortex filaments and examined their motion by numerical analysis. However, this method fails to accurately reproduce the inner portion of the spiral at the tips (vortex core), not due to numerical inaccuracies, but to interaction between vortex filaments that are adjacent to one another on the sheet. Kaden [Ref. 4] used the similarity solution of Prandtl for unsteady roll-up of an infinite sheet to approximate a solution for the finite sheet, but again this fails because of the ever increasing arc length between adjacent point vortices in the vortex core.

The direct calculation of the roll-up process is based on the conservation of certain quantities, namely

I) Conservation of circulation

$$\Gamma_0 = -\int_0^{b/2} d\Gamma(y)/dy dy = \int_0^{b/2} d\Gamma(r)/dr dr \quad (\text{eqn 2.1})$$

II) The Centroid of vorticity

$$\Gamma_0 \bar{y} = \int_0^{b/2} y d\Gamma(y)/dy dy \quad (\text{eqn 2.2})$$

where $b/2$ is the wing semi-span, $d\Gamma/dy$ is the strength of the vortex sheet, Γ_0 is the circulation at the centerline of the wing and \bar{y} is the centroid of vorticity over the semi-span of the wing. The distribution of circulation $\Gamma(y)$ that is set by the wing loading determines the values of Γ_0 and \bar{y} .

spanwise loading of the airfoil. From Helmholtz theorems, that a vortex filament has a constant circulation and cannot end in a fluid, it follows that as the spanwise loading changes the bound vortex must change. This is accomplished by truncating the vortex filaments along the span in increments of Δy which correspond to increments of circulation $\Delta \Gamma$. These filaments run downstream of the lifting surface to infinity (or the starting vortex) and are the trailing vortices. By summing all these filaments an accurate profile of the spanwise loading distribution can be made. This method of modeling has been termed "horseshoe vortex" and is shown in Figure 2. [Ref. 2]

A tangential flow pattern is created by the culmination of these horseshoe vortices. In addition to the effect on following aircraft as indicated on Figure 3, the trailing vortices have a detrimental effect on the generating aircraft. The resultant induced velocity is in a downward direction, particularly in between the vortex pair, and is called downwash. As shown in Figure 4, the downwash velocity, in conjunction with the free stream velocity, acts to tilt the flow seen by the airfoil. Since effective lift acts normal to the effective flow direction, there is a force component which is opposite to the undisturbed flow direction. This drag force is termed induced drag and is common to all finite wingspans.

Various attempts have been made to model the structure of trailing vortices mainly concerned with the far-field structure after the roll-up process has been completed. This is normally within a few spanlengths behind the wing. These studies simplify the roll-up with the assumptions that the process is fast enough to be inviscid (viscosity and turbulence discounted), yet slow enough that it can be modeled as two dimensional. Two methods have been prevalent, a step by step calculation from the initial wake structure or calculations based on preservation of certain invariant quantities.

II. BRIEF REVIEW OF THE FUNDAMENTAL ASPECTS OF WINGTIP VORTICES

The spanwise loading across a two-dimensional airfoil (i.e. of infinite span) is uniform. The lift produced by the camber and/or the increased angle of attack, with respect to the flow direction, is created by the pressure difference between the upper and lower surfaces of the airfoil.

However, when the span is finite, as in practice, the differential pressure between the surface allows air to spill over the wingtips and consequently change the flow field. This equalization of pressure over the wingtips alters the spanwise loading of the airfoil, creating a modified pressure or lift distribution which goes to zero at the wingtips. There are added spanwise velocity components that direct the overall flow outward towards the tips on the lower surface and inward towards the root on the upper surface. When these components meet at the trailing edge of the span, the air rolls up into a number of small vortices. The vorticity shed by the airfoil rolls up into two counter-rotating vortices and its spanwise location is dictated by the spanwise loading. The vorticity is concentrated in areas where the wing loading changes dramatically, therefore they appear more or less near the wingtips (see Figure 1).
[Ref. 1]

The vortex system created by a lifting surface can best be described as a combination of three individual vortices. They are the bound vortex, the trailing vortex, and the starting vortex. The bound vortex is placed at the aerodynamic center of the wing, which is the quarter chord line for subsonic flight. This vortex has a circulation Γ whose strength varies along the span to match the change in

I. INTRODUCTION

Vortex motion has long been a subject of great interest to Hydro and Aero-dynamicists. Only in the last decade has it received renewed emphasis, based mainly on the persistence of trailing vortices created by jumbo jets. These vortices pose a hazard to following aircraft. Additionally, the elimination or the reduction of the intensity of these vortices has the advantages of reducing drag and increasing the aerodynamic efficiency of the wing.

The purpose of this review is to make a critical assessment of the efforts that have been made in the study of trailing vortices and their implication on the understanding and/or control of wingtip vortices. Two possible avenues exist in the alleviation of the wake vortex hazard. The first is their avoidance, where systems are installed at terminal areas to warn aircraft of possible hazards. The second approach, and the one pursued herein, is the modification of vortex patterns in an effort to minimize their effects on the following aircraft and to improve the aerodynamic characteristics of the generating aircraft.

First, a brief review of wingtip vortices is presented. This includes the vortex formation by the roll-up of the vortex sheet and the vortex structure. Then, an investigation of the analytical models which have been devised to describe the structure of the vortices is undertaken. Followed by, wingtip modifications that have thus far been used or proposed in an attempt to attenuate the wingtip vortices.

Investigation of the vortex attenuation attained by varying the thrust levels of the installed jet engines has also been conducted. Using the same model, Patterson and Brown [Ref. 28] found that maximum engine thrust could produce a 20% decrease in vortex-induced rolling moments (1.63 km downstream). They also found that engine positioning and reverse thrusting could reduce the rolling moment (see Figure 14), though at these distances, the probe aircraft still could not resist a sustained roll.

Yuan and Bloom [Ref. 29] demonstrated that a tube (.6 chordlength) extending from the trailing edge of a straight wing tip blowing a sheet of air downward (Figure 15) can significantly decrease the induced rolling moment (7.5 span-lengths downstream). Additionally, the jet momentum coefficient, ($C_{\mu} = .018$), improved the aircraft lift-to-drag ratio (L/D) at moderate angles of attack (Figure 16). The jet momentum coefficient is defined as,

$$C_{\mu} = \rho V_j^2 S_j / \frac{1}{2} \rho U_0^2 S \quad (\text{eqn 3.1})$$

in which, ρ is the medium density, V_j and U_0 are the jet and free stream velocities and S_j and S are the jet and wing areas. However, further investigation [Ref. 30 : pp. 225-226] found that for a transport aircraft model, the improvement of L/D was less pronounced in the cruise configuration. Also, the flapped configuration erased the effect of blowing altogether, and dramatically increased the induced rolling moment (Figures 17, 18).

Recent research conducted by Wu and Vakili [Ref. 31] at the University of Tennessee Space Institute has been directed towards specifically improving wing aerodynamic characteristics. Different configurations of blowing jets,

directed spanwise off the wingtip, have been explored. Three discrete jets, as shown in Figures 19 and 20, with varying angles off the span axis have been most effective in altering the pressure distribution over the wing. Tests were made in the wind tunnel on a NACA 0012-64 airfoil ($Re = 4 \times 10^5$) with C_{μ} varying from .001 to .01. The jet blowing alters the flow field, effectively increasing the wingspan. Flow visualization studies carried out in the water tunnel found that wingtip-jet blowing not only injected turbulence, but generated secondary vortices. All these secondary vortices drew some of their energy from the wingtip vortex and marked interaction was noted which could effectively alleviate the wake vortex hazard. More concentrated blowing in the forward jet produced greater vortex dispersion.

The upwardly-deflected blown flap, located near the wingtip (Figure 21), is another device which has reduced both tangential velocities and induced rolling moments [Ref. 27 : pp. 8,15,73]. Its effects are shown in Figure 22 and Table III. Again, this was for an extremely small momentum coefficient (4.94×10^{-4}) and was demonstrated only in a cruise configuration at 4.42 km downstream. Only one study on this type of device has been found, in spite of the fact that it yields half the rolling moment of the unattenuated case. More research should be conducted in this area.

The blowing concept has one obvious detractor. It requires bleed air from some source which is most logically the engine. This requires drawing power off the engine and an air transport system through the wing. Therefore, this method cannot easily be applied to existing aircraft due to the enormous propulsion/airframe modification requirements. This concept, if effective, must be incorporated into future aircraft design requirements.

Wingtip-mounted jet engines (Figure 23) have been explored [Ref. 30,32 : pp. 224-225, p. 746]. The data, for

TABLE III
Induced Rolling Moment Coefficients for Various Devices
[Ref. 27]

Generating Aircraft (Boeing 747)	Following Aircraft (Gates Learjet)	
Configuration	Induced Rolling Moment Coefficient, C_l	Induced Rolling Velocity, p degrees/second
Cruise-Basic	0.402	1042
Cruise-Vortex Generators (Device I)	0.103	268
Cruise Blown Flap (Device F)	0.202	530
Cruise Spline (Device H-1)	0.304	800
Flaps 30 - Basic	0.845	2200

Note: Maximum rolling-angular velocity corresponding to full aileron deflection on Gates Learjet is 120 degrees per second at an aircraft speed of 120 knots. This corresponds to a rolling moment coefficient $C_l = 0.0463$.

a momentum coefficient of .02, gives results similar to the rearward blowing jet. It decreases the induced drag but is still ineffective in reducing the vortex hazard. Wingtip props are currently being explored by Loth [Ref. 33]. The propeller rotation, opposite to the vortex roll-up, would counter the tip vortex circulation. The wingtip prop produces a flow field where upwash is created inboard of the wingtip, rather than the customary downwash. This upwash can even result in additional thrust. The overall effectiveness is dependent not only on the propeller's diameter, but also on the amount of vorticity it can produce. Wingtip mounted jet engines and propellers have drawbacks, also. The increase in wing weight due to structural considerations may be prohibitive. Furthermore, consideration must be given to the effects of asymmetric thrust in the event of a single engine failure.

Control surface oscillation has produced interesting results with respect to vortex attenuation. Actual flight test investigation [Ref. 34] has examined transport aircraft. Initial results with a B-747 indicated that past 3 nautical miles (NM) the use of specific aileron/spoiler configuration produced wakes with no rotary motion (Figure 24). This was at a set frequency of 6 sec/cycle and required complex manipulation of the control surfaces by the pilot. Subsequent tests on the L-1011 could not reproduce the favorable results of the B-747. Attempts to recreate the 747 maneuvers required inputs from both the pilot and co-pilot. The attenuation levels were attained by landing-configured aircraft with landing gear extended. However, the oscillation surfaces produced generating aircraft rolling motion that would be unacceptable for final approach.

C. PASSIVE DEVICES

Numerous studies have involved the use of splines as an attenuation device. The earliest study by Uzel and Marchman [Ref. 35] used various crossed blades (Figure 25, 25a) at the wingtips. They showed their capability of reducing both the maximum tangential velocity and increasing core size. Kirkman, et al. [Ref. 27 : pp. 16-18, 101] with towing tank results for a 3/100 scale model B-747 showed similar effects with his spline (Figure 26). But, at 4.42 km downstream, the rolling moment was still outside the controllable aileron limits of the Learjet. Additionally, the drag increase due to those devices was between 70-280% in cruise configuration. Croca [Ref. 36, 37 : pp. 4-7, 6-10] showed that the spline was much less effective in reducing the rolling moment when the aircraft was in the flapped condition ($Re=5.74 \times 10^5$, $C_L = 1.25$). The effectiveness was

dependent on the flap settings in conjunction with the location of the spline along the span. Flap settings drastically changed the vorticity pattern off the span, so that a spline located near the wingtip might be fine for cruise, but little help at lower speeds when flaps are extended. Actual flight testing by Hastings, et al. [Ref. 38] has also demonstrated the effectiveness of wingtip-mounted splines in reducing rolling moments. The spline diameter was 55% of the chordlength and mounted 50% of the chordlength aft the wing trailing edge. Aileron control could only be maintained beyond 2.5 NM downstream of the unattenuated vortex while the spline reduced this distance to .62 NM. These results were obtained with a Douglas C-54 as the generating aircraft and a Piper Cherokee as the probe aircraft. The spline appears quite effective, and its construction allows it to be deployed for takeoff and landing just as the spokes on an umbrella (Figures 27, 28). Placement of the spline is critical and multiple splines may be necessary on heavily flapped aircraft.

The cabled drogue cone and cabled chute, shown in Figure 29, have been mentioned just in passing. The drogue cone [Ref. 27 : p. 17] was towed approximately 1.5 spanlengths behind the model with little change in the velocity field farther downstream. It appears that this technique was unacceptable based on the difficulties in intercepting the vortex. Patterson [Ref. 32 : pp. 745-746], examining the cabled chute, found velocity profiles similar to those of the spline. Yet, the tremendous increase in drag produced by the chute made its use impractical.

The use of vortex generators or wingfins has been examined in a tow tank, but more extensively in a wind tunnel. Kirkman, et al. [Ref. 27 : p. 19], again using the .03 scale model B-747, mounted 18 wingfins along the 75% chordline of each semispan (Figure 30). These wingfins were

angled 20 degrees to the freestream to produce vortices that rotated opposite those originating from the wingtips. While in a clean configuration ($C_L = 0.4$), the wingfins were extremely effective at reducing the downwash (4.42 km downstream). However, they demonstrated little effect in the flapped configuration ($C_L = 1.2$, 2.25 km downstream). Also, there was a four fold reduction in the induced rolling moment on a following aircraft, over the basic aircraft, with the use of vortex generators. Croom [Ref. 39] ran tests of semicircular fins, placing one to two on the upper surface of each semi-span, at various spanwise locations and incidence angles (Figure 31). These tests were made at a Reynolds number of 4.7×10^5 on a 3/100 scale model of the B-747 with gear and flaps down. Reductions of 50-60% in the induced rolling moments were obtained at .25 NM downstream of the generating aircraft as shown in Figure 32. Various wingfin configurations, varying fin shape, aspect ratio, and incidence angles were investigated by Iversen and Moghadam [Ref. 40]. The optimization was done maximizing the vortex strength terms of angular velocity and rolling moment for individual fins. This study did not explore the interaction between the shed wingtip vortices and wingfin vortices. However, based on their findings, low aspect ratio parabolic fins (Figures 33-35) produced sufficient vortices for successful use in wake vortex alleviation. Furthermore, these wingfins increase the drag and add a positive nose pitch-up moment.

The use of spoilers, as spanwise load altering devices, has received a lot of attention. The first experimental investigations were made with a small rectangular plate, mounted perpendicular to the flow direction, on the upper surface of the wing close to the wingtip (Figure 36) [Ref. 27,41 : p. 20, pp. 229-241]. These studies, both wind tunnel and flight testing, showed decreased maximum

tangential velocities and increased core size under cruise conditions. But, again when the aircraft transitioned to a flapped condition, the advantage was lost. Croom [Ref. 36 : p. 7] investigated an unswept wing with an aspect ratio of eight in both the flapped and cruise conditions. He found reductions in the rolling moment of approximately 25% at all downstream distances using a midspan spoiler (Figures 37, 38). Further studies were made by the same author [Ref. 42, 43] with the 3/100 scale model B-747 in the Langley V/STOL wind tunnel at a Reynolds number of 4.7×10^5 . The model was set in a landing configuration (inner and outer flaps deflected 30 degrees) with gear both up and down. Four spoilers were outfitted on each wing just as on existing aircraft, as shown in Figures 39-40. Various combinations of spoilers and deflection angles produced results with optimum reductions of 50-70% in the maximum rolling moments at .25 NM downstream (see Figure 41). With a 47/1000 scale model of the DC-10 (Figures 42, 43), similar results were obtained (35-60% reduction) at downstream distances between 0.25-0.5 NM (Figure 44) [Ref. 44]. Flight tests have verified that the decreased separation distances can be obtained for the spoiler-attenuated vortex with control power adequate to handle vortex induced roll [Ref. 45]. Pilots also indicated that the spoiler deflections did not adversely effect the B-747's landing performance.

Changes in trailing edge flap settings have shown a tremendous effect on the characteristics of the vortex roll-up. This research has focused on the B-747 aircraft (see Figure 45). Two sets of flaps are located on the inboard portion of the wings. Normally, in landing configuration, they are both set at 30 degrees deflection, but they can be varied. With landing gear up, (30 degrees deflection inboard, 1 degree deflection outboard) at a $C_L = 1.2$, penetration with the T-37 could be made down to 1.8 NM

separation, but when the gear was extended, the distance was diminished to 4.5 NM. Interestingly, but of no real use, vortex augmentation was obtained with a 5 degree-30 degree flap setting [Ref. 37,47 : pp. 8-10, 2-33]. The trailing edge flap which alters the spanwise loading of the wing has shown some promise and NASA has extended their basic research with the use of the variable twist wing [Ref. 48].

Smith [Ref. 49] has examined the use of porous sections at the wingtips, as shown in Figure 46, to equalize the pressure difference between the upper and lower surfaces. Experiments conducted on a full-scale aircraft (O-1A) resulted in a 60% reduction in tangential velocities at approximately one chordlength downstream and 10% reduction several thousand feet downstream (see Figures 47, 48). This was for a 10% porous tip. Additionally, the porous tip creates an inflection in the circulation distribution and two distinct vortices were formed off each semispan (Figure 49). Although the reduction in tangential velocity is favorable, the study did not investigate the rolling moment coefficient.

Wingtip edge shaping has shown a marked effect on the rolled-up structure of the trailing vortices. Thompson [Ref. 20 : pp. 910-911] examined the axial velocities produced at varying angles of attack by three alternate tip shapes: square, semi-circular and sharp edged (see Figure 50). The NACA 6412 and NACA 0012 sections were tested in the tow tank at Reynolds numbers of 3.4×10^6 and 6.8×10^6 . His results indicate a centerline velocity excess, for all tip edge shapes, immediately downstream of the wing. However, this reverts to a centerline velocity deficit within 1.5 to 5.5 chordlengths and increasing the angle of attack accelerates this transition for all cases (Figure 51). Faery and Marchman [Ref. 50 : pp. 208-211] extended the research on these same shapes to include tangential

velocity profiles (NACA 0012, $Re = 3.7 \times 10^5$). While the centerline axial velocity deficit was noted in the rolled-up region for all tip shapes, only the sharp edged tip exhibited no velocity excess outside the core as shown in Figure 52. Additionally, this pointed tip showed decreased maximum tangential velocities along with decreased core size over the square and rounded tips (see Figure 53). This result seems to contradict those observed previously where decreased maximum tangential velocities were associated with increased core size. However, the vortex created by the pointed tip was found to have an increased circulation. The authors suggest that the absence of an axial velocity excess may be one feature that produces this reduction in tangential velocity. El-Ramly and Rainbird [Ref. 51 : pp. 196,201], investigating various wingtip shapes at $Re = 5 \times 10^6$, found little success in reducing the maximum induced rolling moments for short downstream distances.

Wingtip extension devices, although showing limited vortex hazard reduction capabilities, have been extensively researched. It was recognized for many years that non-planar lifting surfaces should have less drag than conventional planar wings. As early as 1897, Lanchester obtained a patent for vertical surfaces at the wingtips. In 1955, Clements [Ref. 52] investigated the use of canted end plates (NACA 0012 Airfoil) with 30% chord flaps as a drag controlling device. The optimum decrease in drag was obtained ($Re = 3.5 \times 10^5$) with an outward endplate cant of 5 degrees and a 15 degree flap deflection in the same direction. The emphasis was on reducing the drag. Therefore, the data on the downstream vortex structure was limited to tuft grid photography at two chordlengths downstream. Patterson [Ref. 32 : p. 745], using stationary airflow visualization techniques (smoke screen), also found that the use of endplates and wingtip extensions (Figure 54) had a marked

effect on the near-field vortex resulting in a reduction in induced drag. However, he additionally noted that these devices were of little use as vortex attenuator since only a small effect in the far-field flow was observed. El-Ramly and Rainbird's [Ref. 51 : p. 201] results are only for short distances downstream (2.5 span lengths), but support the belief that the endplate modification is ineffective in reducing the maximum induced rolling moment.

The Whitcomb winglet, which has resulted in improvements in lift-to-drag ratios, has altered the roll-up of wingtip vortices. The design, shown in Figures 55 and 56, incorporates a larger primary winglet rearward on the upper surface and a smaller winglet mounted forward on the lower surface. Whitcomb [Ref. 53] tested the design at a Mach number of .78 and a Reynolds number of 6.9×10^6 . Figure 57 indicates the improvement in lift for a constant drag coefficient. In a follow-on study [Ref. 54], the same transonic pressure tunnel was used at Mach numbers of 0.7, 0.8 and 0.83 and a constant Reynolds number of 5.8×10^6 . The results give the same significant reductions in induced drag, but indicate that "the winglet spreads the vorticity behind the tip to such an extent that a discrete vortex core is not apparent." This was not found to be the case in a study conducted by Faery and Marchman [Ref. 50 : p. 215]. Using the same winglet geometry on a NACA 0012 airfoil of eight inch chord, two distinct vortices were created which persisted for the twenty chord lengths downstream. The difference may lie in the fact that the Reynolds number for these tests were much lower (3.7×10^5) and the Mach number never exceeded 0.1. Figures 58 and 58a show their results. At twenty chord-lengths downstream, the maximum tangential velocity in each of the two vortices, shed off from the semi-span, was about 64% less than that of the rounded tip, even though there was increased circulation. The velocity defect that the winglet

produces, shown in Figures 59 and 59a, as with the sharp-edged tip, may be a factor in reducing the tangential velocities within the vortex. The spanwise pressure distribution obtained by Faery and Marchman (see Figure 60) is not consistent with their finding of two distinct vortices off the wingtip. Rather, Whitcomb's spanwise distribution (Figure 61), which indicates an inflection point near the tip, would produce two distinct vortices.

Continuing research into the reduction of induced drag, with the use of wingtip sails, is being conducted at the Cranfield Institute of Technology. Spillman [Ref. 55], in 1978, observed that the effective flow direction near the tip varied drastically from the free stream. He surmised that a smaller auxiliary surface mounted on the wingtip might exploit this change in flow direction to obtain thrust in the direction of motion (Figure 62). To reduce the spiralling flow around the tip, Spillman decided to employ a cascade of sails set such that the flow off the preceding sails would not interfere with those that followed. These sails have camber and twist, which varied from root to tip, to efficiently turn the flow back towards the free stream direction. Wind tunnel and flight tests on the Paris Aircraft (Figure 63) with one or three sails (see Figure 64), have produced reductions in drag due to lift of 10 to 29% respectively. Comparison of the data is shown in Figure 65. The flight and wind tunnel tests vary by over an order of magnitude in Reynolds number which explains the difference in zero lift drag. High Reynolds numbers produced less separation and therefore decreased the drag and increased the efficiency of the wing. Experiments were conducted by varying the number of sails, the spiral angle of successive sails, and the sail span. Increasing the number of sails beyond four or increasing the sail span beyond three-tenths of the wingtip chord indicated a diminishing reduction in

induced drag. Spiral angles of 15 to 20 degrees between successive sails produced the best results.

A follow-on study [Ref. 56] showed that the Paris aircraft fitted with three sails had reduced the total drag and improved the fuel economy above a lift coefficient of 0.22. Spillman and McVitie [Ref. 57] reported another study in 1984 that reaffirmed the previous works. Overall drag with the three sail configuration was reduced above a lift coefficient of approximately 0.25. Again, improved fuel economy was noted with the Cessna Centurion fitted with sails over a speed range from 120-160 knots. The strength of the mounting techniques for the sails have limited the airspeeds at which testing has been accomplished. Although the author mentions the possibility of reduced trailing vortex strength, no measurements were conducted to substantiate it.

Interested purely in improving the aerodynamic characteristics of the aircraft, Gall and Smith [Ref. 58] have researched the use of winglets applied to biplanes. This winglet has been structured as an airfoil spanning the tips of the two wings, as shown in Figure 66 .

TABLE IV
Biplane Winglet Addition Efficiency Factors
[Ref. 58]

	Theory		Experimental	
	e winglet	e no winglet	e winglet	e no winglet
Monoplane	-	.975	-	-
Biplane I Ga = 1.0 St = 1.0 Dec = 0°	1.091	.974	.991	.870
Biplane II Ga = 1.0 St = 1.0 Dec = -5°	1.166	1.083	.981	.831

The theoretical and experimental (wind tunnel, $Re=5.1 \times 10^5$) results, shown in Table IV, approximate the improved wing

efficiency factor at between 8 and 13% depending on the incidence angle between the two biplane wings. One interesting note, made in an additional parametric study, was that the effectiveness of the winglet was relatively unaffected until less than 30% of the original chord remained forward of the trailing edge.

IV. SUMMARY

In the previous chapter, all the known active and passive devices that have been investigated in an effort to minimize trailing vortex effects, were discussed. Their performance and claimed advantages were examined in as much detail as possible. It has been discovered that most of the existing devices have not been extensively investigated under all possible aircraft configurations and velocities to allow immediate application. It has also been found that some of these devices are quite promising and with further research may be developed into effective vortex minimization techniques. Recognizing the need for vortex hazard alleviation and the consequences if the present trend towards heavier aircraft is continued, one must address two important questions:

- (1) What can be done with the existing devices?
- (2) On what types of devices should additional research be carried out for future use?

To facilitate the response to these questions, one needs a comparison of the advantages and disadvantages of the existing devices in a compact form, as shown in Tables 5 and 6.

In assessing the information summarized in these Tables, some consideration must be given to the following factors:

- (1) Does the addition of the device adversely affect the aerodynamic characteristics of the aircraft? (e.g. lift and drag forces, weight, takeoff and landing distances and the stability, maneuverability and ride quality of the aircraft, etc.);
- (2) Can the device be incorporated into existing aircraft?;

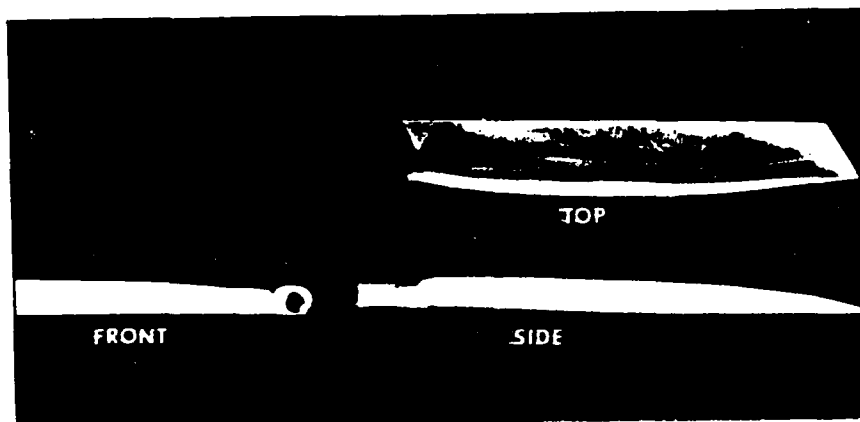
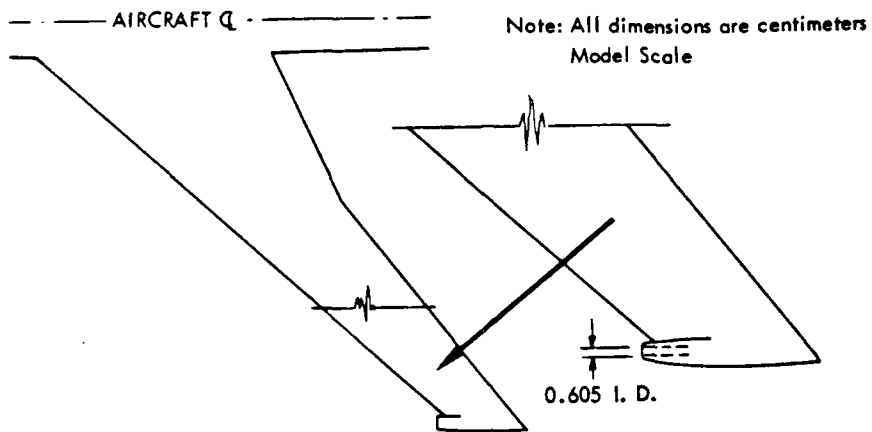


Figure 9 Sketch and Close-Up Views of a Forward Blowing Jet [Ref. 27].

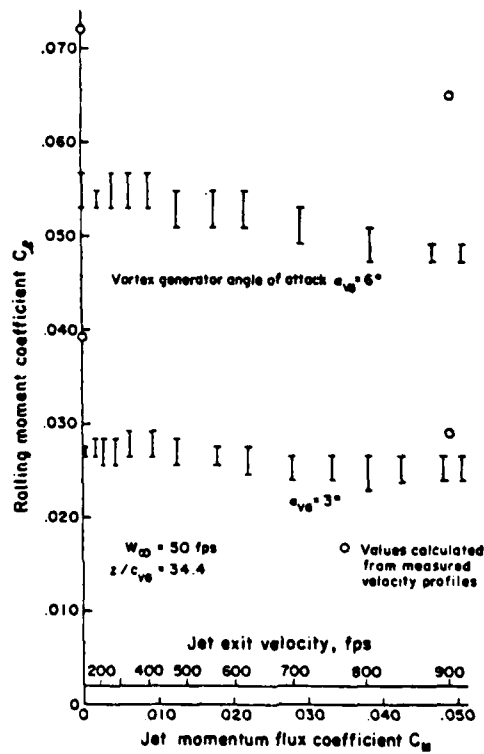


Figure 8 Effects of Central Jet on the Rolling Moment Coefficient [Ref. 25].

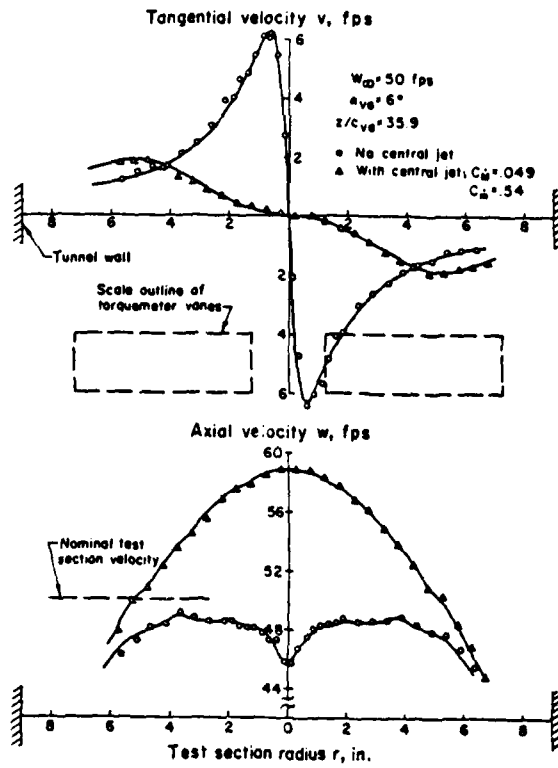


Figure 7 Effects of Central Jet on the Measured Tangential and Axial Mean Velocity Profiles [Ref. 25].

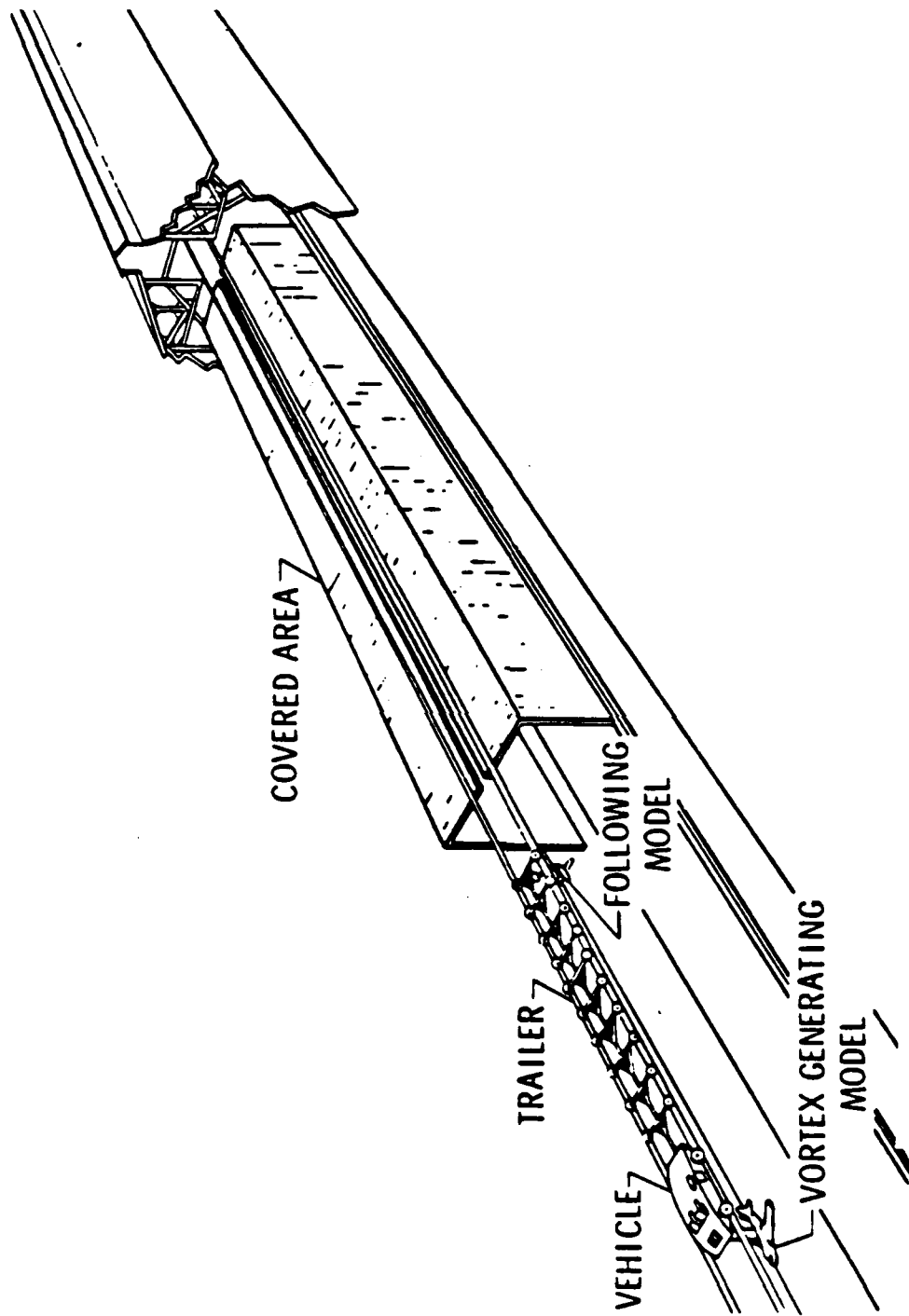
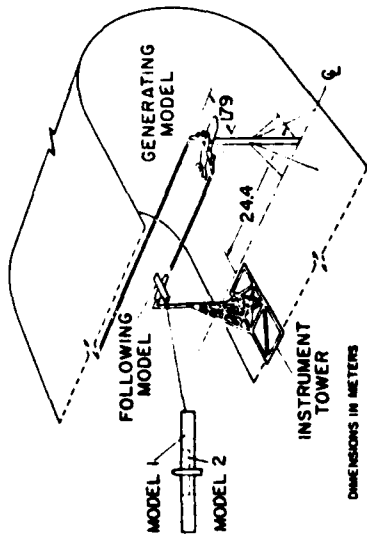
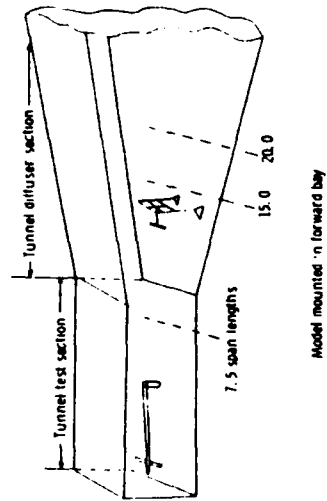


Figure 6 Arrangement of the Langley Vortex Research Facility [Ref. 28].

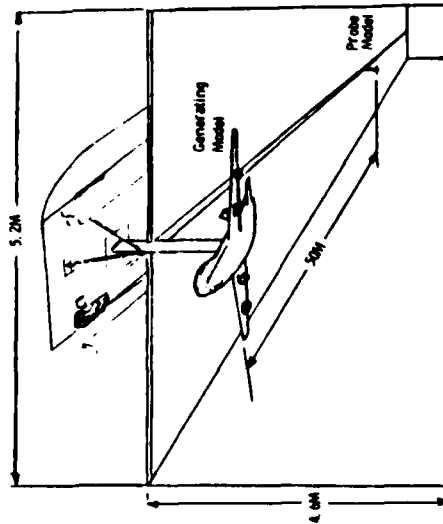
40 BY 80 FOOT WIND TUNNEL



VISTOL TUNNEL



VORTEX FLOW FACILITY



HYDRONAUTICS SHIP MODEL BASIN

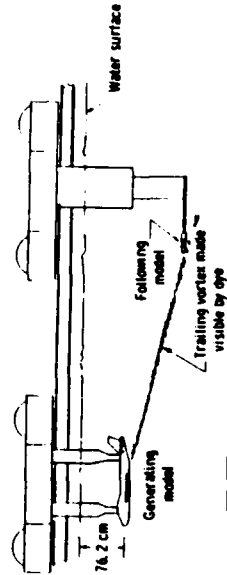


Figure 5 Test Arrangement in NASA Facilities [Ref. 23].

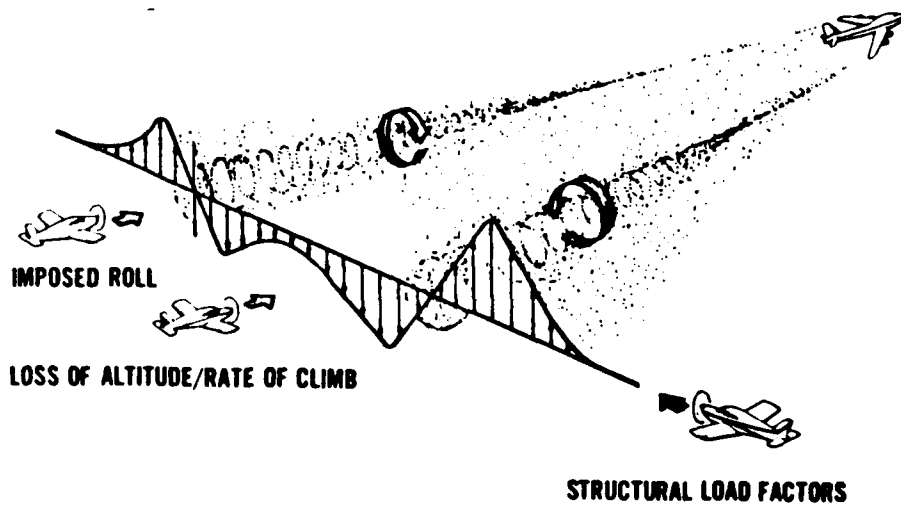


Figure 3 Trailing Vortex Hazard Potentials [Ref. 1].

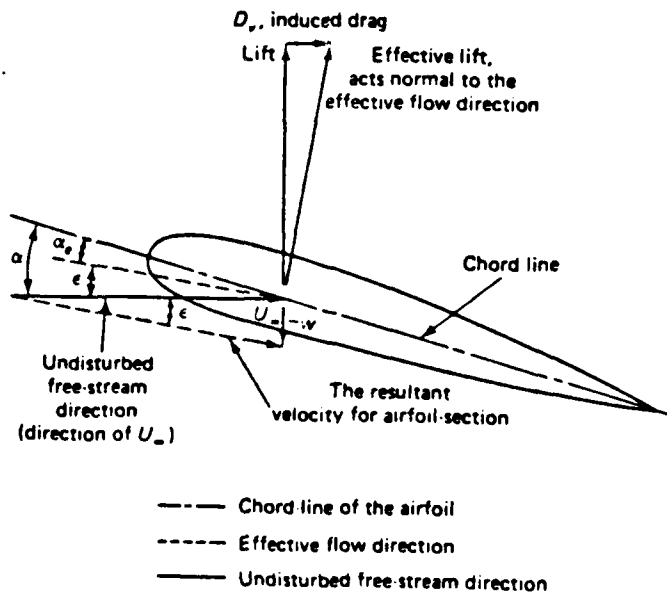


Figure 4 Sketch of the Induced Flow [Ref. 2].

**APPENDIX A
FIGURES**

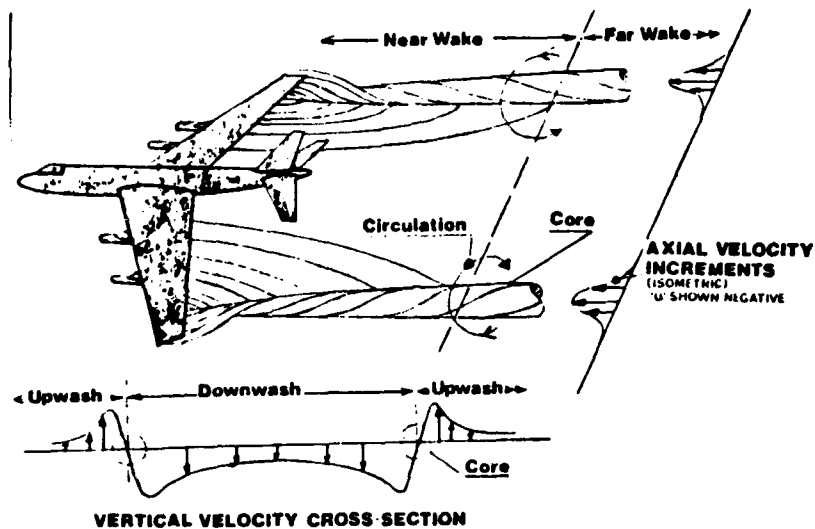


Figure 1 Formation of Wake Vortex Showing Induced Velocities [Ref. 1].

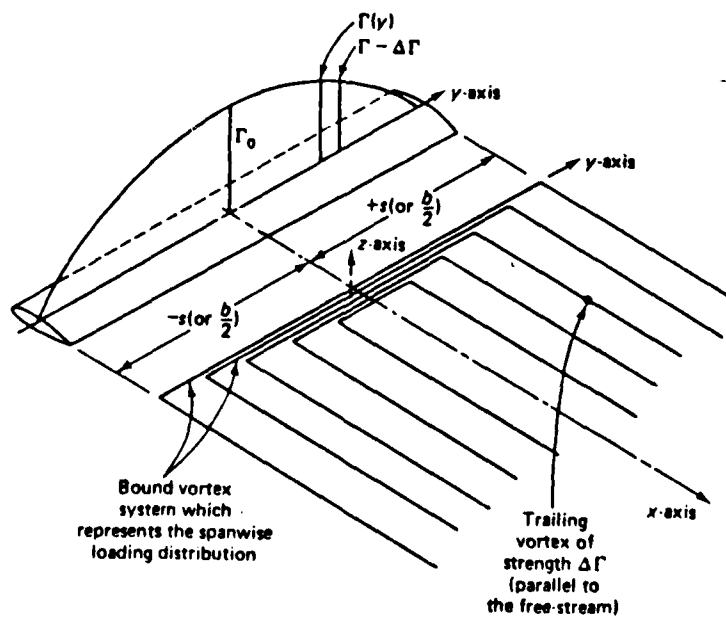


Figure 2 Sketch of Trailing Vortex System [Ref. 2].

V. CONCLUSIONS

A survey and critical assessment of the known active and passive devices for wake vortex minimization warranted the following conclusions:

- (1) None of the devices has been sufficiently investigated under laboratory and environmental conditions for immediate use on new or existing aircraft;
- (2) Among the devices which do not require energy input from the aircraft, the wingtip sails and winglets have certain advantages. However, there is no information regarding their effectiveness on the demise of the vortices far downstream;
- (3) Among the devices which do require energy input by the aircraft, discrete wingtip jets appear to be most effective;
- (4) All the devices examined in this investigation require extensive research if their full potential on various aircraft is to be realized. Such research should clearly identify the effectiveness of each device on the near wake as well as the far wake several miles downstream of the aircraft;
- (5) It appears that there is room for the development of new concepts, means and/or devices, in addition to those considered herein, which will lead to an overall effective solution of the most important problem of modern aviation.

The introduction of a pulsating jet or nozzle which would provide step input changes to the circulation of the wingtip vortex might very well lead to the early destruction of the trailing vortex system. Also, a method might be devised for slicing the wingtip vortex, with jets normal to the vortex.

possible that further downstream these vortices could coalesce into a single vortex recreating the vortex hazard to the following aircraft. Only with continued research can one answer the question of whether these devices dissipate or reinforce the trailing vortex.

The employment of passive devices seems a much simpler approach. However, the benefits of active devices, such as the wingtip jets, cannot be ignored. The ability to vary flow rates and directions to changing flight conditions, the lack of additional wing stresses at moderate blowing angles off the spanwise axis, the lack of ground clearance problems, and the ON-OFF capability make the wingtip jets attractive for use on civilian as well as military aircraft provided that the bleed air requirements do not degrade the engine performance significantly.

The use of wingtip jets would entail considerable aircraft modification. This would rule out a retrofit capability. The details of a bleed air piping system ducted through the wings, engine tapping for high pressure air, and control/monitoring devices for air flow and jet orifice positioning are enormous. One must also consider that passive devices, like the winglet and wingtip sail, cannot simply be fabricated and attached to the wingtips. These devices, to be structurally sound when operated over a wide variety of airspeeds and maneuver forces, must be an integral part of the wing itself. This would require completely new wings on anything other than possibly light aircraft.

While further research on the above devices is recommended, there are certainly other possible avenues which could be explored. All proposed devices have tried to destroy the vortex core by imposing adverse pressure gradients on the flow, in hopes that this will lead to vortex breakdown. Another concept, which may prove to be fruitful, is the attempt to vary the vortex strength periodically.

- 2.
- (3) Is the device going to create additional wing stress problems? (e.g. gust loading or other unsteady flow effects, higher wing root moments, wing fatigue (high frequency vibration), structural limits on the device and its attachment points, etc.);
 - (4) What are the effects on ground and terminal area operations? (Ground clearance for the device, mobility around the device (fueling, taxiing, loading, etc.), and the noise characteristics);
 - (5) Will the device still produce favorable results under varying conditions of flight? (cruise, flaps extended for takeoff/landing, gear extended or retracted);
 - (6) Can the loss of the device on a single wingtip be handled without producing catastrophic results?;
 - (7) What are the effects of the device on the trailing vortices further downstream?; and
 - (8) Is the device applicable to the military as well as civilian aircraft?

With these factors in mind, it appears that only three of the existing devices hold any promise. They are the discrete wingtip jets, the Whitcomb winglet, and the wingtip sails. While these devices have shown improvements in the aircraft lift-to-drag ratio, all the research has been limited to near-field effects alone. Therefore, no tangible evidence exists that these devices really do reduce the wake vortex hazard further downstream. However, based solely on the data reported, the existence of secondary vortices and the possible dissipation that their interaction can create, it is conjectured that these devices can achieve some degree of vortex attenuation. Both the wingtip jets and the Whitcomb winglet produced multiple vortices at short distances downstream. The wingtip sails are also expected to produce multiple vortices even though there is not yet any experimental data to confirm it. It is of course

Table VI
 Recapitulation of the Advantages and Disadvantages of Passive Devices (cont'd.)

Device	Figs.	Advantages	Disadvantages	Refs.
(9) Trailing Edge Flaps	39, 42, 45	a) changes spanwise loading drastically. b) has some present-day surface uses. c) decreases separation distances. d) cambers wing-- increasing lift Coeff.	a) increases drag.	37, 47, 48
(10) Porous Wingtip	46	a) produces near-field reductions in tangential velocity. b) has an inflection in spanwise loading (two vortices off wingtip).	a) losses some lifting surface (dependent on porosity). b) has far-field effectiveness which is less pronounced.	49
(11) Wingtip-Edge Shaping	50	a) decreases maximum tangential velocity. b) affects axial velocity profile.	a) has little effect on the induced rolling moment.	50, 51
(12) Wingtip Extensions (winglets, sails)	54, 56, 63	a) has lift-to-drag ratio improvements. b) Whitcomb--has two distinct vortices. c) sail--provides a force in direction of motion. d) improves fuel economy.	a) no data available on following aircraft performance.	32, 50, 52, 53, 54, 55, 56, 57, 58

TABLE VI
Recapitulation of the Advantages and Disadvantages of Passive Devices

Device	Figs.	Advantages	Disadvantages	Refs.
(5) Spline	25, 26, 25a,	a) can be extended and retracted from pod. b) has produced mixed to favorable results for induced rolling moments.	a) Placement is critical. b) greatly increases drag (increased engine noise, decreased fuel econ.) c) decreased climb performance.	32, 35, 36, 37, 38, 45
(6) Cabled Drogue Ccne or Chute	29	a) increases turbulence.	a) has difficulty in intercepting the vortex core. b) chute--one time shot/ high drag. c) cone--deployable /will be damaged on landing rollout	27, 32
(7) Vortex Generators	30	a) greatly reduces induced rolling moments.	a) slightly decreases the lift coeff. with nominal drag rise. b) are permanently set surfaces.	27, 39, 40
(8) Spoiler	39, 43	a) surfaces already exist on aircraft. b) greatly decreases induced rolling moments. c) is effective in every flight config.	a) increases drag. b) increases engine noise in terminal areas.	36, 37, 41, 42, 43, 44, 46

TABLE V
Recapitulation of the Advantages and Disadvantages of Active Devices

Device	Figs.	Advantages	Disadvantages	Refs.
(1) Blowing Jet	9, 10, 11, 12, 15, 19	a) increases turbulence. b) creates secondary vortices. c) improves the lift-to drag ratio. d) flow rates can be varied to flight conditions.	a) requires bleed air and piping system to the wingtip. b) cannot be applied easily to existing fleet.	24, 25, 26, 27, 28, 29, 30, 31
(2) Blown Flap	21	a) reduces rolling moments. b) can be extended or retracted as necessary.	same as above.	27
(3) Wingtip Propeller/Jet Engine	23	a) decreases induced drag. b) possibly creates force in flight direction. c) adds turbulence to the vortex core.	a) increases wing weight (long moment arm). b) produces asymmetric thrust given single engine failure.	28, 31, 33
(4) Control Surface Oscillation	39, 42, 45	a) uses existing aircraft surfaces. b) significantly decreases wake.	a) are frequency dependent. b) increases pilot/co-pilot workload during takeoff/land. c) degrades a/c ride quality.	34

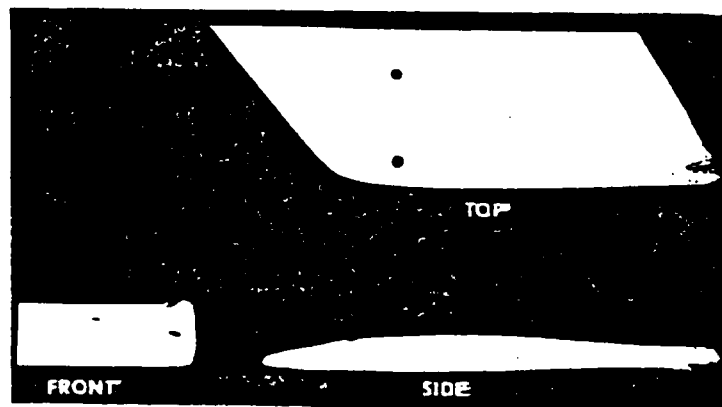
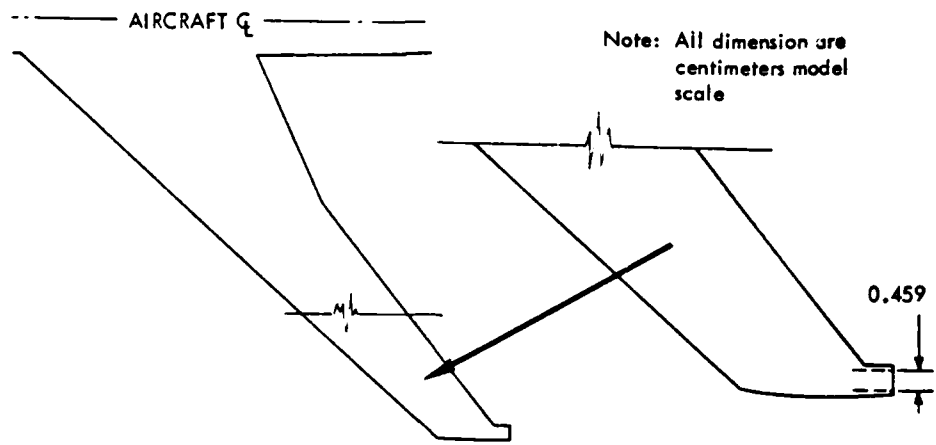


Figure 10 Sketch and Close-Up Views of a Rearward Blowing Jet [Ref. 27].

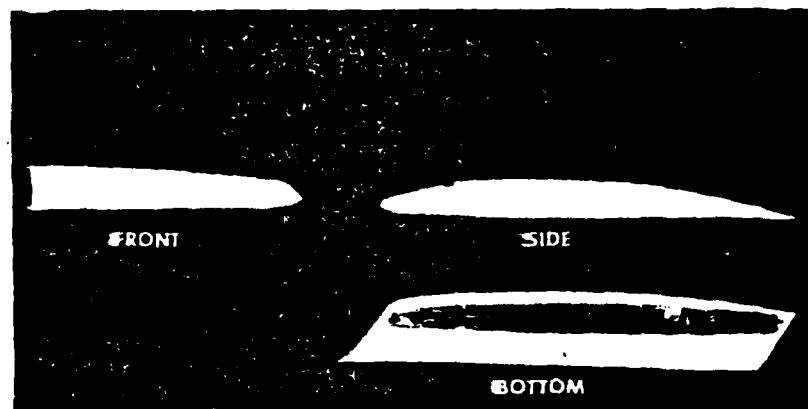
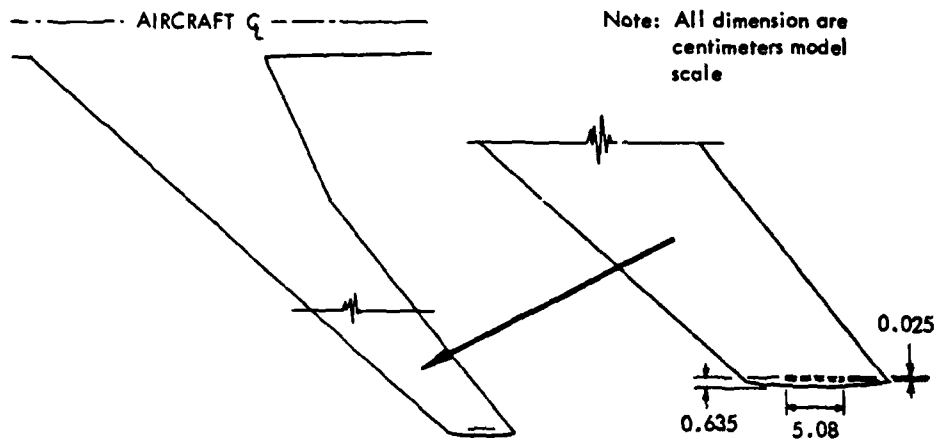


Figure 11 Sketch and Close-Up Views of a Downward Blowing Jet [Ref. 27].

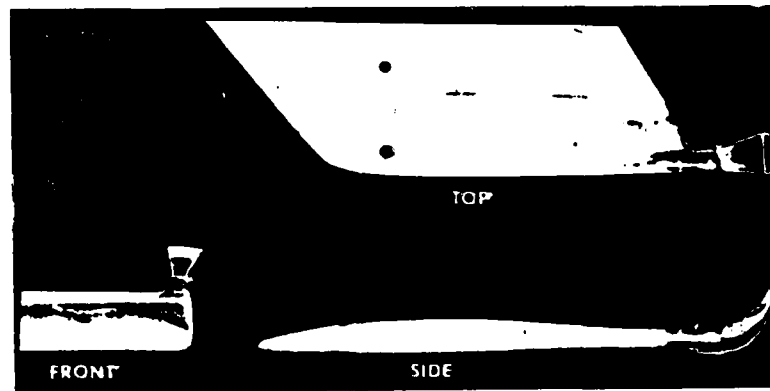
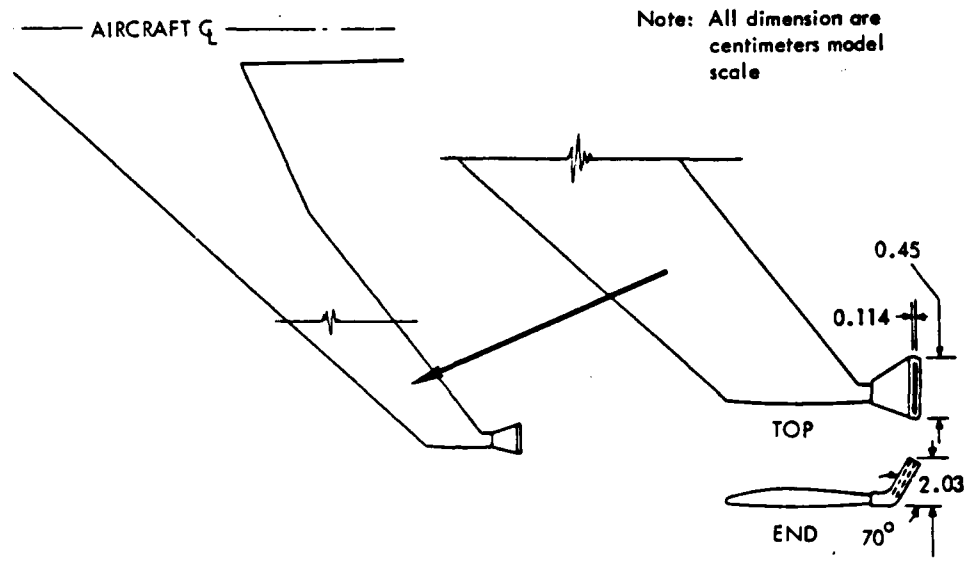


Figure 12 Sketch and Close-Up Views of a Deflected Jet [Ref. 27].



Figure 13 Basic Model of a Boeing 747 Aircraft [Ref. 27].

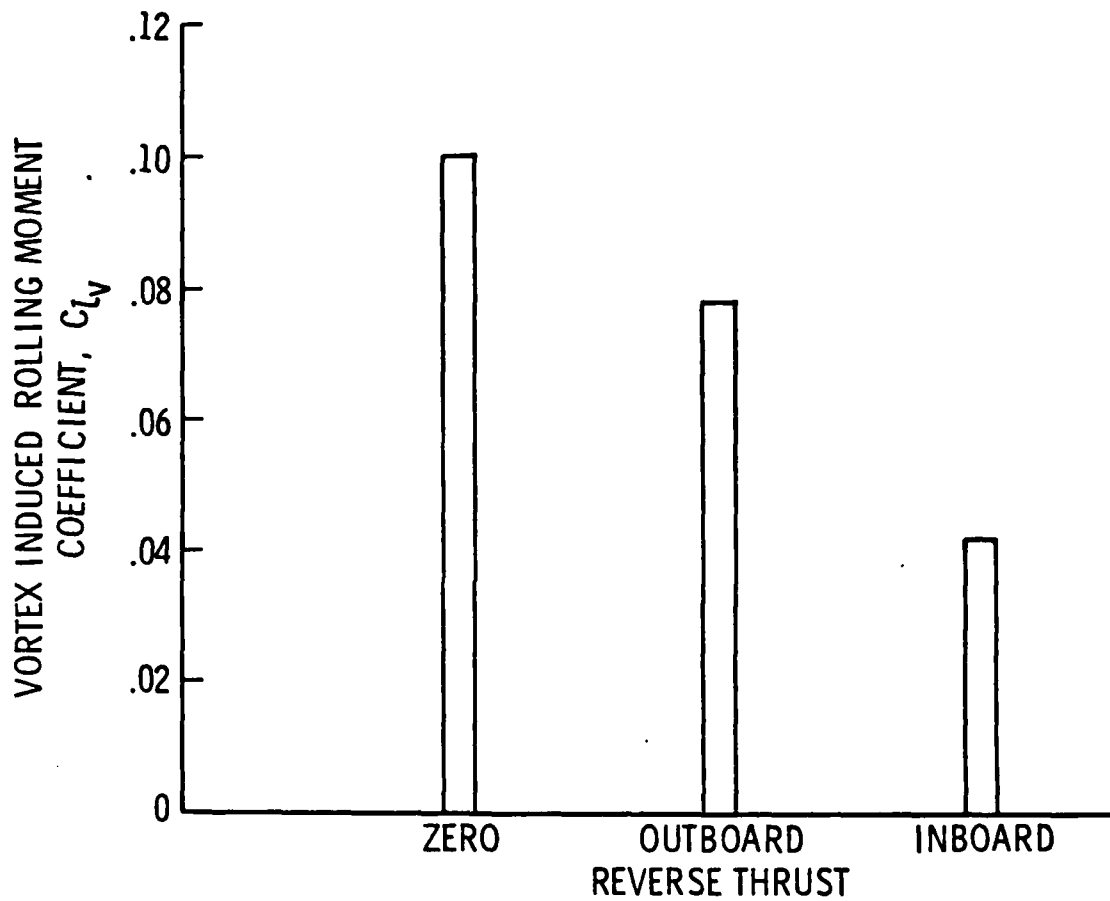


Figure 14 Effect of Engine Reverse Thrust on the Vortex Induced Rolling Moment Coefficient on a Learjet Probe Model [Ref. 28].

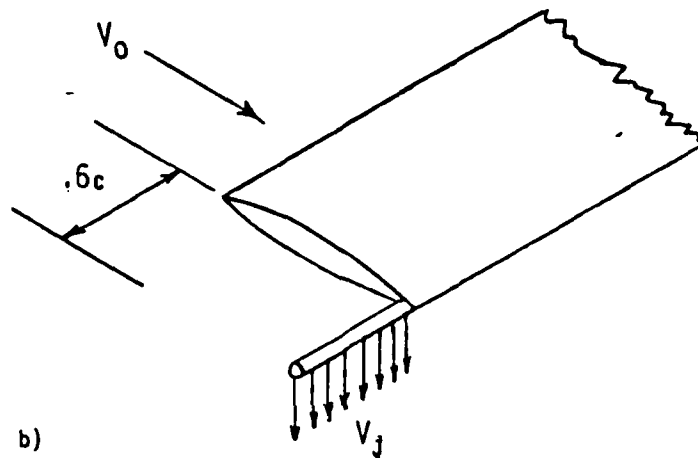


Figure 15 Sketch of a Spanwise Extended Blowing Tube [Ref. 30].

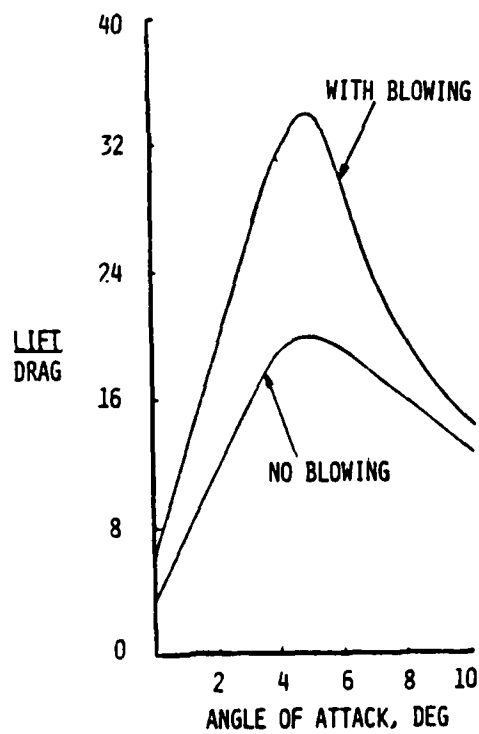


Figure 16 Effect on Lift-to-Drag Ratio from Spanwise Extended Tube Blowing [Ref. 30].

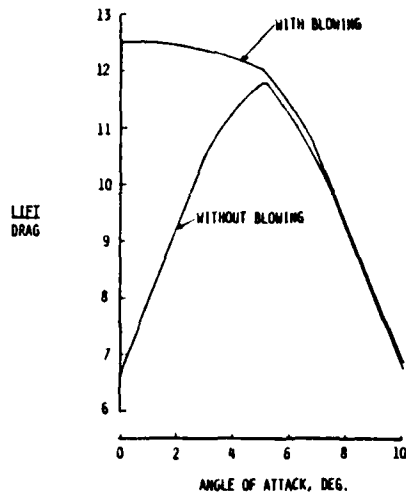


Figure 17 Effect on Lift-to-Drag Ratio from Spanwise Extended Tube Blowing at Transport Model Wingtip [Ref. 30].

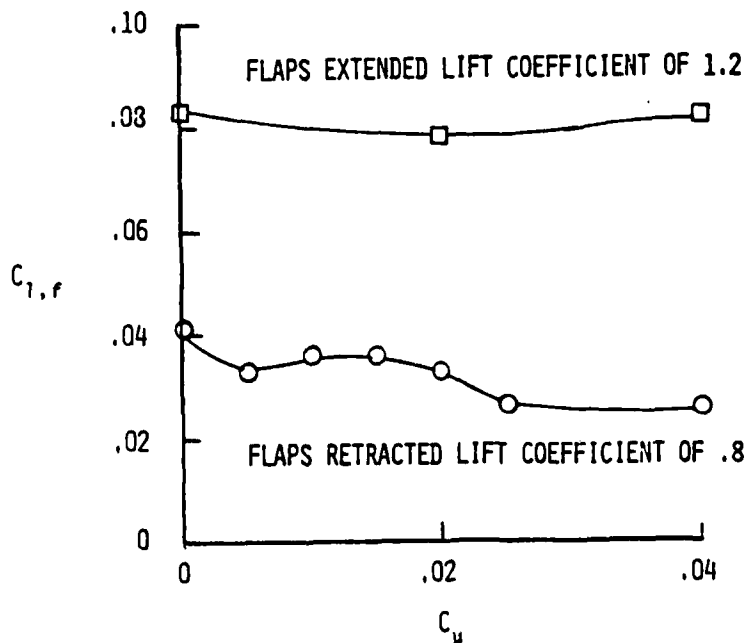


Figure 18 Rolling Moments Measured by a Small-Wing Model at 7.5 Spans Downstream a Transport Model with a Blowing Tube [Ref. 30].

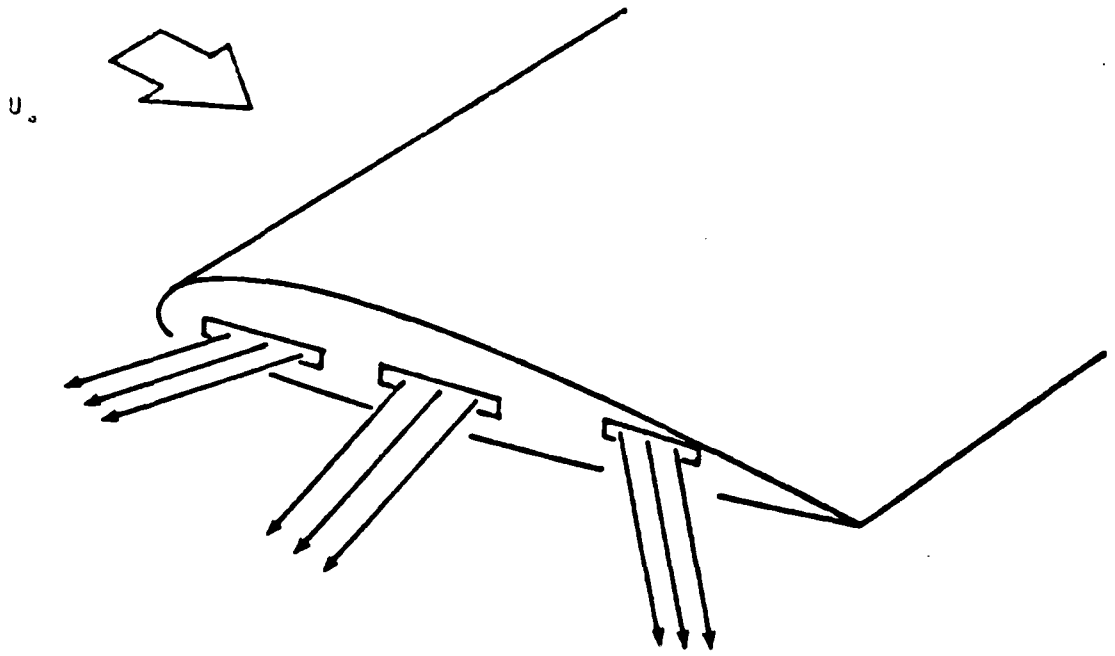
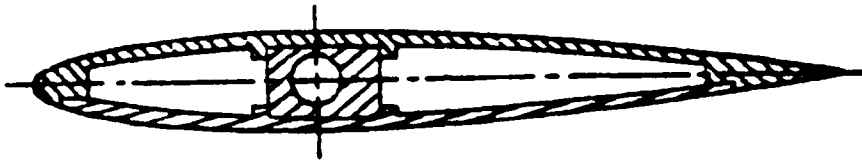
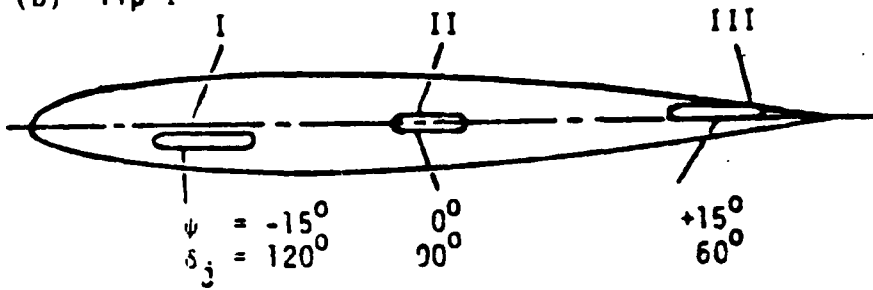


Figure 19 Sketch of Individually Controlled Discrete Wingtip Jets [Ref. 31].

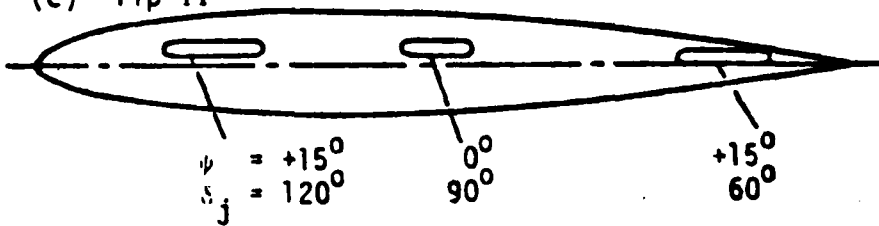
(a) Cut-off View of Wing Model



(b) Tip I



(c) Tip II



ψ = dihedral angle from x-y plane
 δ_j = sweep angle from the x-axis

Figure 20 Two Typical Wingtip Jet Configurations [Ref. 31].

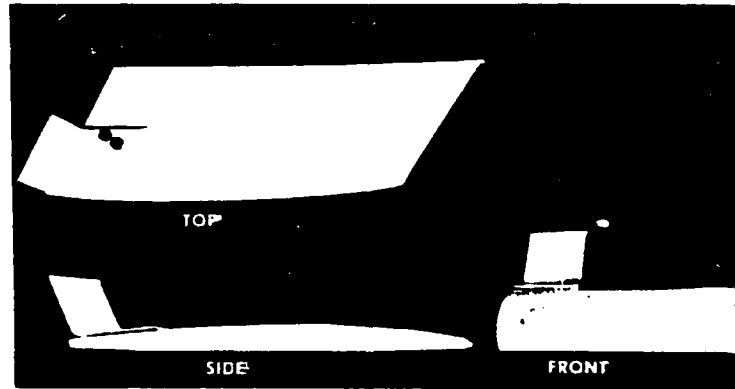
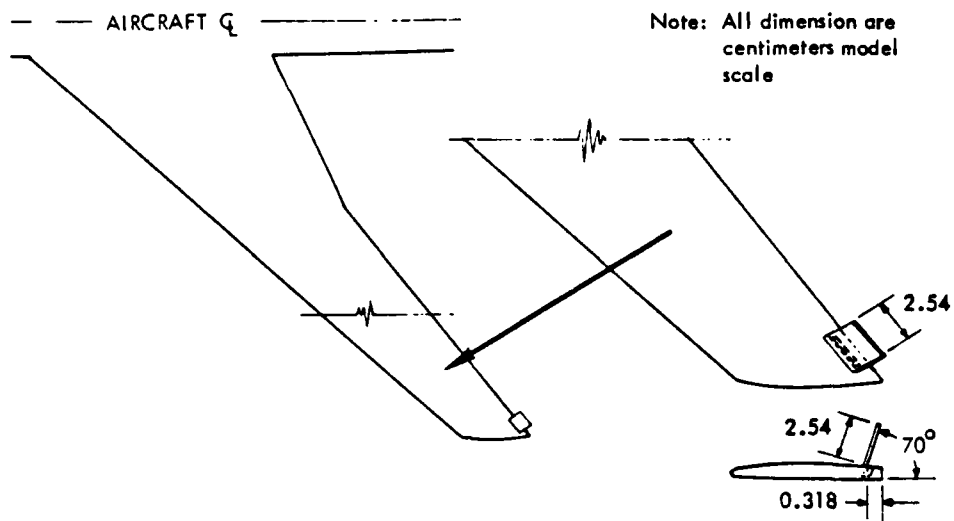


Figure 21 Sketch and Close-Up Views of a Blown Flap
[Ref. 27].

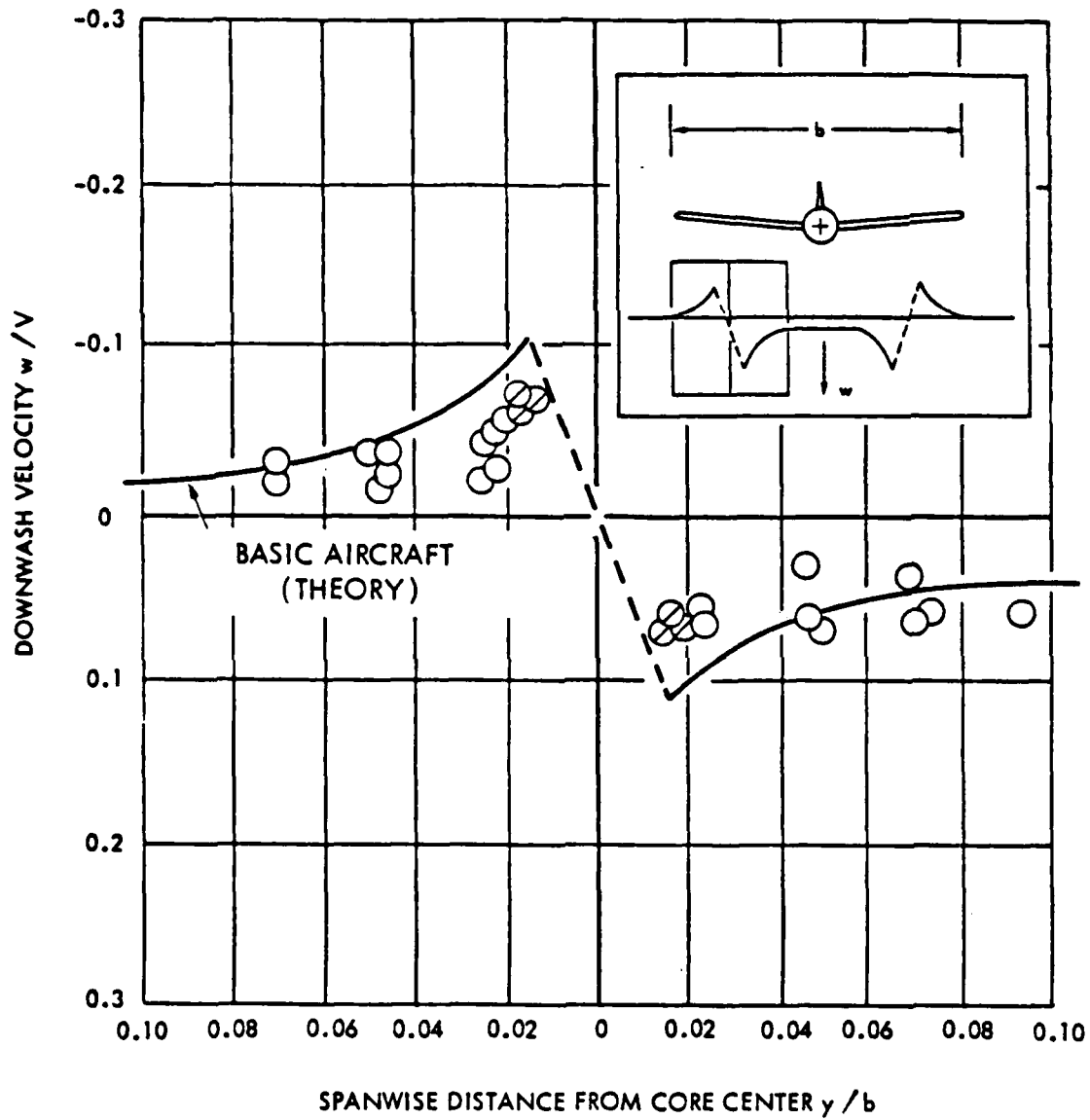


Figure 22 Effect of a Blown Flap on the Vortex Velocity Distribution [Ref. 27].

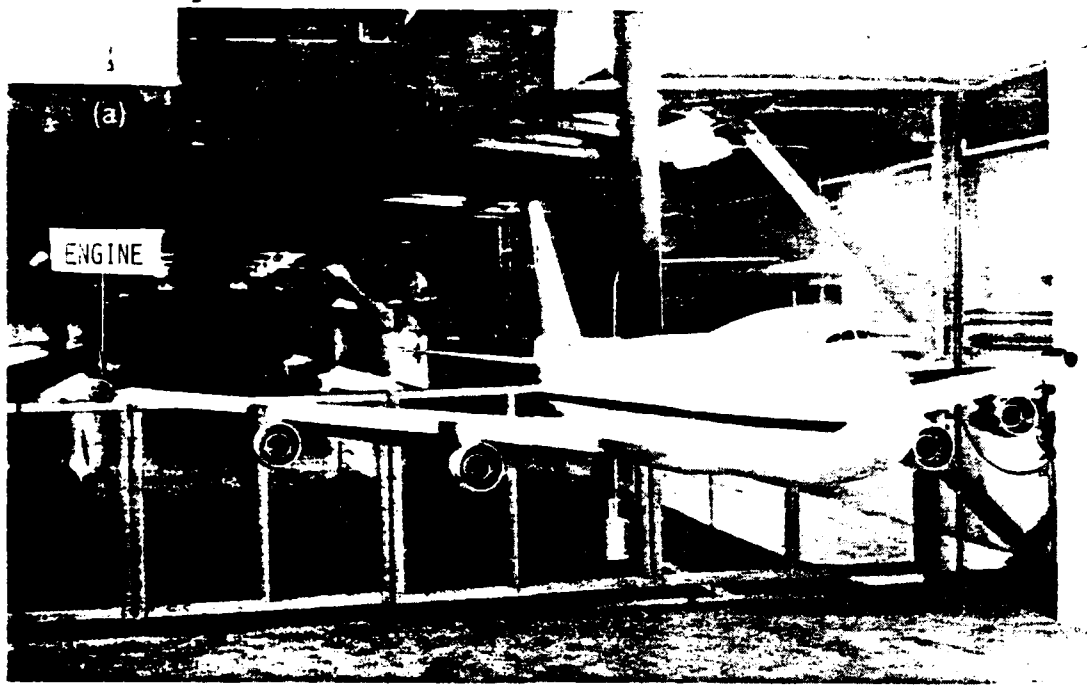


Figure 23 Wingtip-Mounted Engines on a Transport Model:
Front and Side Views [Ref. 30].

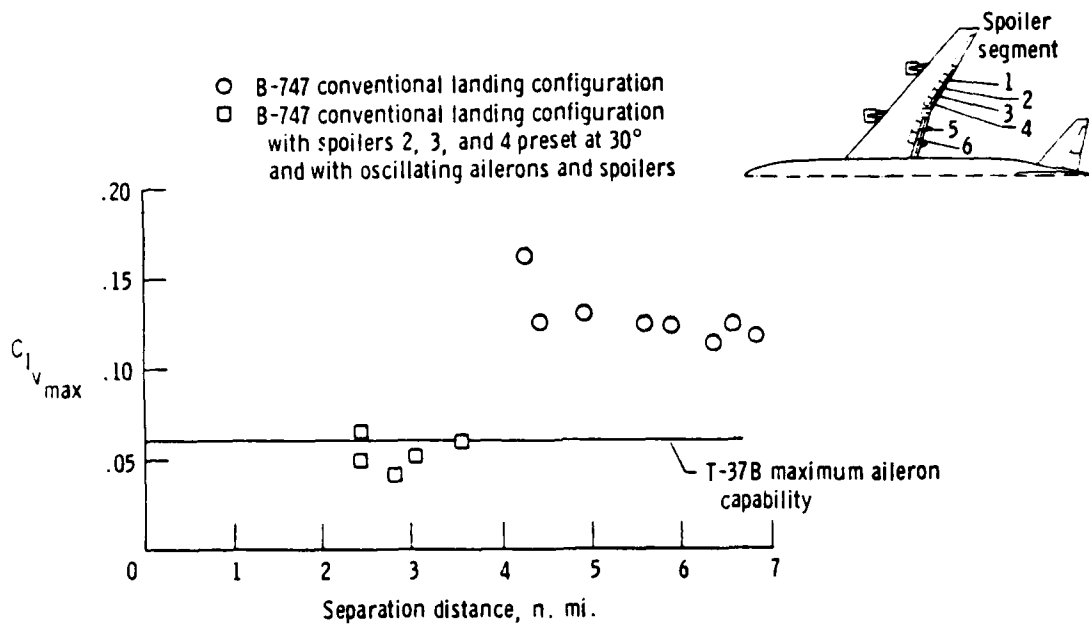


Figure 24 B-747 Wake Vortex Disturbance on a T-37B Probe Aircraft--Oscillating Ailerons and Spoilers [Ref. 34].

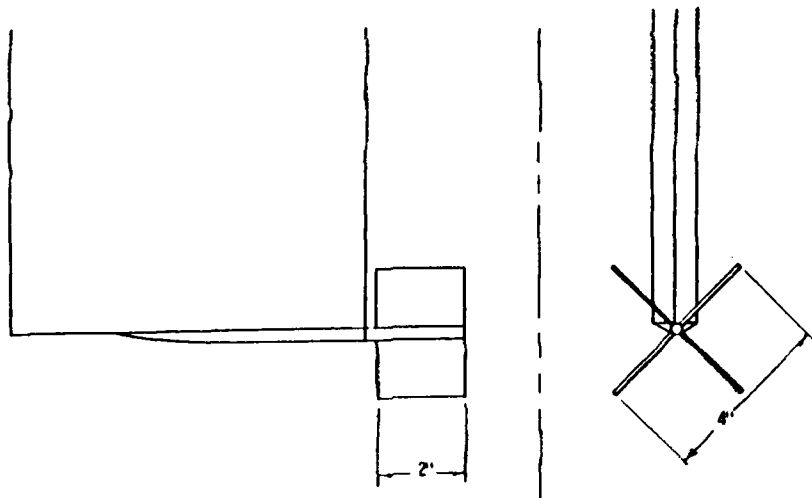


Figure 25 Sketch of Fixed Crossed Blades (Four Inch)
[Ref. 35].

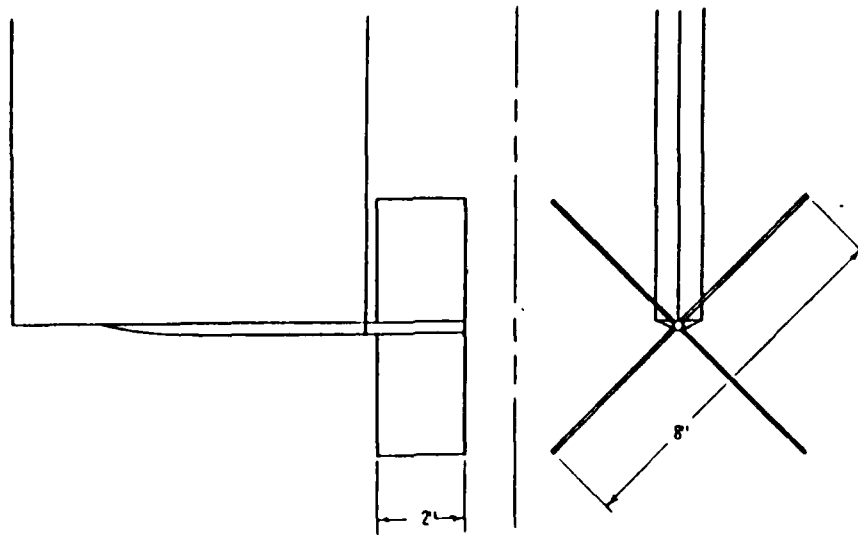


Figure 25a Sketch of Fixed Crossed Blades (Eight Inch)
[Ref. 35].

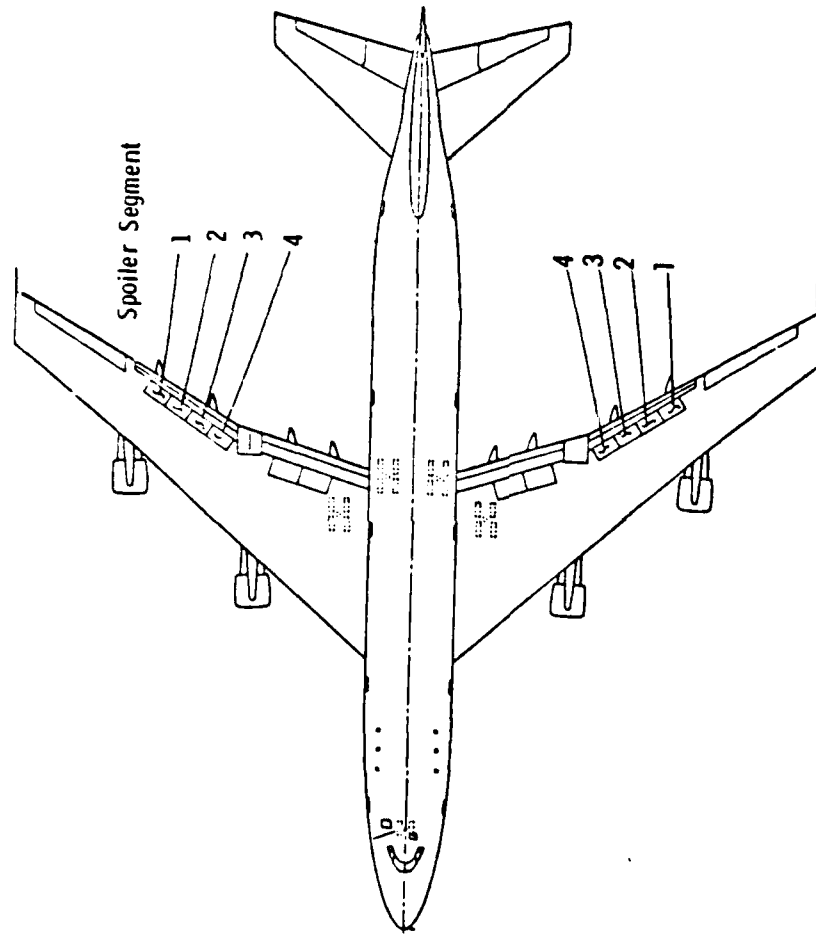


Figure 39 Sketch of Flight Spoilers on a B-747 Aircraft Model
[Ref. 42].

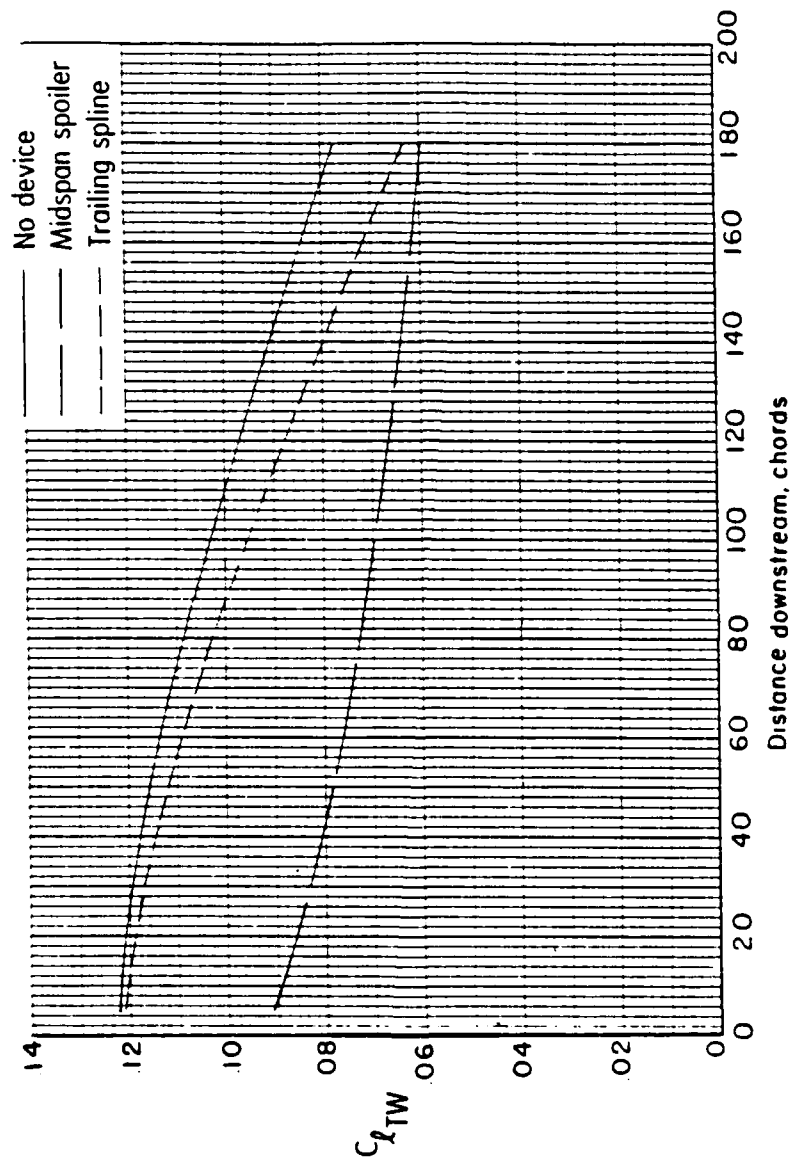


Figure 38 a Variation of Rolling Moment Coefficient with Distance behind a Flapped Model: No Device, Spoiler, Spline [Ref. 36].

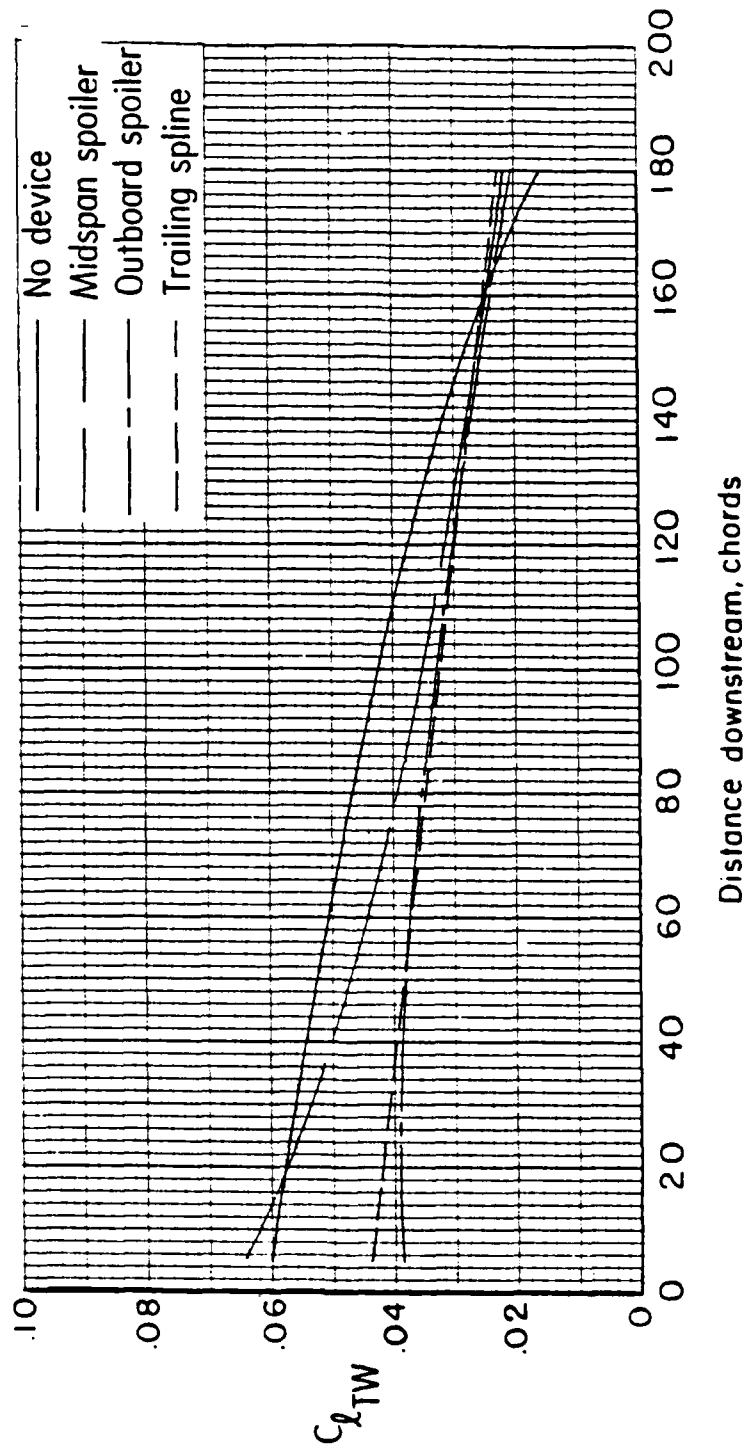


Figure 37 Variation of Rolling Moment Coefficient with Distance behind a Basic Model: No Device, Spoiler, Spline [Ref. 36].

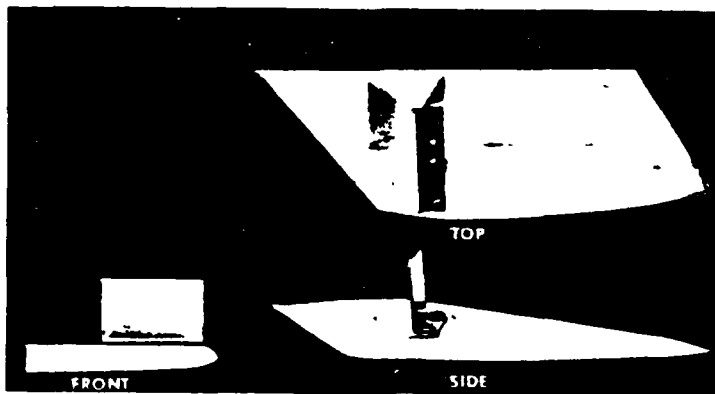
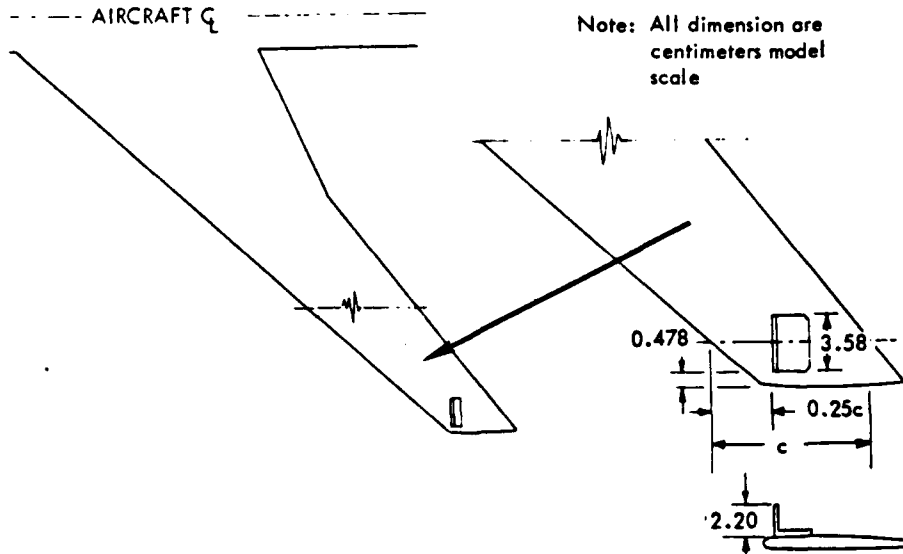


Figure 36 Wingtip Mounted Spoiler [Ref. 27].

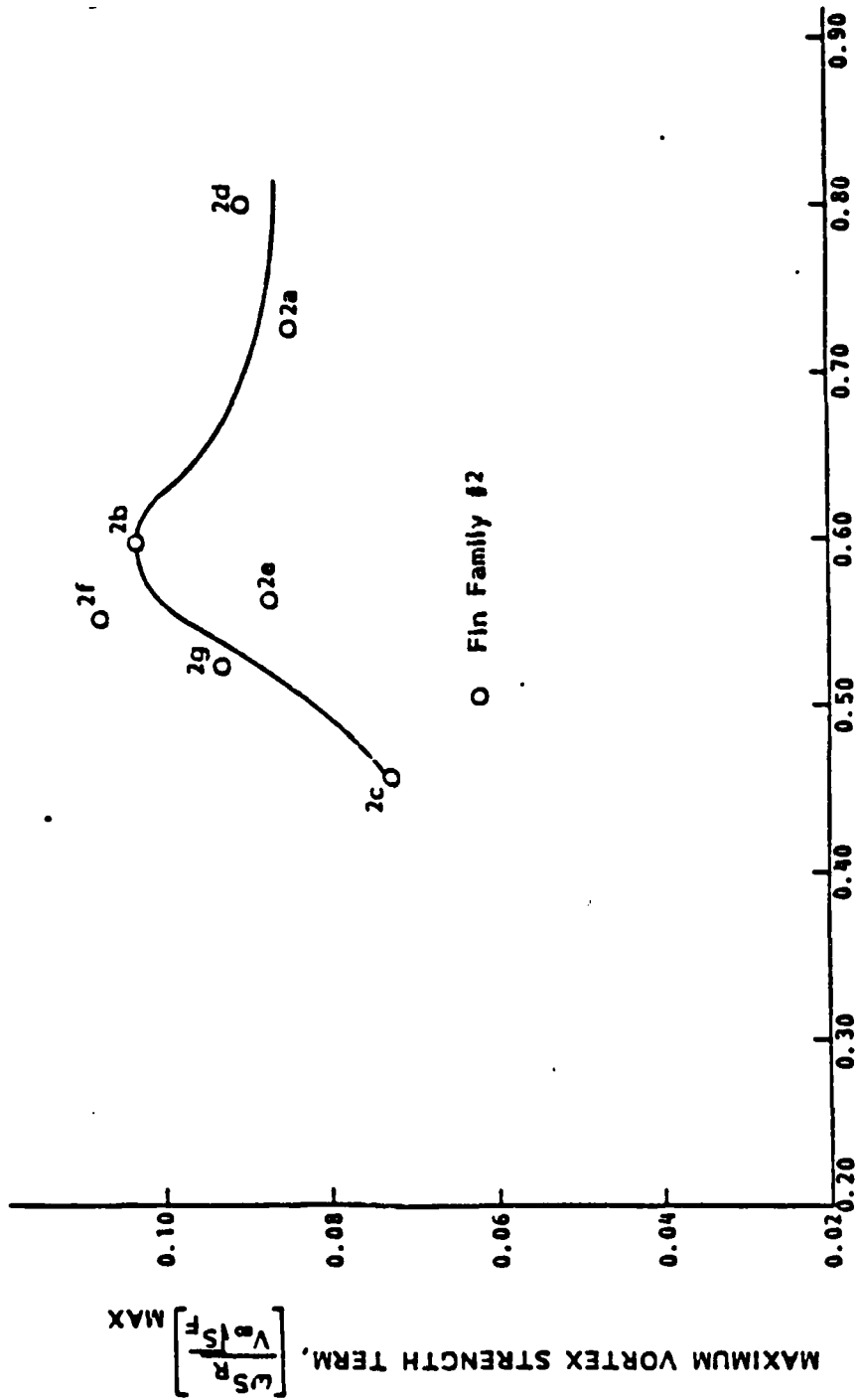


Figure 35 Maximum Vortex Strength Term vs. Fin Aspect Ratio [Ref. 40].

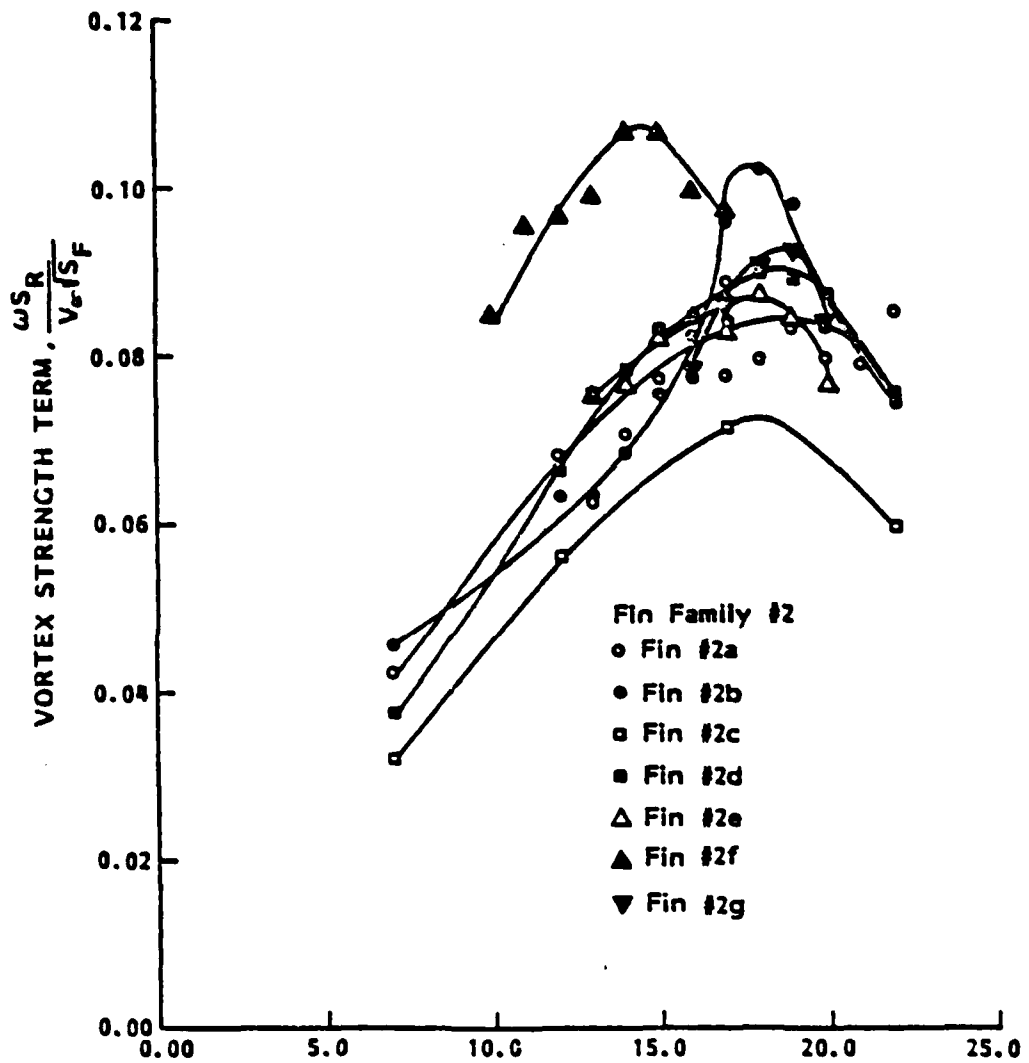


Figure 34 Vortex Strength Term vs. Pin Angle of Attack [Ref. 40].

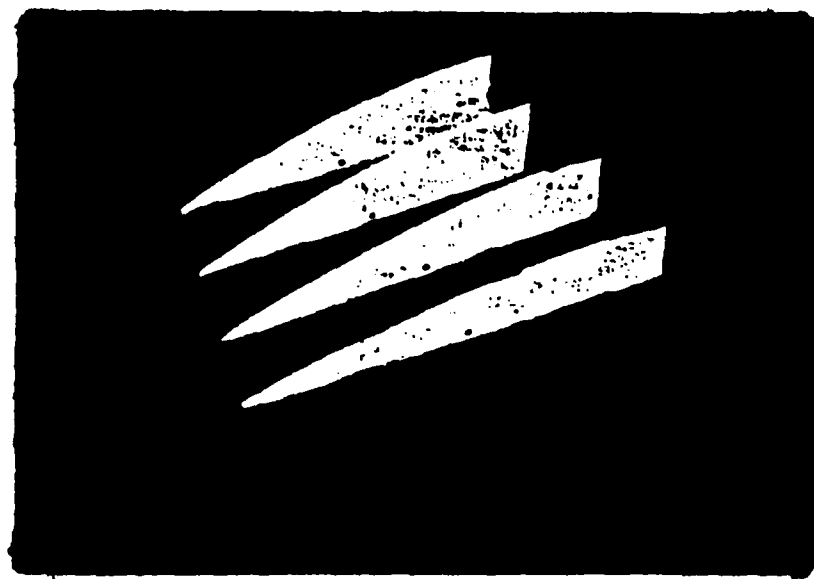


Figure 33 Parabolic Wingfins [Ref. 40].

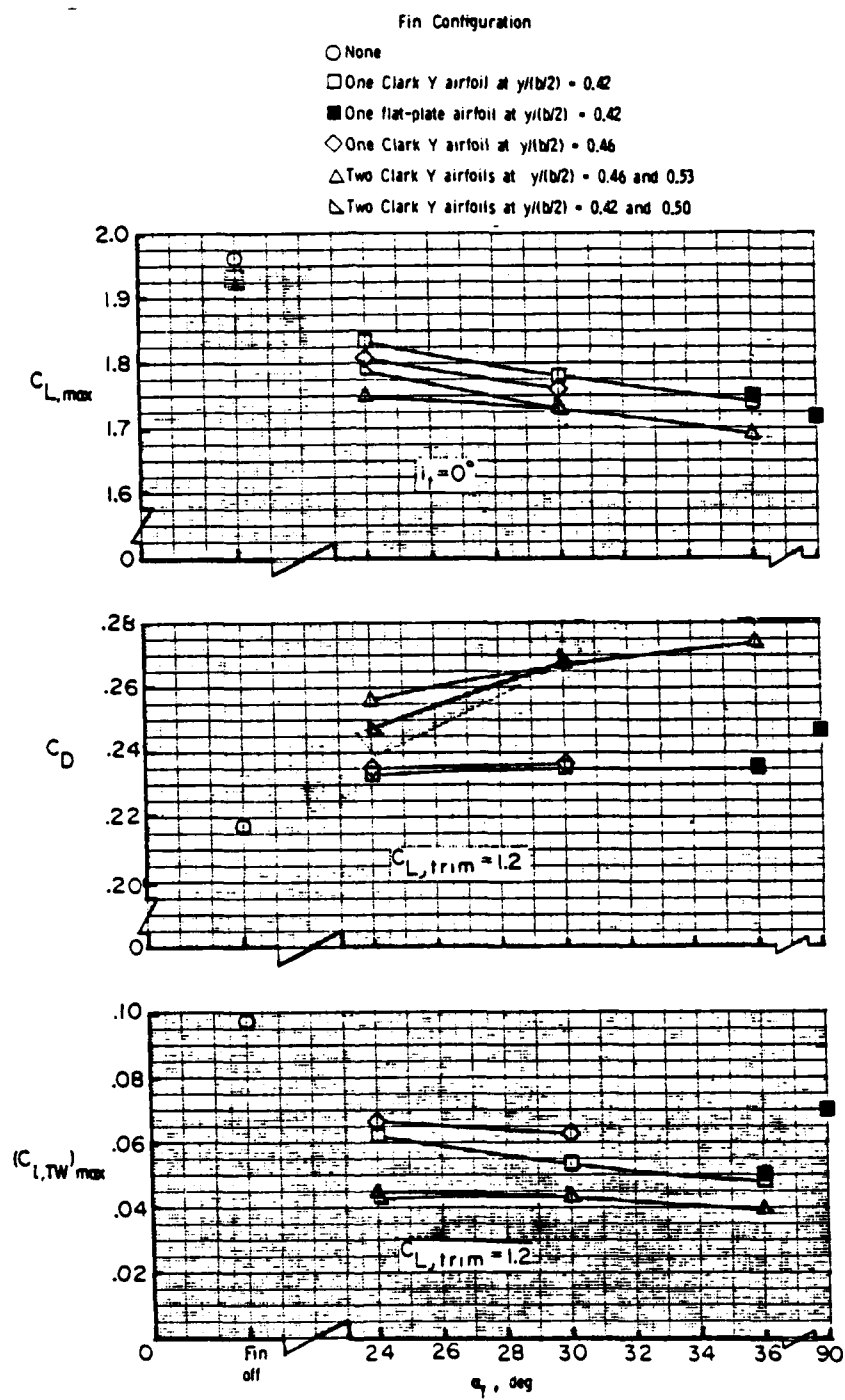


Figure 32 Summary of Reductions in Rolling Moment Coefficient for Various Wingfin Configurations (7.8 Spans Downstream) [Ref. 39].

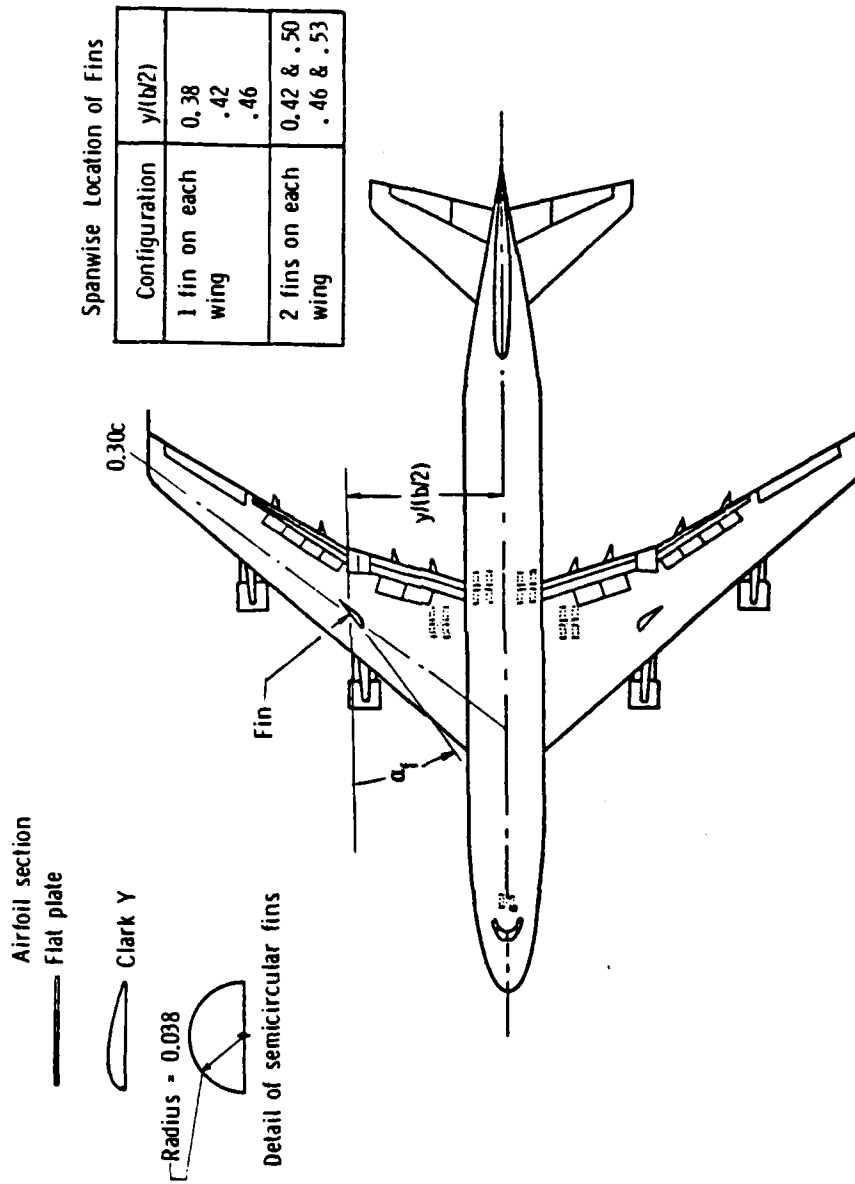


Figure 31 Sketch of Wingfins on a Transport Aircraft Model [Ref. 39].

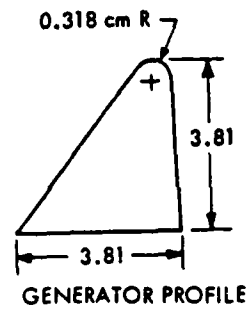
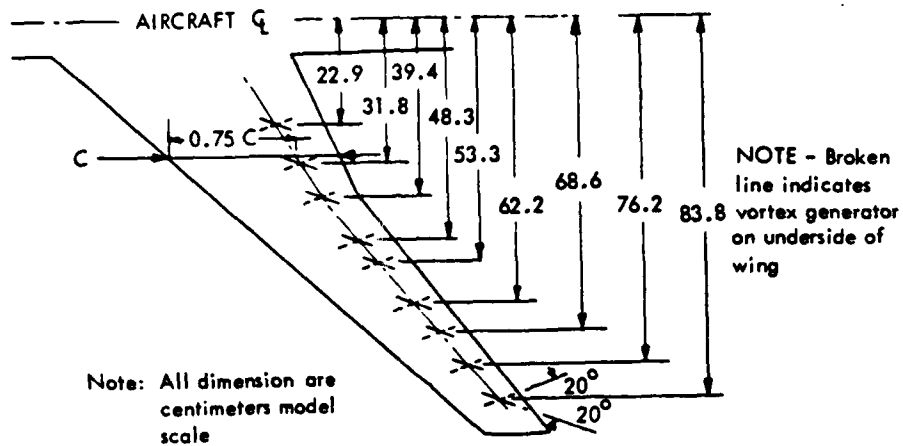
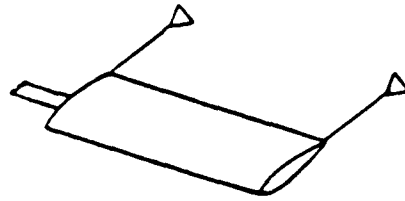


Figure 30 Sketch and Close-Up Views of a Vortex Generator [Ref. 27].

Cabled drogue
cones



Cabled chutes

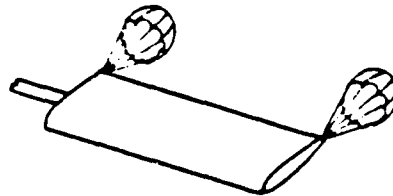


Figure 29 Sketch of Cabled Drogue Cone and Cabled Chute
[Ref. 38].

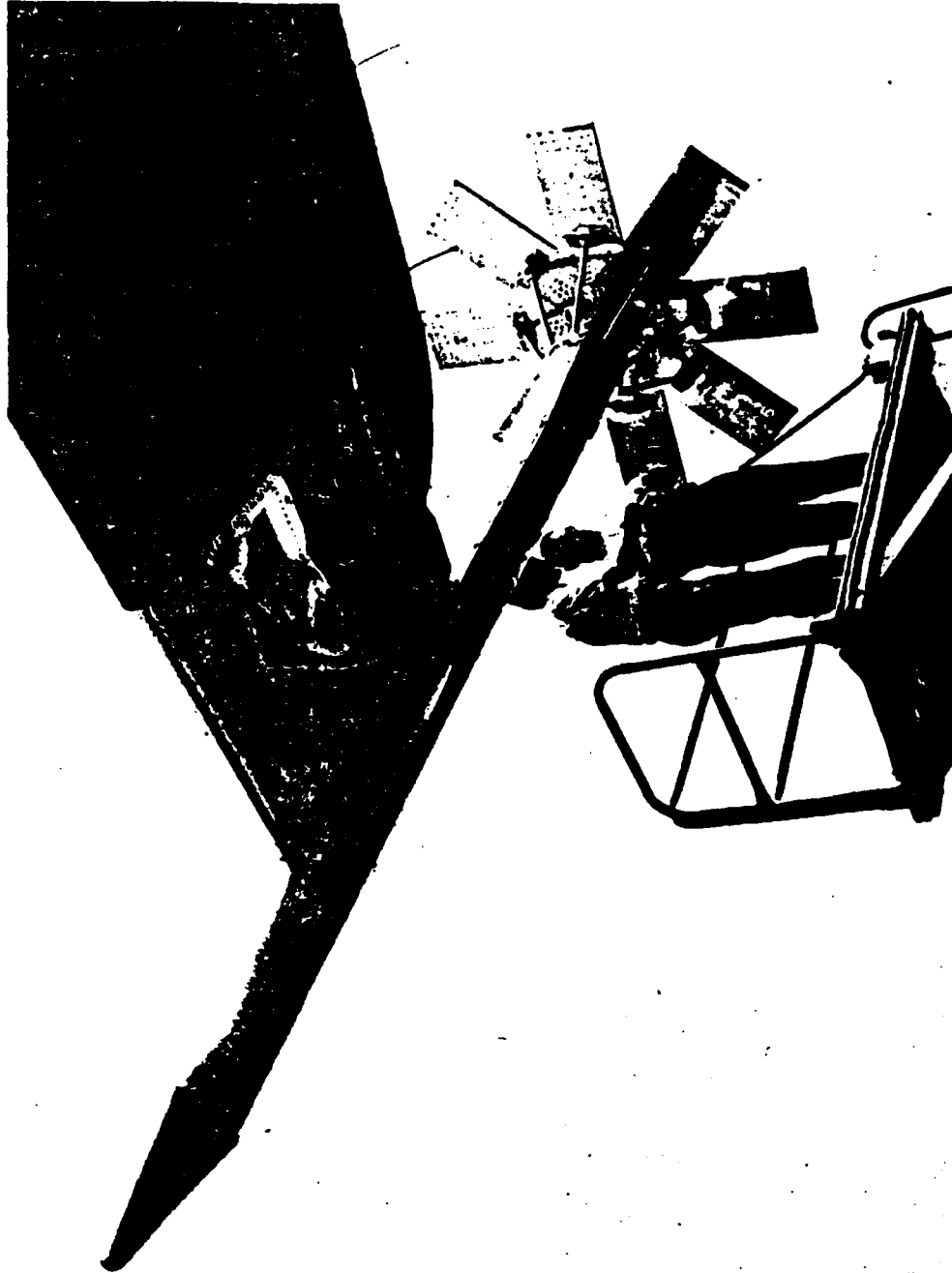


Figure 28 Photograph of the Spline Assembly on the Wingtip
[Ref. 38].

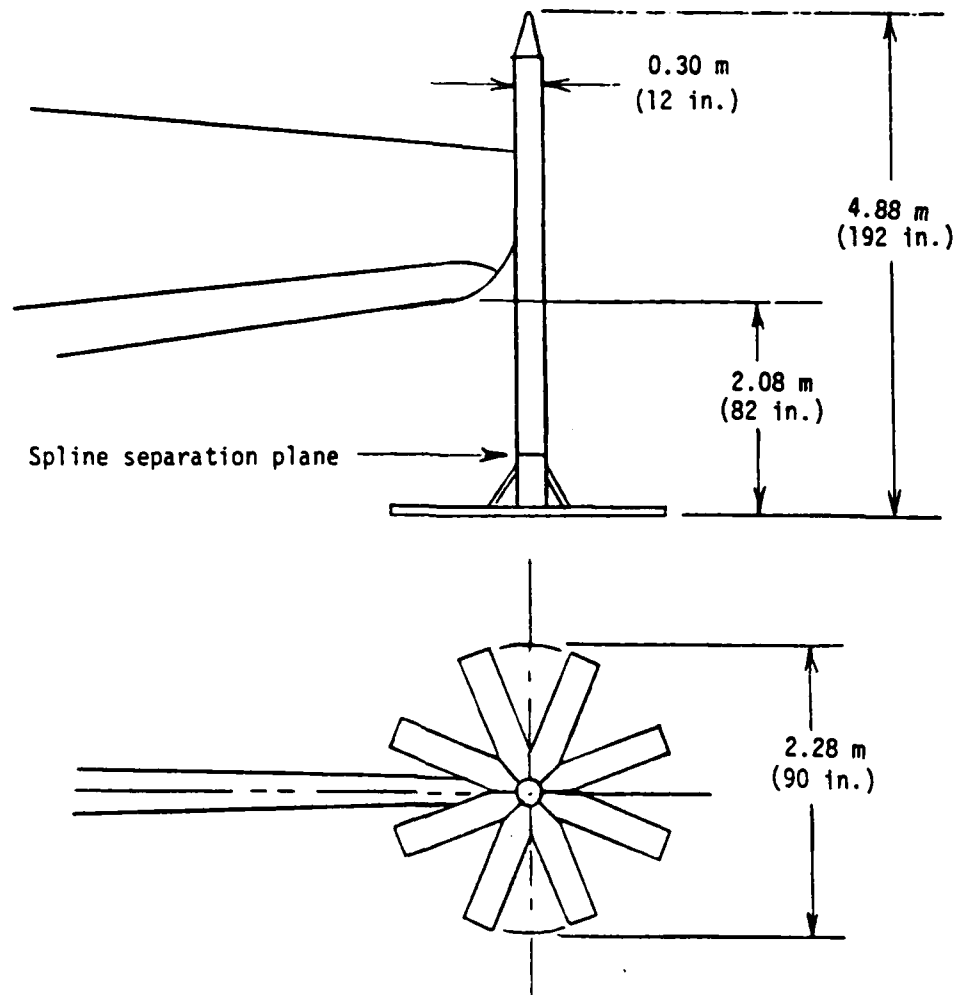


Figure 27 Sketch of Spline Assembly at Wingtip [Ref. 38].

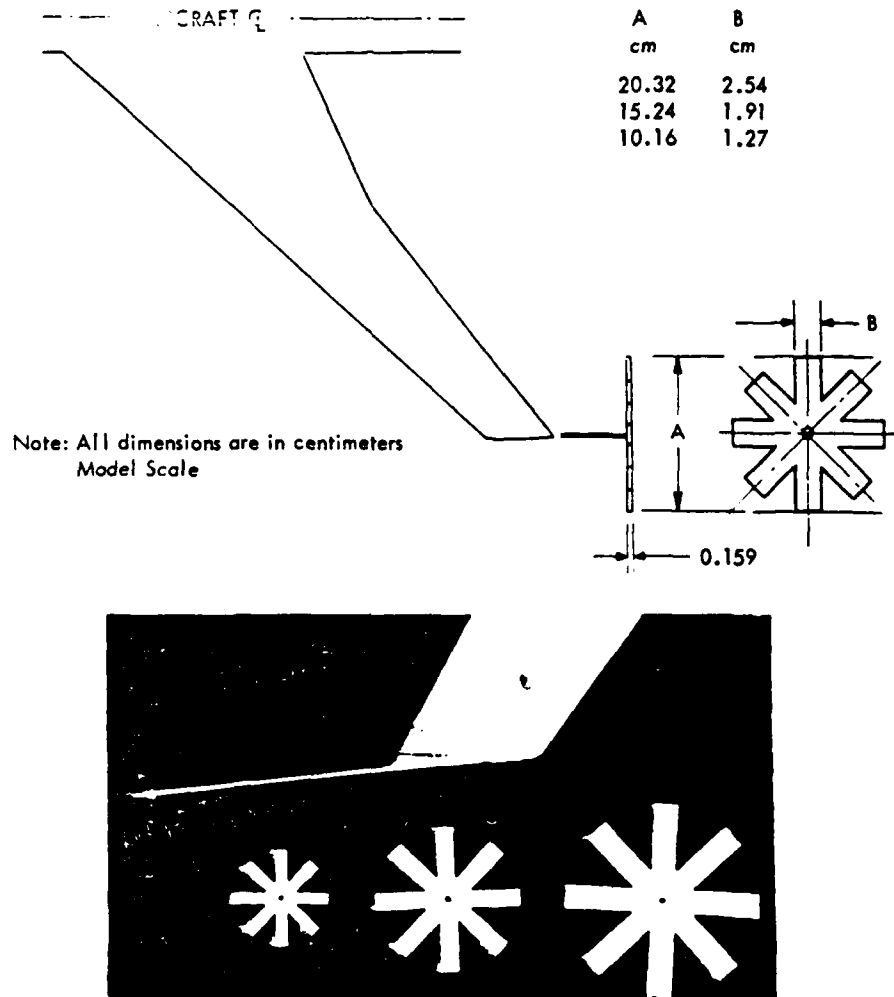


Figure 26 Sketch and Close-Up Views of Wingtip Mounted Splines [Ref. 27].

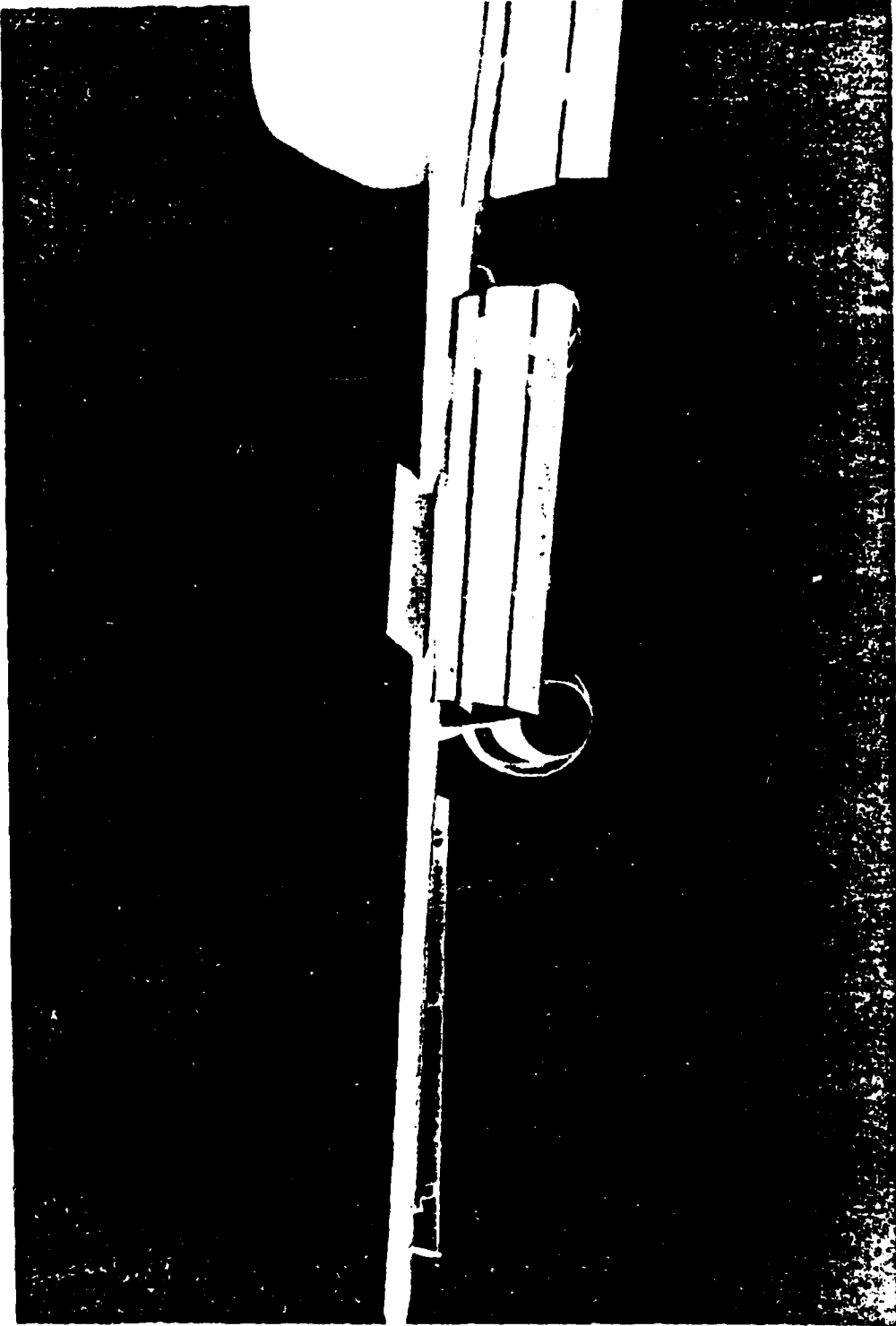


Figure 40 Photograph of Flight Spoilers on a B-747 Aircraft Model:
Segments 1 and 2 Deflected 45 Degrees [Ref. 42].

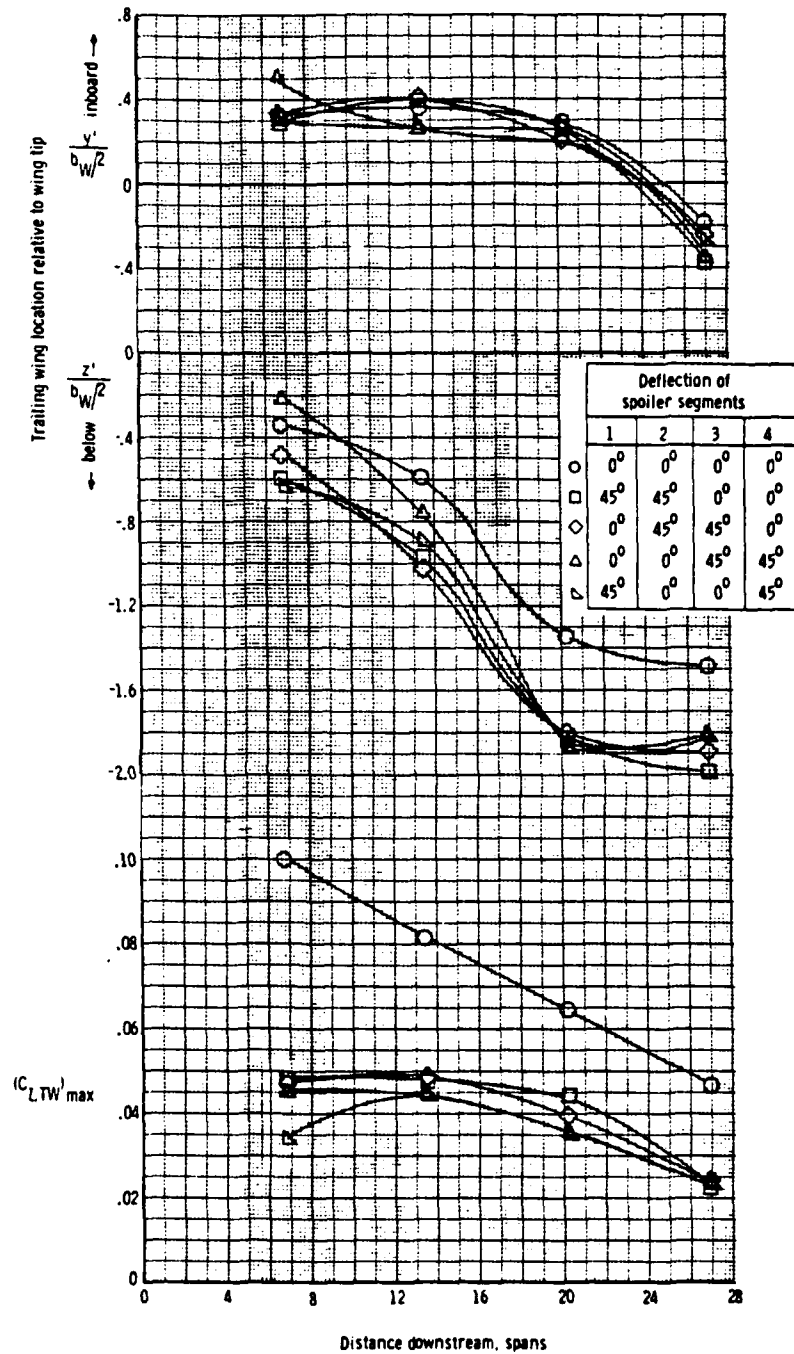


Figure 41 Variation of Rolling Moment Coefficient with Distance behind the B-747 Aircraft Model (Spoiler Deflection) [Ref. 42].

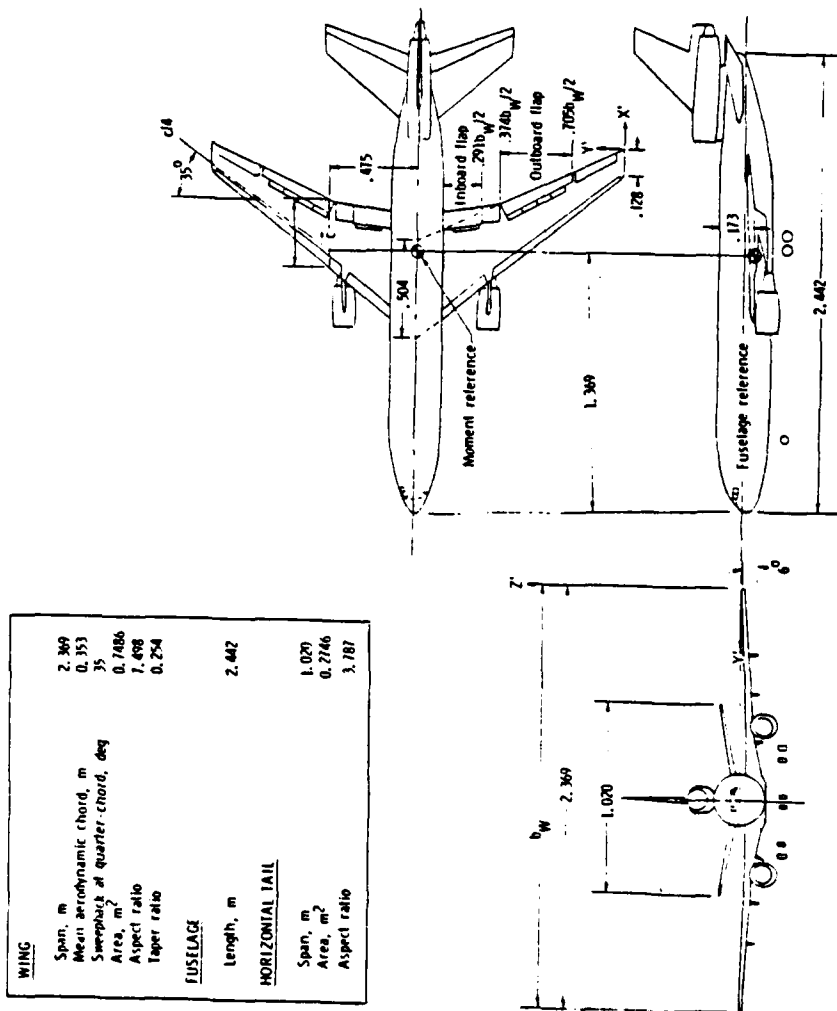


Figure 42 Three View Sketch of DC-10 Model with Flaps Retracted [Ref. 44].

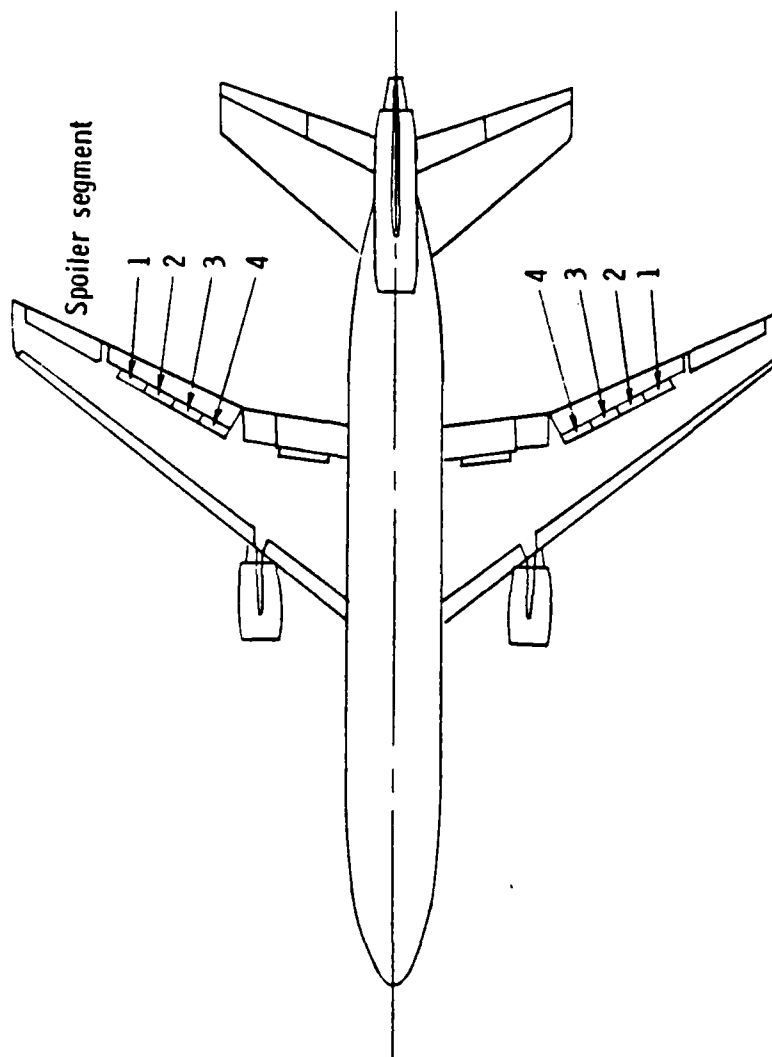


Figure 43 Sketch of Flight Spoilers on a DC-10 Model [Ref. 44].

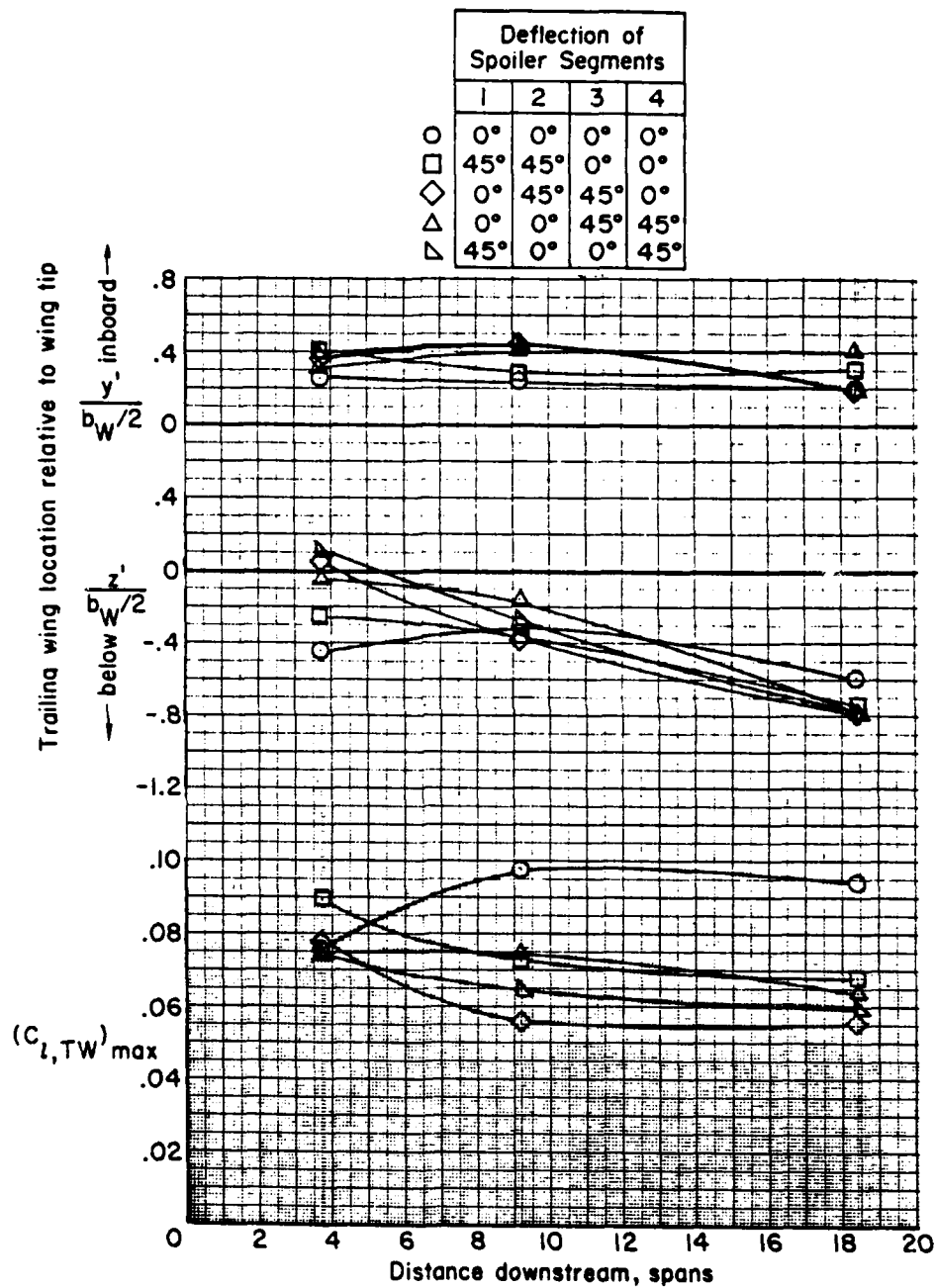
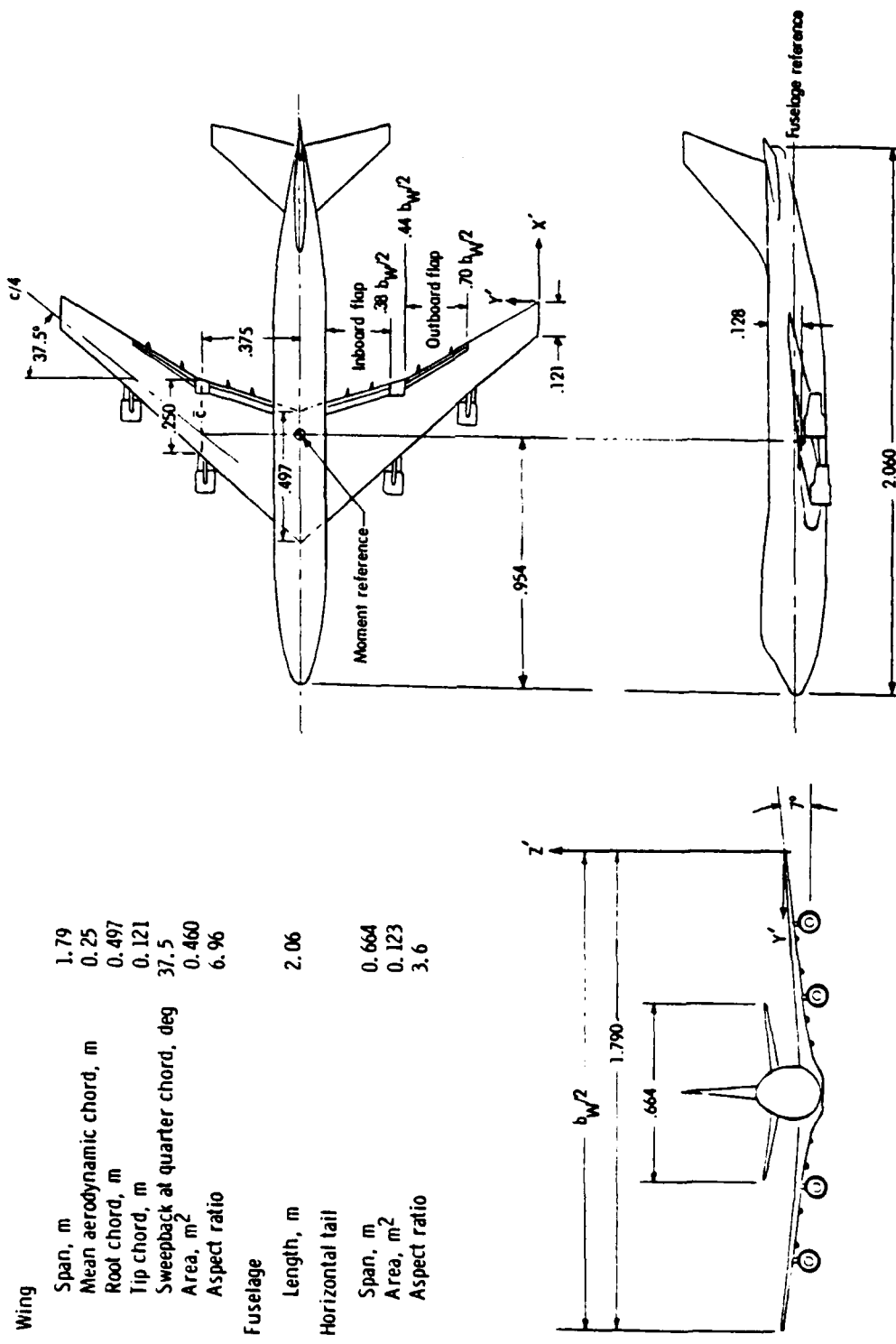


Figure 44 Variation of Rolling Moment Coefficient with Distance behind the DC-10 Aircraft Model (Spoiler Deflection) [Ref. 44].



Wing	
Span, m	1.79
Mean aerodynamic chord, m	0.25
Root chord, m	0.497
Tip chord, m	0.121
Sweepback at quarter chord, deg	37.5
Area, m ²	0.460
Aspect ratio	6.96
Fuselage	
Length, m	2.06
Horizontal tail	
Span, m	0.664
Area, m ²	0.123
Aspect ratio	3.6

Figure 45 Three View Sketch of B-747 Model with Flaps Retracted [Ref. 37].

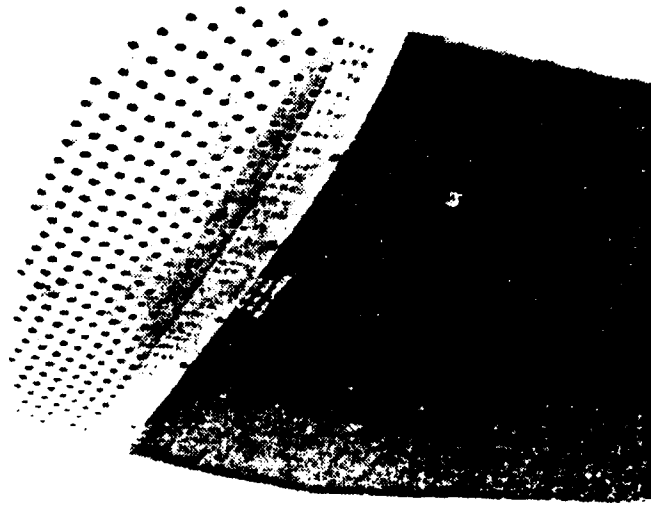


Figure 46 Photograph of a Porous Wingtip [Ref. 49].

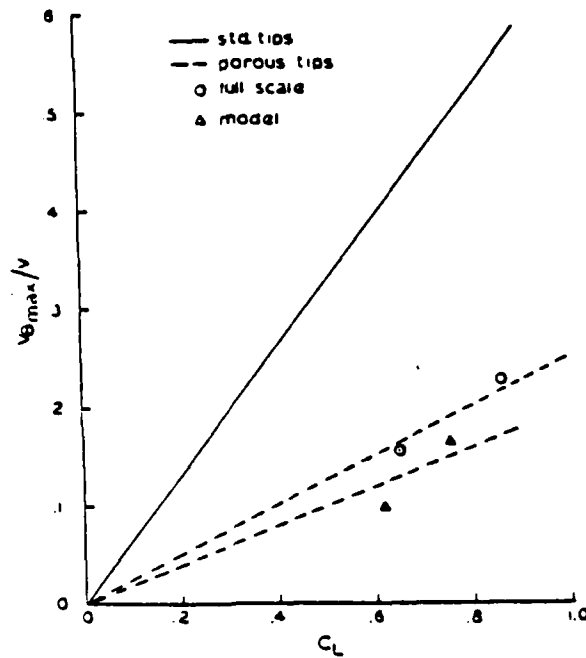


Figure 47 Nondimensional Maximum Tangential Velocity vs. Lift Coefficient [Ref. 49].

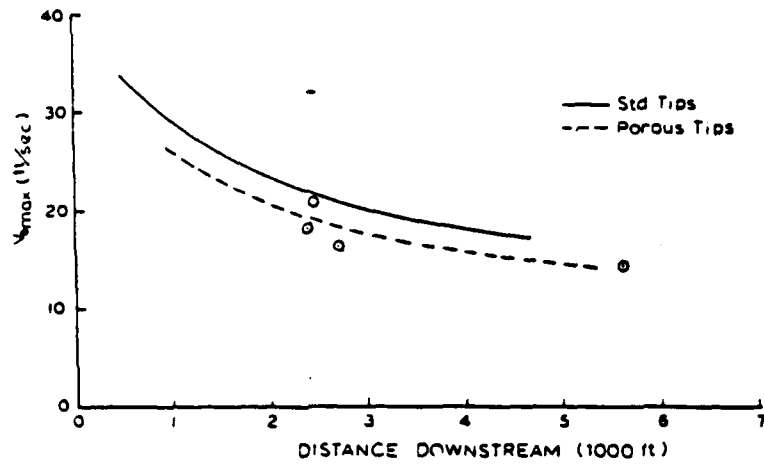


Figure 48 Maximum Tangential Velocity vs. Downstream Distance [Ref. 49].

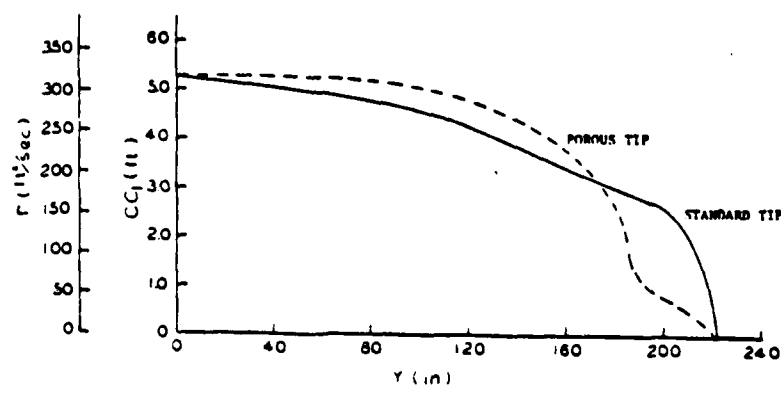


Figure 49 Lift Distribution on O-1A Wing with and without Porous Tip [Ref. 49].

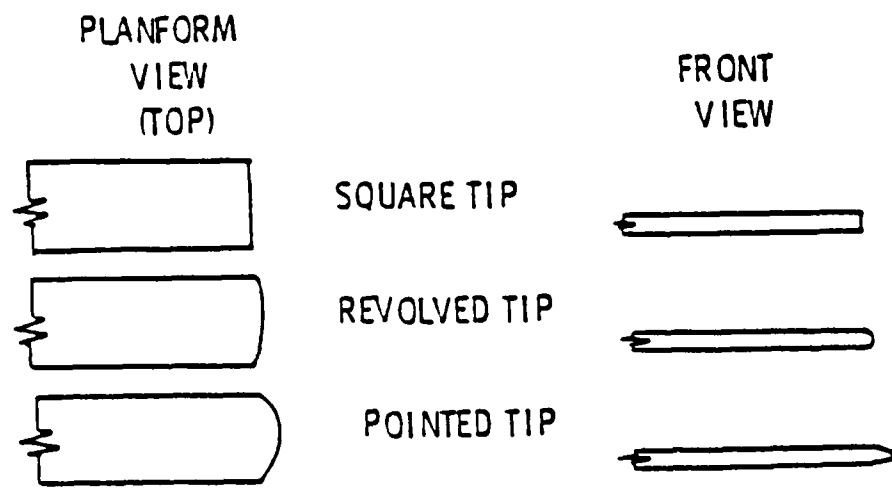
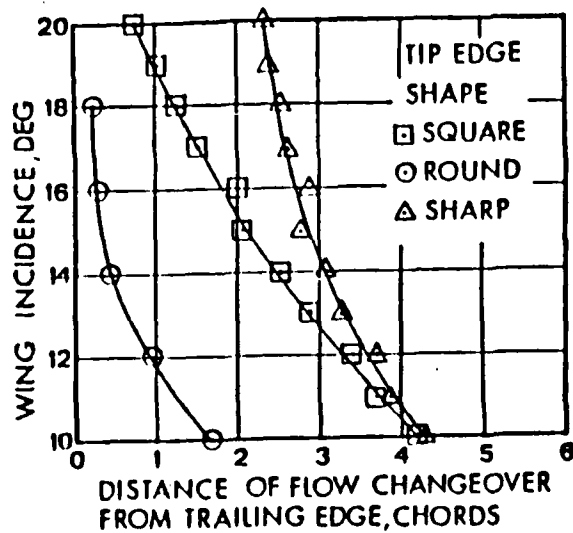
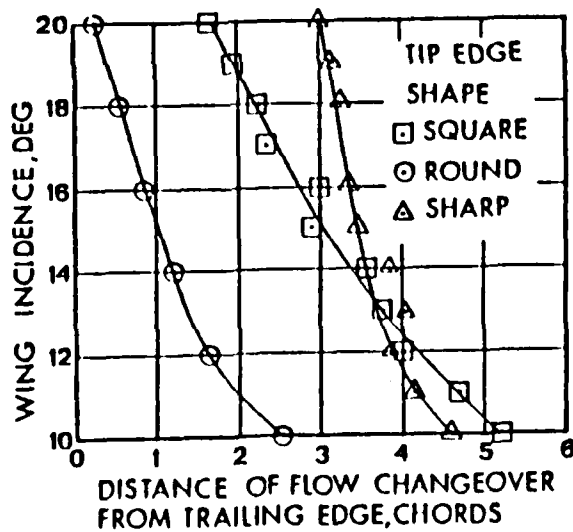


Figure 50 Wingtip Edge Shape Configurations [Ref. 50].



a) REYNOLDS NUMBER = 3.4×10^4



b) REYNOLDS NUMBER = 6.8×10^4

Figure 51 Changeover Position from Axial Velocity Excess to Axial Velocity Deficit behind NACA 6412 Wing Section [Ref. 20].

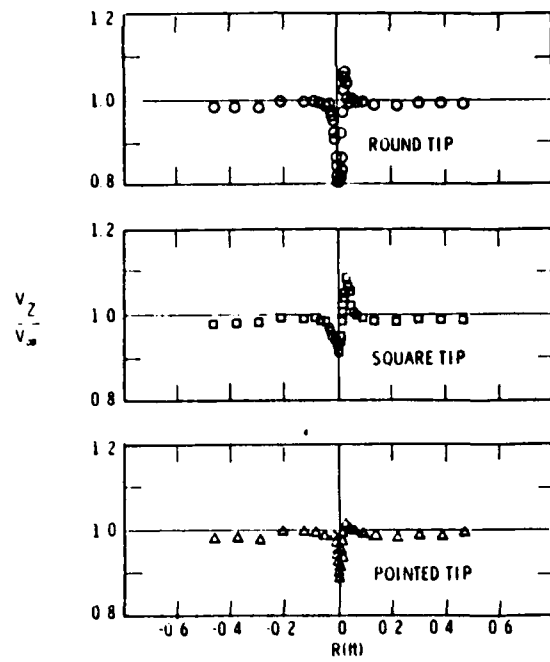


Figure 52 Comparison of Axial Velocity Profile for Various Wingtip Edge Shapes (20 Chordlengths Downstream) [Ref. 50].

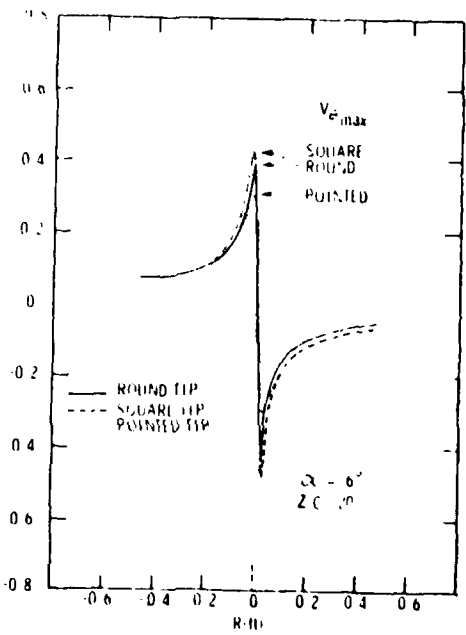


Figure 53 Comparison of Tangential Velocity Profile for Various Wingtip Edge Shapes (20 Chordlengths Downstream) [Ref. 50].

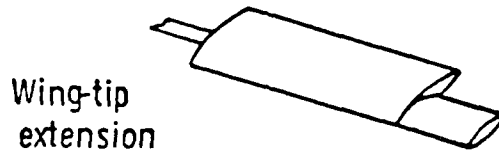
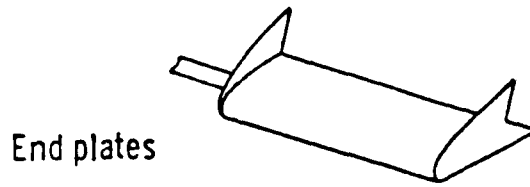


Figure 54 Sketch of End Plate and Wingtip Extension [Ref. 38].

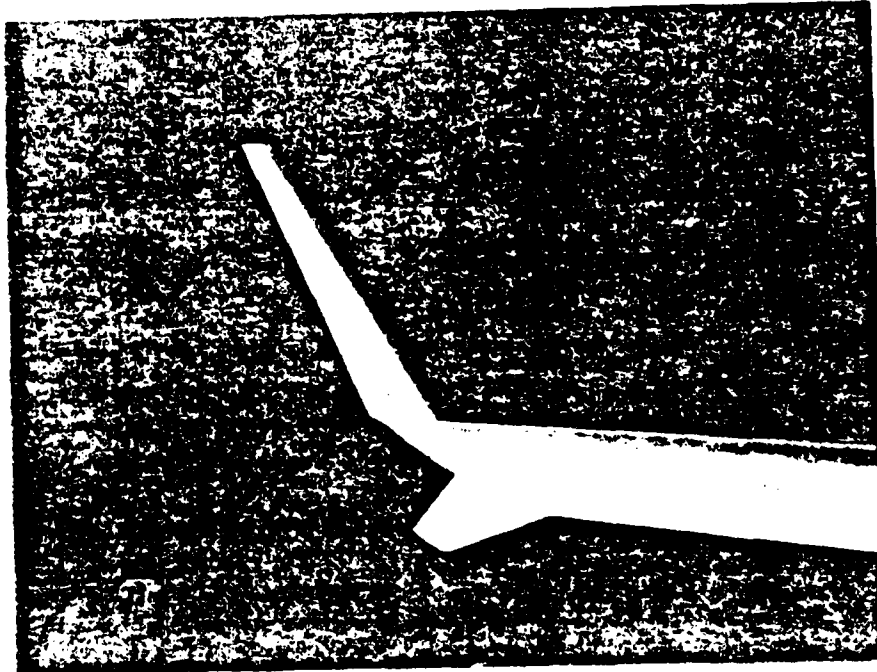


Figure 55 Photograph of Whitcomb Winglet [Ref. 53].

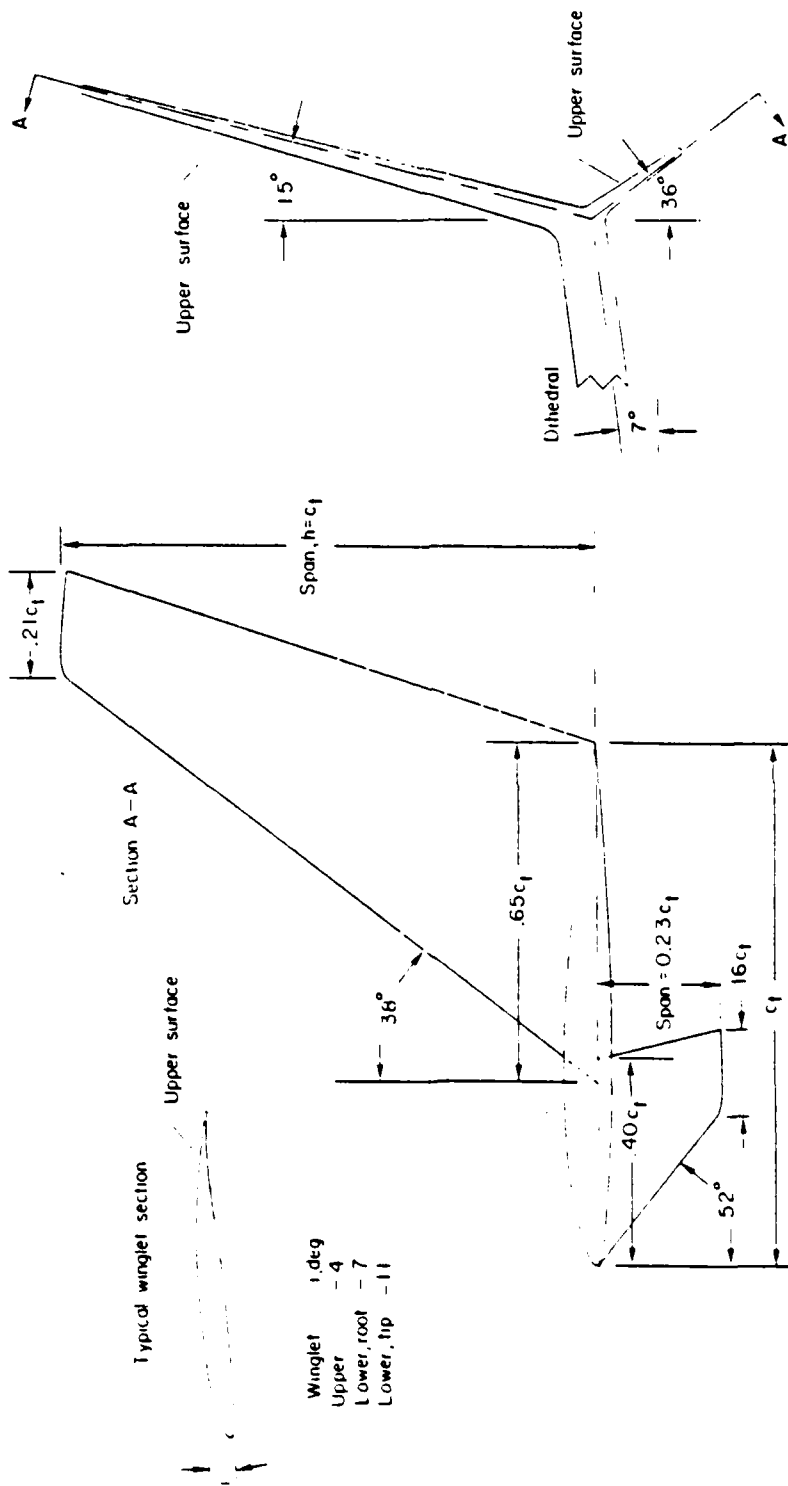


Figure 56 Geometric Drawing of the Whitcomb Winglet [Ref. 53].

AD-A159 535

TRAILING VORTEX ATTENUATION DEVICES(U) NAVAL
POSTGRADUATE SCHOOL MONTEREY CA K G HEFFERNAN JUN 85

2/2

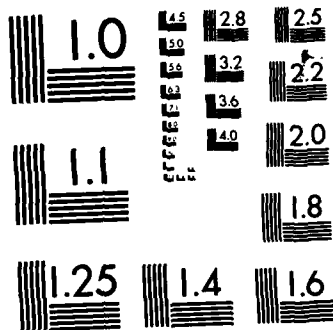
UNCLASSIFIED

F/G 28/4

NL



		END
		FILMED
		DTIC



MICROCOPY RESOLUTION TEST CHART
NATIONAL BUREAU OF STANDARDS-1963-A

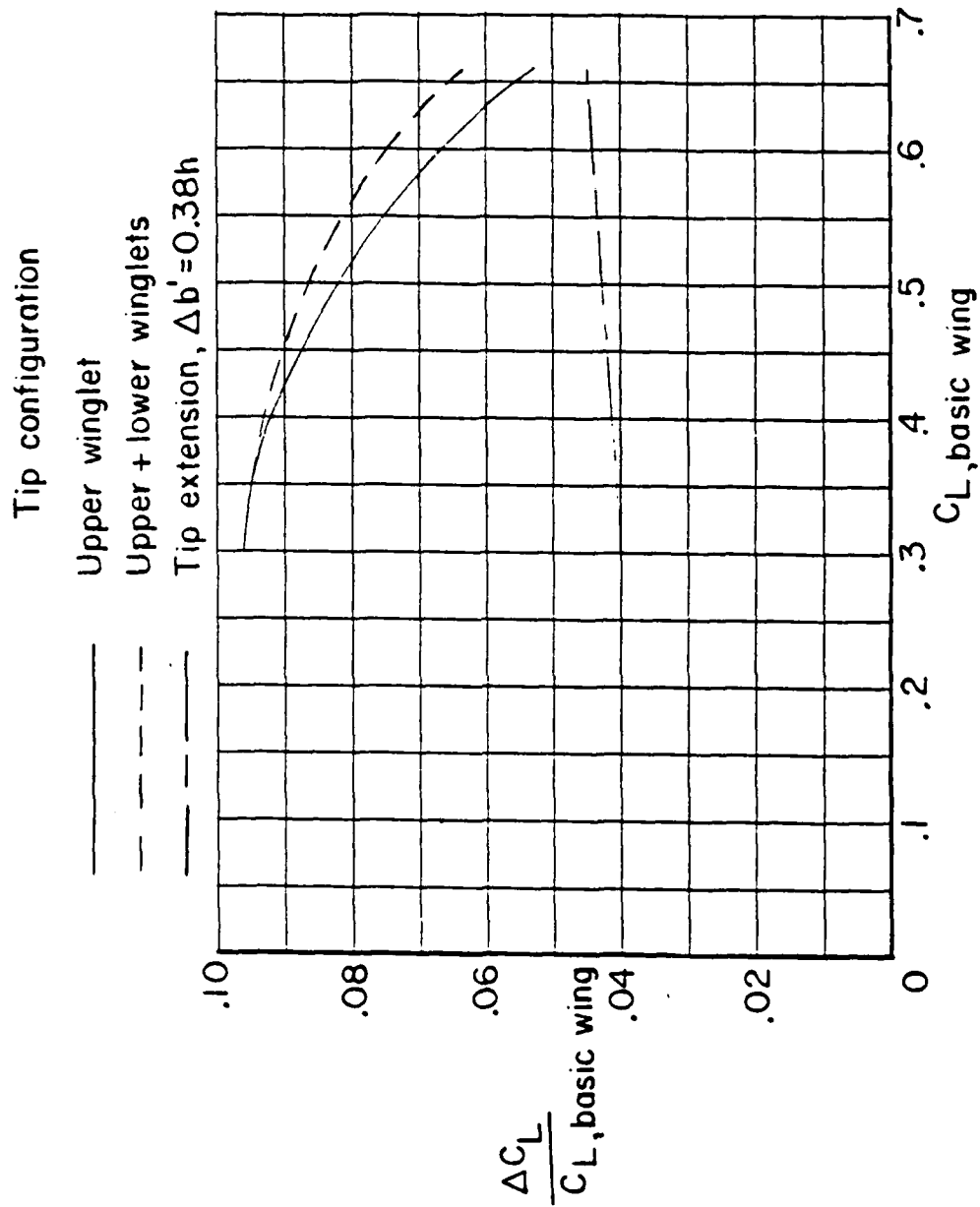


Figure 57 Incremental Lift Coefficient Variation for Constant Drag Coefficient ($H=0.78$) [Ref. 53].



Figure 58 Tangential Velocity Profile Downstream Whitcomb Winglet (5 Chordlengths) [Ref. 50].

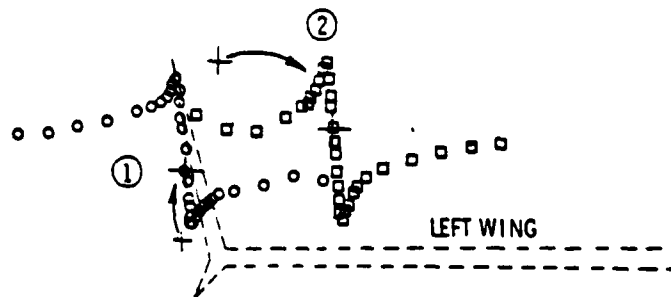


Figure 58a Tangential Velocity Profile Downstream Whitcomb Winglet (20 Chordlengths) [Ref. 50].

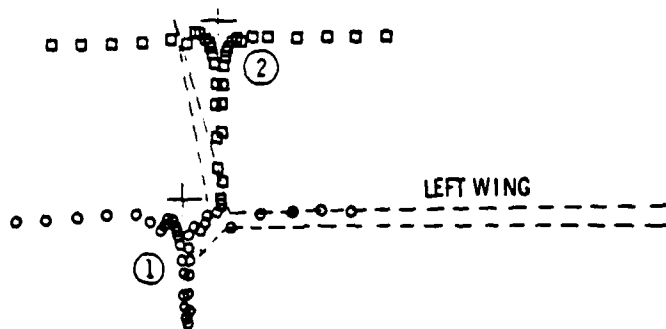


Figure 59 Axial Velocity Profile Downstream Whitcomb Winglet (5 Chordlengths) [Ref. 50].

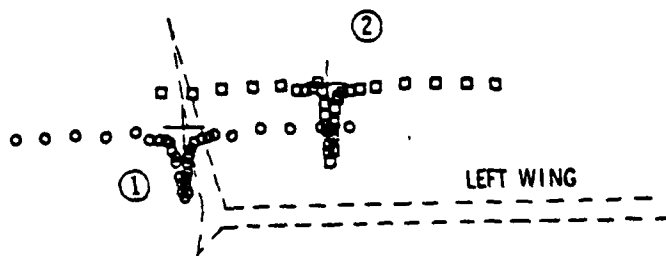


Figure 59a Axial Velocity Profile Downstream Whitcomb Winglet (20 Chordlengths) [Ref. 50].

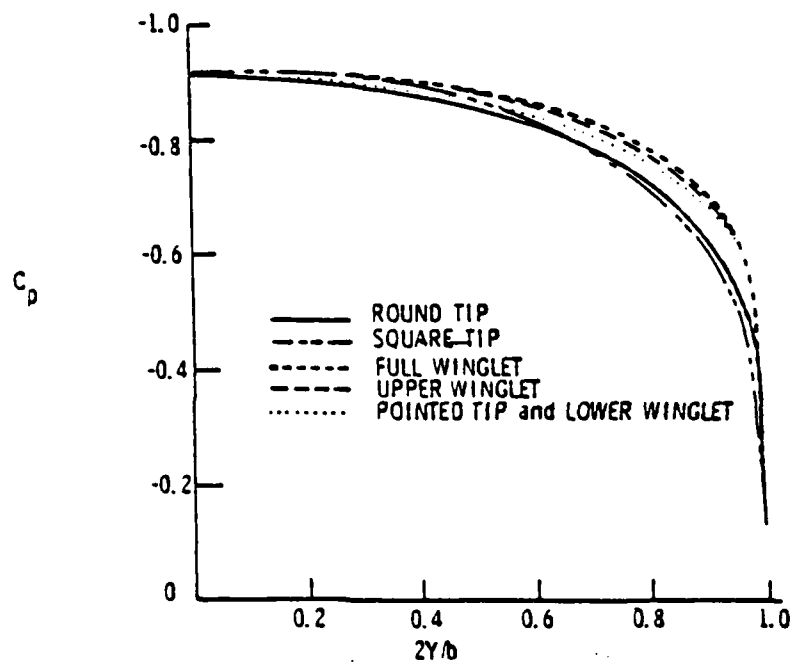


Figure 60 Spanwise Pressure Distribution for Various Wingtip Edge Shapes and Whitcomb Winglet [Ref. 50].

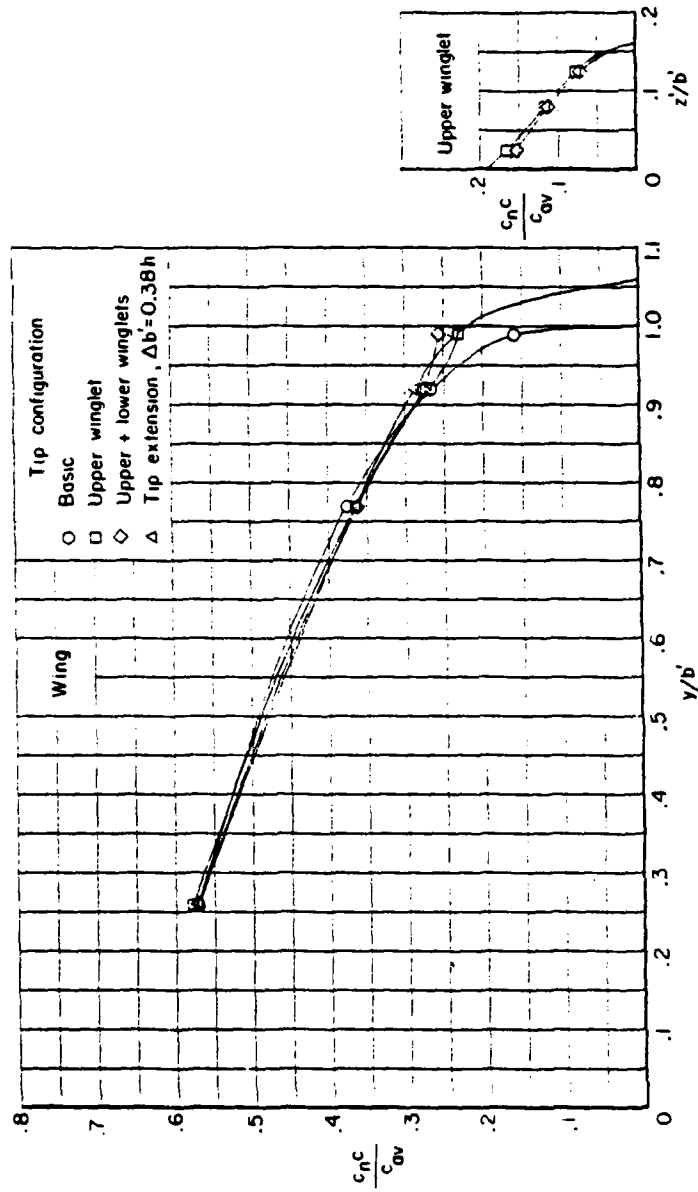


Figure 61 Spanwise Load Distribution of Whitcomb Winglet ($M=0.78$) [Ref. 53].

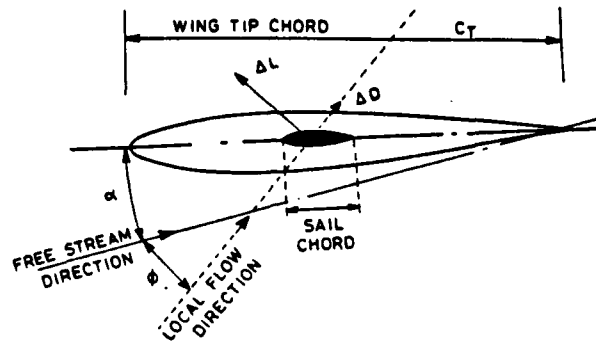


Figure 62 Forces on an Auxiliary Surface Mounted on the Tip of a Wing [Ref. 55].

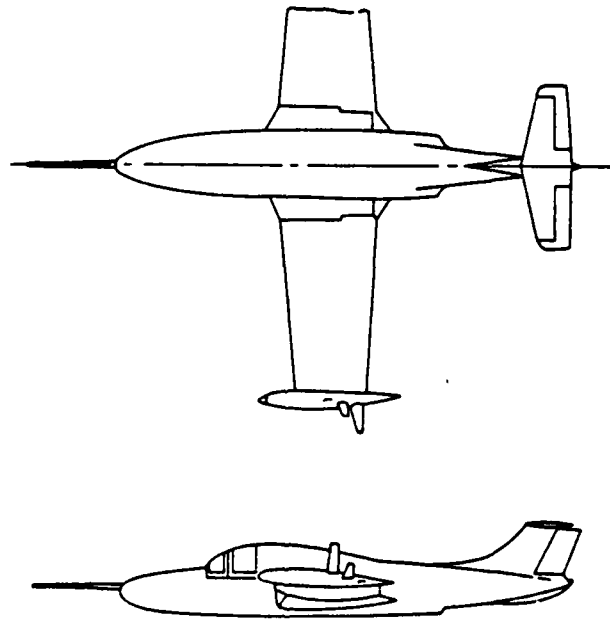


Figure 63 View of Paris Aircraft Fitted with Wingtip Sails [Ref. 55].

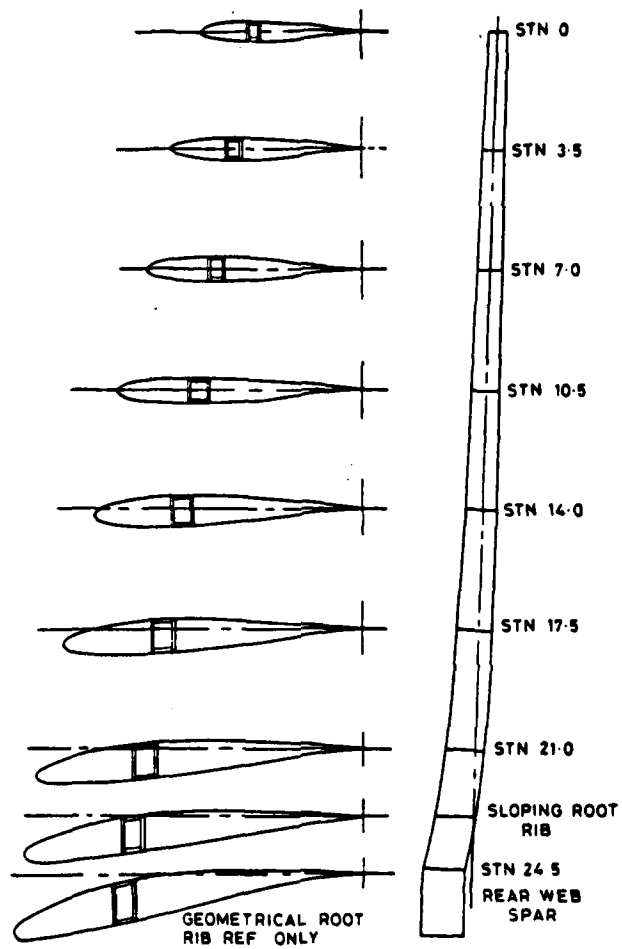


Figure 64 Wingtip Sail Geometry [Ref. 55].

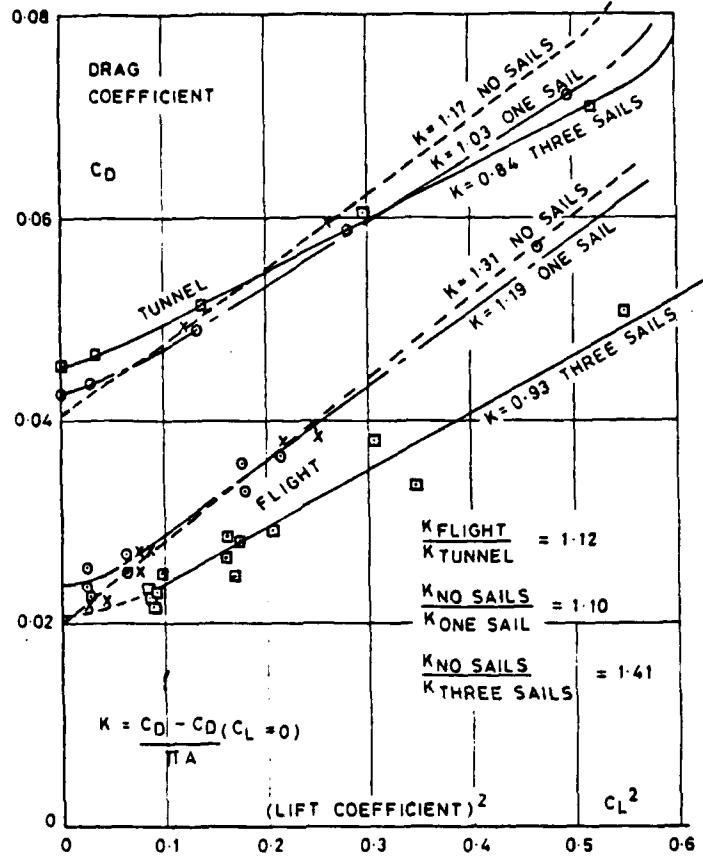


Figure 65 Effect of Wingtip Sails on Lift-Induced Drag [Ref. 55].

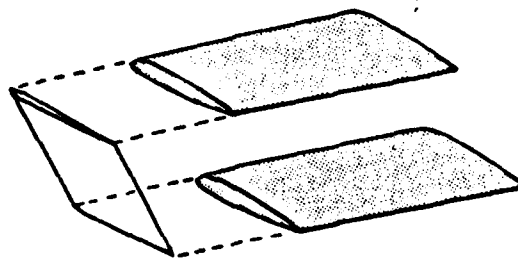


Figure 66 Sketch of Biplane Winglet [Ref. 58].

LIST OF REFERENCES

1. Lee, G.H., "Trailing Vortex Wakes," Aeronautical Journal, pp. 377-388, September 1975.
2. Bertin, John J. and Smith Michael L., Aerodynamics for Engineers, Prentice-Hall, pp. 163-170, 1979.
3. Westwater, E. L., "The Rolling Up of a Surface of Discontinuity," Aeronautical Research Reports and Memoranda, no. 1962, pp. 116-131, 1936.
4. Kaden, H., "Aufwicklung Einer Unstetigkeitsfläche," Ingenieur-Archiv 2, pp. 140-168, 1931.
5. Spreiter, J.R. and Sacks, A.H., "The Rolling Up of a Trailing Vortex Sheet and its Effect on the Downwash behind Wings," Journal of Aeronautical Science, vol. 18, no. 1, pp. 27-32, Jan. 1951.
6. Betz, A., Behavior of Vortex Systems, NACA TM 713, June 1933.
7. Donaldson, C. duP., A Brief Review of the Aircraft Trailing Vortex Problem, ARAP Report 155, Aeronautical Research Associates of Princeton, Princeton, N.J., May 1971.
8. Donaldson, C. duP., Snedeker, R.S., and Sullivan, R.D., "Calculation of Aircraft Wake Velocity Profiles and Comparison with Experimental Measurements," Journal of Aircraft, vol. 11, no. 9, pp. 547-555, September 1974.
9. Rossow, V., "On Inviscid Rolled-Up Structure of Lift-Generated Vortices," Journal of Aircraft, vol. 10, no. 11, pp. 647-650, November 1973.
10. Moore, D.W. and Saffman, P.G., Axial Flow in Laminar Trailing Vortices, Proceedings of Royal Society A333, pp. 491-508, 1973.
11. Lamb, H., Hydrodynamics, Sixth Edition, p. 592, Dover, 1945.
12. Dosanjh, D.S., Grasperek, E.P., and Eskinazi, S., "The Decay of a Viscous Trailing Vortex," Aeronautical Quarterly, vol. 13, no. 167, pp. 167-188, 1962.

13. Squires, H.B., "On the Growth of a Turbulent Vortex in Flow," Aeronautical Research Council CP666, 1954.
14. Govindaraju, S.P. and Saffman, P.G., "Flow in a Turbulent Trailing Vortex," The Physics of Fluids, vol. 14, no. 10, pp.2074-2080., October 1971.
15. Hoffmann, E.R. and Joubert, P.N., "Turbulent Line Vortices," Journal of Fluid Mechanics, vol. 16, no.3, pp.395-411, July 1963.
16. Batchelor, G.K., "Axial Flow in Trailing Line Vortices," Journal of Fluid Mechanics, vol. 20, no. 2, pp.645-648, December 1964.
17. Brown, Clinton E., "Aerodynamics of Wake Vortices," AIAA Journal, vol. 11, no. 4, pp.531-536, April 1973.
18. Chigier, N.A. and Corsiglia, V.R., "Wind Tunnel Studies of Wing Wake Turbulence," Journal of Aircraft, vol. 9, no. 12, pp. 820-825, December 1972.
19. Panton, R.L., Cberkamp, W.L., and Soskic, N., "Flight Measurements of a Wingtip Vortex," Journal of Aircraft, vol. 17, pp. 250-259, April 1980.
20. Thompson, D.H., "Experimental Study of Axial Flow in Wingtip Vortices," Journal of Aircraft, vol. 12, no. 11, pp. 910-911, November 1975.
21. Ciffone, D.L. and Orloff, K.L., "Application of Laser Velocimetry to Aircraft Wake-Vortex Measurements," Wake Vortex Minimization, NASA SP-409, pp. 157-192, 1977.
22. Staufenbiel, Rolf W., "Structure of Lift-Generated Rolled-Up Vortices," Journal of Aircraft, vol. 21, no. 10, pp. 737-744, October 1984.
23. Stickle, J.W. and Kelly, M.W., "Ground Based Facilities for Evaluating Vortex Minimization Concepts," Wake Vortex Minimization, NASA SP-409, pp. 129-155, 1977.
24. Rinehart, S.A., Balcerak, J.C., and White, R.P. Jr., An Experimental Study of Tip Vortex Modifications by Mass Flow Injection, Rochester Applied Science Associates, Inc., NASA Report 71-01, January 1971.
25. Snedeker, R.S., "The Effects of Air Injection on the Torque Produced by a Trailing Vortex," Journal of Aircraft, vol. 9, no. 9, pp.682-684, September 1972.

26. Poppleton, E.D., "Effect of Air Injection into the Core of a Trailing Vortex," Journal of Aircraft, vol. 8, no. 8, pp. 672-673, August 1971.
27. Kirkman, K.L., Brown, C.E., and Goodman, A., Evaluation of the Effectiveness of Various Devices for Attenuation of Trailing Vortices Based on Model Tests in a Large Towing Basin, NASA CR-2202, December 1973.
28. Patterson, J.C. Jr. and Jordan, F.L. Jr., "Thrust-Augmented Vortex Attenuation," Wake Vortex Minimization, NASA SP-409, pp. 251-270, 1977.
29. Yuan, S.W. and Bloom, A.M., Experimental Investigation of Wingtip Vortex Abatement, Ninth Conference of the International Council of Aeronautical Science, Haifa, Israel, August 25-30, 1974.
30. Dunham, R.E. Jr., "Unsuccessful Concepts for Aircraft Wake Vortex Minimization," Wake Vortex Minimization, NASA SP-409, pp. 221-249, 1977.
31. Wu, James and Vakili, A. Aerodynamic Improvements by Discrete Wing Tip Jets, Air Force Wright Aeronautical Laboratory, AFWAL-TR-84-3009, March 1984.
32. Patterson, James C. Jr., "Vortex Attenuation Obtained in the Langley Vortex Research Facility," Journal of Aircraft, vol. 12, no. 9, pp. 745-749, September 1975.
33. DeMeis, R., "New Tricks for Cutting Drag," Aerospace America, pp. 75-77, January 1985.
34. Barber, M.R. and Tymczyszyn, J.J., "Wake Vortex Attenuation Flight Tests," A Status Report: 1980 Aircraft Safety and Operating Problems, NASA CP-2770, Part II, pp. 387-408, 1981.
35. Uzel, J.N. and Marchman, J.F. III, The Effect of Wing-Tip Modifications on Aircraft Wake Turbulence, VPI-E-72-8, July 1972.
36. Croom, Delwin R., Low-Speed Wind-Tunnel Investigation of Forward-Located Spoilers and Trailing Splines as Trailing-Vortex Hazard Alleviation Devices on an Aspect-Ratio 8 Wing Model, NASA TM X-3166, February 1975.
37. Croom, D.R. and Dunham, R.E. Jr., Low-Speed Wind-Tunnel Investigation of Span Load Alteration, Forward Located Spoilers, and Splines as Trailing-Vortex-Hazard Alleviation Devices on a Transport Aircraft Model, NASA TN D-8133, December 1975.

38. Hastings, E.C. Jr., and others, Development and Flight Tests of Vortex-Attenuating Splines, NASA TN D-8083, December 1975.
39. Croom, D.R. and Holbrook, G.T., Low-Speed Wind-Tunnel Investigation of Wing Trailing-Vortex-Alleviation Devices on a Transport Airplane Model, NASA TP-1453, June 1979.
40. Iversen, J. and Moghadam, M., Experimental Investigation of Vortices Shed by Various Wing Fin Configurations, NASA CP-163874, January 1981.
41. Corsiglia, V.R., Jacobsen, R.A., and Chigier, N., "An Experimental Investigation of Trailing Vortices Behind a Wing with a Vortex Dissipator," Aircraft Wake Turbulence and its Detection, Plenum Press, pp.229-242, 1971.
42. Croom, D.R., Low-Speed Wind-Tunnel Investigation of Various Segments of Flight Spoilers as Trailing-Vortex-Alleviation Devices on a Transport Aircraft Model, NASA TN D-8162, March 1976.
43. Croom, D.R., Low-Speed Wind-Tunnel Parametric Investigation of Flight Spoilers as Trailing-Vortex-Alleviation Devices on a Transport Aircraft Model, NASA TP-1479, April 1979.
44. Croom, D.R., Vogler, R.D., and Thelander, J.A., Low-Speed Wind-Tunnel Investigation of Flight Spoilers as Trailing-Vortex-Alleviation Devices on an Extended-Range Wide-Body Tri-Jet Airplane Model, NASA TN D-8373, December 1976.
45. Barber, M.R., and others, "Vortex Attenuation Flight Experiments," Wake Vortex Minimization, NASA SP-409, pp. 369-403, 1977.
46. Corsiglia, V.R. and Dunham, R.E. Jr., "Aircraft Wake-Vortex Minimization by use of Flaps," Wake Vortex Minimization, NASA SP-409, pp. 305-338, 1977.
47. FAA/NASA Proceedings Workshop on Wake Vortex Alleviation and Avoidance, FAA-RD-79-105, September 1979.
48. Morris, D.J. and Holbrook, G.T., "Basic Research in Wake Vortex Alleviation using a Variable Twist Wing," A Status Report, 1980 Aircraft Safety and Operating Problems, NASA CP-2170, Part II, pp. 409-424, 1981.
49. Smith, Hubert C., "Method for Reducing the Tangential Velocities in Aircraft Trailing Vortices," Journal of Aircraft, vol. 17, no. 12, pp. 861-866, December 1980.

50. Faery, H.F. Jr. and Marchman, J.F. III, "Effect of Whitcomb Winglets and other Wingtip Modifications on Wake Vortices," Proceedings of the Aircraft Wake Vortices Conference, March 15-17, FAA-RD-77-68, pp. 207-215, June 1977.
51. El-Ramly, Z. and Rainbird, W.J., "Effects of Wing-Mounted Devices on the Trailing Vortex System in the Near Field," Proceedings of the Aircraft Wake Vortices Conference, March 15-17, FAA-RD-77-68, pp. 194-206, June 1977.
52. Clements, Harry R., "Canted Adjustable End Plates for the Control of Drag," Aeronautical Engineering Review, vol. 14, no. 7, pp. 40-44, July 1955.
53. Whitcomb, R.T., A Design Approach and Selected Wind-Tunnel Results at High Subsonic Speeds for Wing-Tip Mounted Winglets, NASA TN D-8260, July 1976.
54. Flechner, S.G., Jacobs, P.F., and Whitcomb, R.T., A High-Speed Wind Tunnel Investigation of Winglets on a Representative Second-Generation Jet Transport Wing, NASA TN D-8264, July 1976.
55. Spillman, J.J., "The Use of Wing Tip Sails to Reduce Vortex Drag," Aeronautical Journal, pp. 387-395, September 1978.
56. Spillman, J.J., Ratcliffe, H.Y., and McVitie, A.M., "Flight Experiments to Evaluate the Effect of Wingtip Sails on Fuel Consumption and Handling Characteristics," Aeronautical Journal pp. 279-281, July 1979.
57. Spillman, J.J. and McVitie, A.M., "Wingtip Sails which give Lower Drag at all Normal Flight Speeds," Aeronautical Journal, pp. 362-369, October 1984.
58. Gall, P.D. and Smith, H.C., Study of Winglets Applied to Biplanes, AIAA Paper 85-0279, January 1985.

INITIAL DISTRIBUTION LIST

	No.	Copies
1. Defense Technical Information Center Cameron Station Alexandria, Virginia 22304-6145	2	
2. Superintendent Attn: Library, Code 0142 Naval Postgraduate School Monterey, California 93943-5100	2	
3. Professor T. Sarrkaya, Code 69S1 Mechanical Engineering Naval Postgraduate School Monterey, California 93943-5100	10	
4. Department of Mechanical Engineering, Code 69 Naval Postgraduate School Monterey, California 93943-5100	2	
5. Department Chairman, Code 67P1 Department of Aeronautics Naval Postgraduate School Monterey, California 93943-5100	1	
6. Lieutenant Kenneth G. Heffernan, USN USS Saratoga (CV-60) Miami, Florida 34078-2740	2	

END

FILMED

11-85

DTIC